Improvement of poly(L-lactide)-*b*-poly(ethylene glycol)-*b*-poly(L-lactide) film properties with nanocellulose

Chutima Banthao

A Thesis Submitted in Partial Fulfillment of Requirements for

degree of Master of Science in Chemistry

June 2020

พหุน ปณฺ ฑิโต ชีเว

พหุน ปณฺ ฑิโต ชีเว

การปรับปรุงสมบัติของฟิล์มพอลิแอล-แล็กไทด์-บล็อก-พอลิเอทิลีนไกลคอล-บล็อก-พอลิแอล-แล็กไทด์ด้วยนาโนเซลลูโลส

วิทยานิพนธ์

ของ

ชุติมา บรรเทา

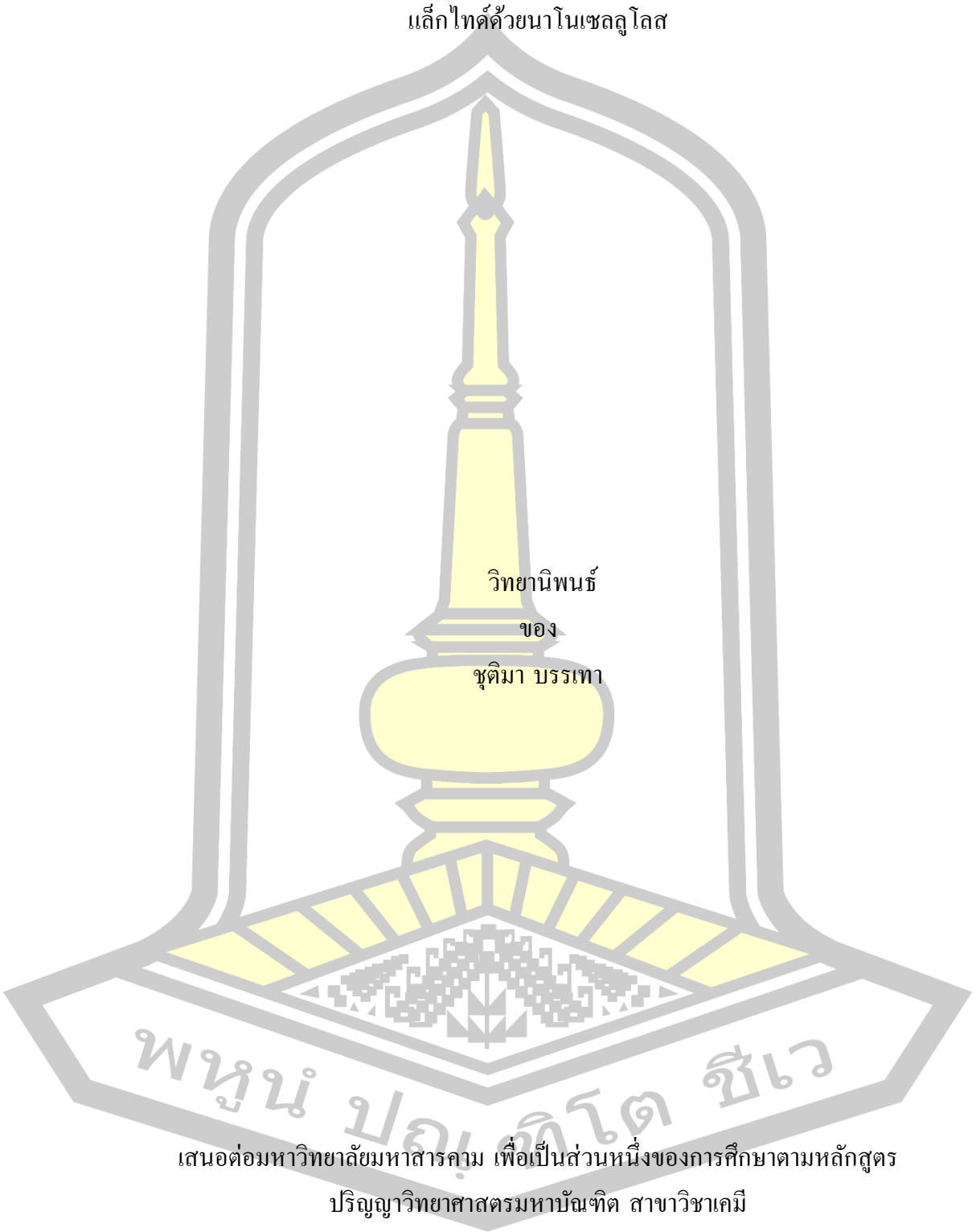

เสนอต่อมหาวิทยาลัยมหาสารคาม เพื่อเป็นส่วนหนึ่งของการศึกษาตามหลักสูตร

ปริญญาวิทยาศาสตรมหาบัณฑิต สาขาวิชาเคมี

มิถุนายน 2563

Improvement of poly(L-lactide)-*b*-poly(ethylene glycol)-*b*-poly(L-lactide) film properties with nanocellulose

Chutima Banthao

A Thesis Submitted in Partial Fulfillment of Requirements

for Master of Science (Chemistry)

June 2020

The examining committee has unanimously approved this Thesis, submitted by Miss Chutima Banthao , as a partial fulfillment of the requirements for the Master of Science Chemistry at Mahasarakham University

Examining Committee

.....Chairman
(Assoc. Prof. Sittipong Amnuaypanich , Ph.D.)

.....Advisor
(Asst. Prof. Kansiri Pakkethati , Ph.D.)

.....Co-advisor
(Assoc. Prof. Yodthong Baimark , Ph.D.)

.....Committee
(Asst. Prof. Khongvit Prasitnok , Ph.D.)

.....Committee
(Asst. Prof. Onanong Cheerarot , Ph.D.)

Mahasarakham University has granted approval to accept this Thesis as a partial fulfillment of the requirements for the Master of Science Chemistry

.....
(Prof. Pairot Pramual , Ph.D.)
Dean of The Faculty of Science

.....
(Assoc. Prof. Krit Chaimoon , Ph.D.)
Dean of Graduate School

TITLE Improvement of poly(L-lactide)-*b*-poly(ethylene glycol)-*b*-poly(L-lactide) film properties with nanocellulose

AUTHOR Chutima Banthao

ADVISORS Assistant Professor Kansiri Pakkethati , Ph.D.

Associate Professor Yodthong Baimark , Ph.D.

DEGREE Master of Science **MAJOR** Chemistry

UNIVERSITY Mahasarakham University **YEAR** 2020

ABSTRACT

The improvement and study properties of PLLA and PLLA-PEG-PLLA was mixed nanocellulose (NC) and modified NC. The NC in this work was extracted from rice straw by alkali treatment (2M, NaOH), bleaching process with 18.5% H_2O_2 and hydrolysis (64%, H_2SO_4). The size of the NC was obtained (after the hydrolysis process) around 50-91 nm and 225-396 nm by particle size analyzer. While the diameter of size NC from transmission electron microscope (TEM) displayed 30.22±1.7 nm. However, NC displayed high hydrophilicity which has low compatibility with polymer matrix (hydrophobicity). Thus, in this research, the NC was modified by [3- (2,3-Epoxypropoxy) -propyl] -trimethoxysilane. The size of the modified NC presented 225-396 nm (particle size analyzer) and 35.53±1.6 nm (TEM). The composite films were prepared by solution casting method using PLLA or PLLA-PEG-PLLA and NC or modified NC with different weight ratios (100/0, 99/1, 97/3and 95/5). The composite films were characterized by fourier transform infrared spectrometer (FTIR) and X-ray photoelectron spectroscopy (XPS) for an analysis functional group, X-ray diffractometer (XRD) for study crystallinity properties, scanning electron microscope (SEM) and transmission electron microscopy (TEM) for analysis morphology, differential scanning calorimeter (DSC) and Thermogravimetric analyzer (TGA) for examining the thermal properties, universal testing machine for study mechanical properties. The thermal properties, mechanical properties, crystallinity properties and water adsorption of composite films were increased when increasing the amount of NC or modified NC. It can be used as reinforcing agents to increase the thermal and mechanical properties of PLLA and PLLA-PEG-PLLA. Meanwhile, the composite films containing 1% modified NC showed the best thermal and mechanical properties.

Keyword : poly(L-lactide), block copolymer, nanocomposite, nanocellulose, biodegradable polymers

ACKNOWLEDGEMENTS

This thesis has been successfully accomplished because of the merciful and help from many parties. Both academic data and instrumentals were useful for research.

I would like to express my sincere thanks to my thesis advisor, Asst. Prof. Dr. Kansiri Pakkethati her invaluable help and constant support throughout the course of this research. I am most grateful for her teaching and advising, not only the research methodologies but also many other methodologies in life. I wouldn't have accomplished this far, and this thesis would not have been completed without all the support that I have always received from her.

I would like to express my sincere gratitude and great appreciation to Assoc. Prof. Dr. Yodthong Baimark, my co-advisor for their kind inspiring guidance, encouragement and helpful discussion throughout this thesis.

I would like to express my great sincere gratitude to Asst. Prof. Dr. Khongvit Prasitnok and Asst. Prof. Dr. Onanong Cheerarot for their kind, provided useful suggestions support as members of my thesis committee.

I would like to express my deepest gratitude to Assoc. Prof. Dr. Sittipong Amnuaypanich. Department of Chemistry, Faculty of Science, Khon Kaen University for the chairman, comment, and suggestion of my thesis.

I would like to express my great sincere gratitude to The Center of Excellence for Innovation in Chemistry (PERCH-CIC), Ministry of Higher Education, Science, Research and Innovation and the Thailand Research Fund (TRF) for the scholarship.

I would like to acknowledge to Department of Chemistry, Faculty of Science, Mahasarakham University for a courtesy location as well as chemicals and instrumentals for experiments of my thesis. I would like to thanks the Scientific Instrument Academic Service Unit, Faculty of Science, Laboratory equipment center and the Faculty of Pharmacy University Mahasarakham University for instrumentals used in this thesis research.

I would like to gratitude to Department of Chemistry, Faculty of Science, Khon Kaen University, the Center for Scientific and Technological Equipment, Suranaree University of Technology, Thailand Center of Excellence in Physics (ThEP Center), Chiang Mai University, for instrumentals used in this thesis research.

I would like to thanks Dr. Supasin Pasee for teaching the use of instrumentals and encouragement for this thesis.

I would like to thanks deeply imprinted to Mr. Aekkaphon Mokkarat, Department of Chemistry, Faculty of Science, Mahasarakham University for all the support, inspiration and encouragement for this thesis.

I would like to thank my best friends for their help, encouragement always being a good consultant and impressive friendship.

Most importantly, I would like to express their heartfelt thanks to my family for their love and tender care, encouragement and continued support throughout my study.

Chutima Banthao

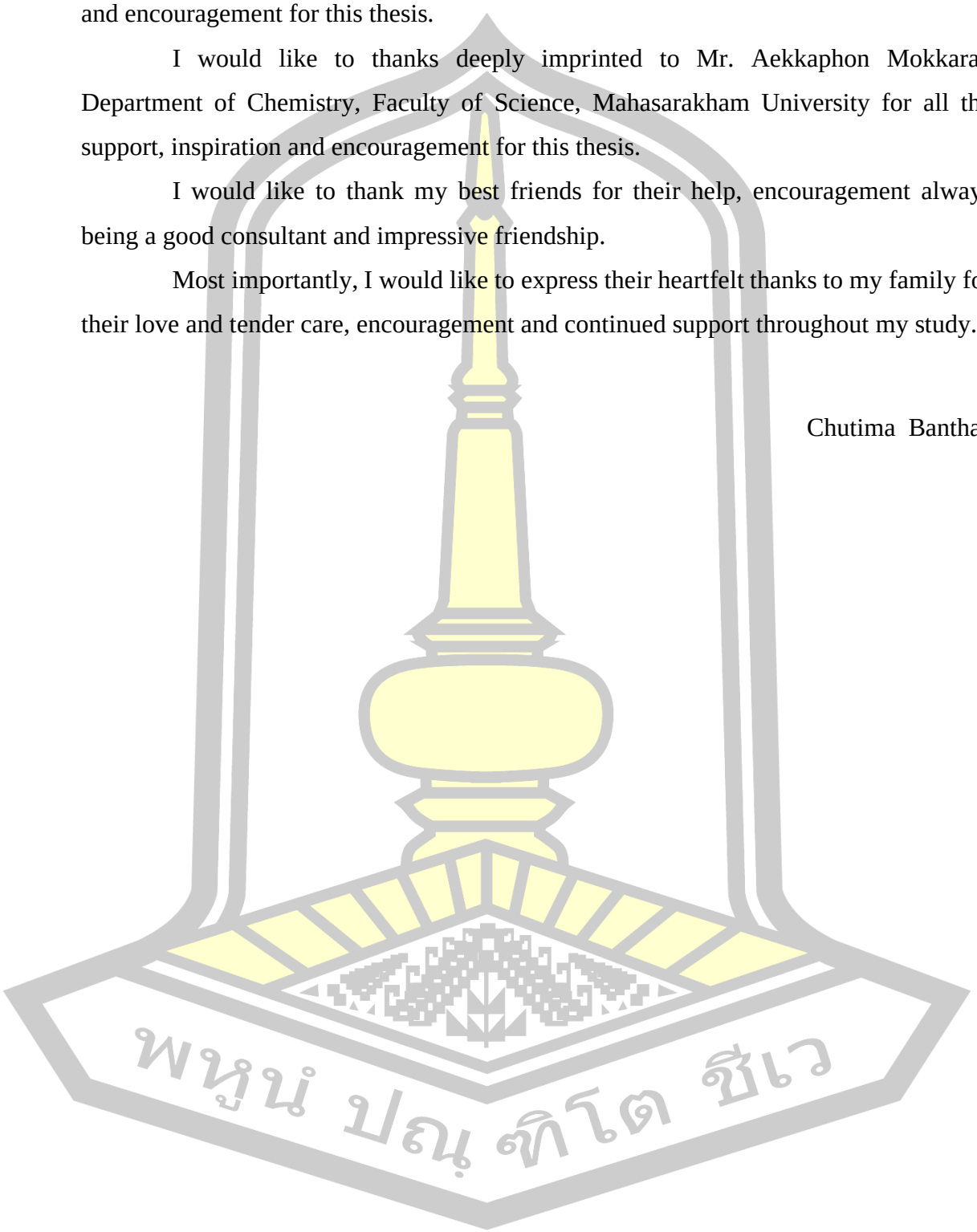

TABLE OF CONTENTS

Page

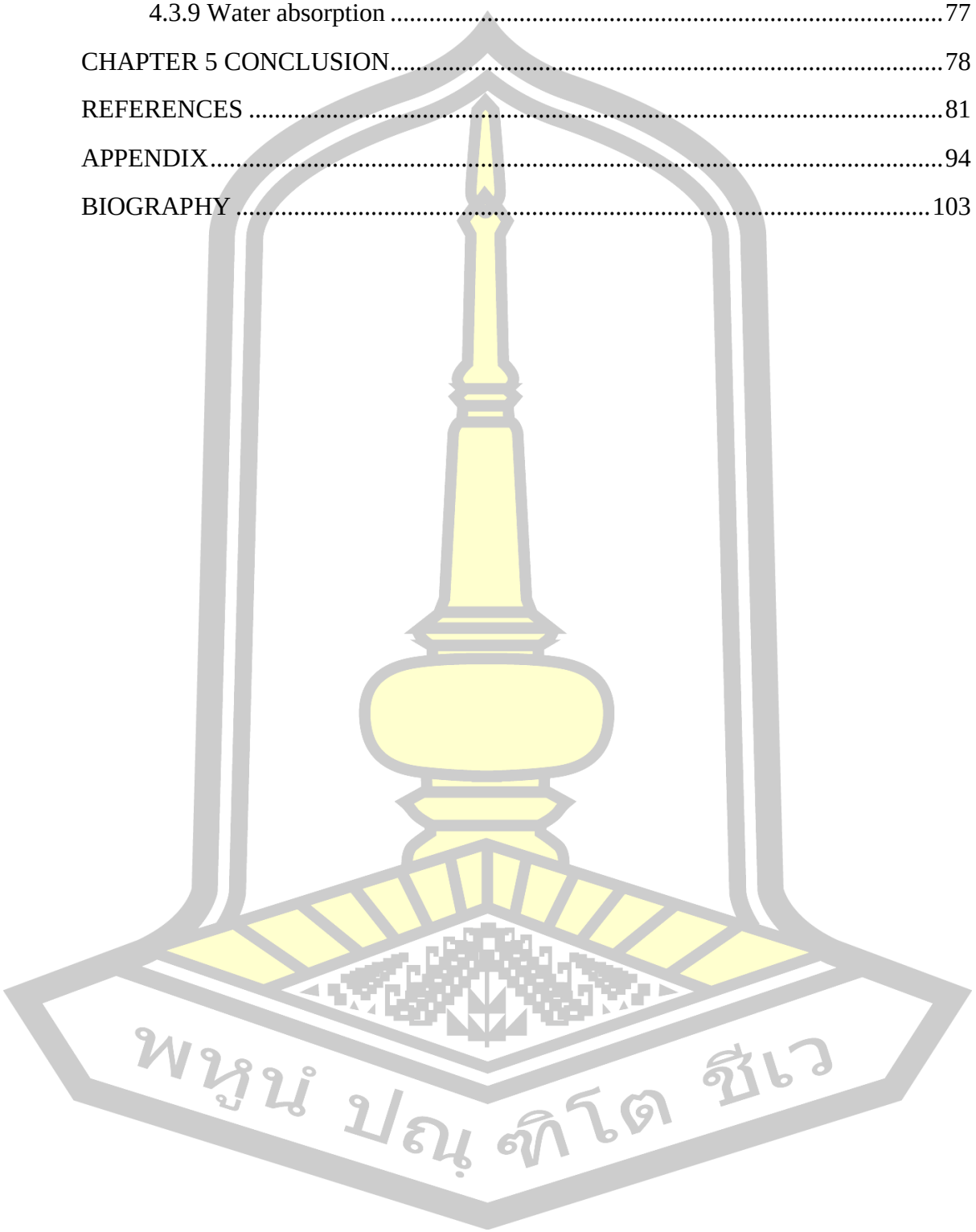

LIST OF TABLES

Page

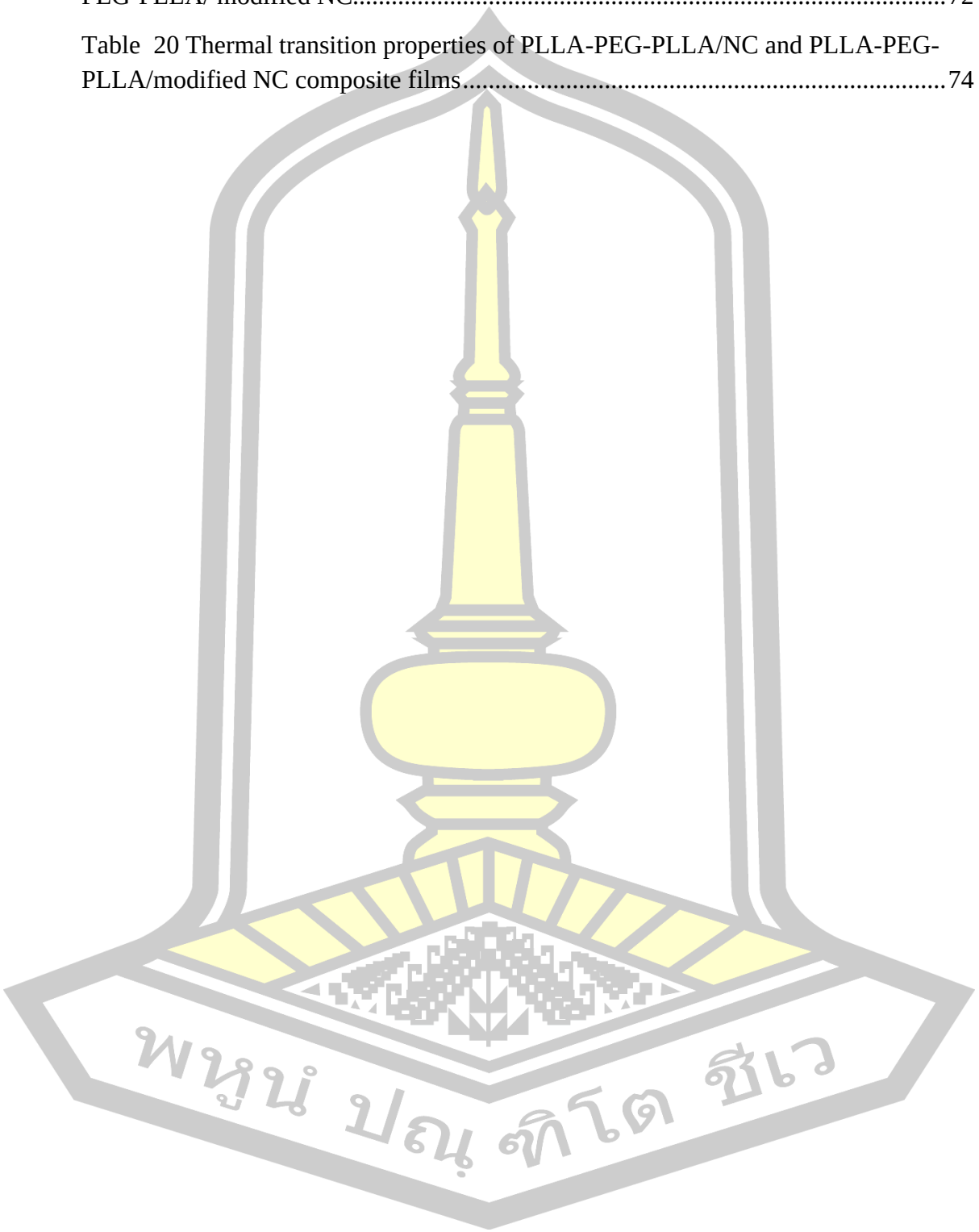

LIST OF FIGURES

Page

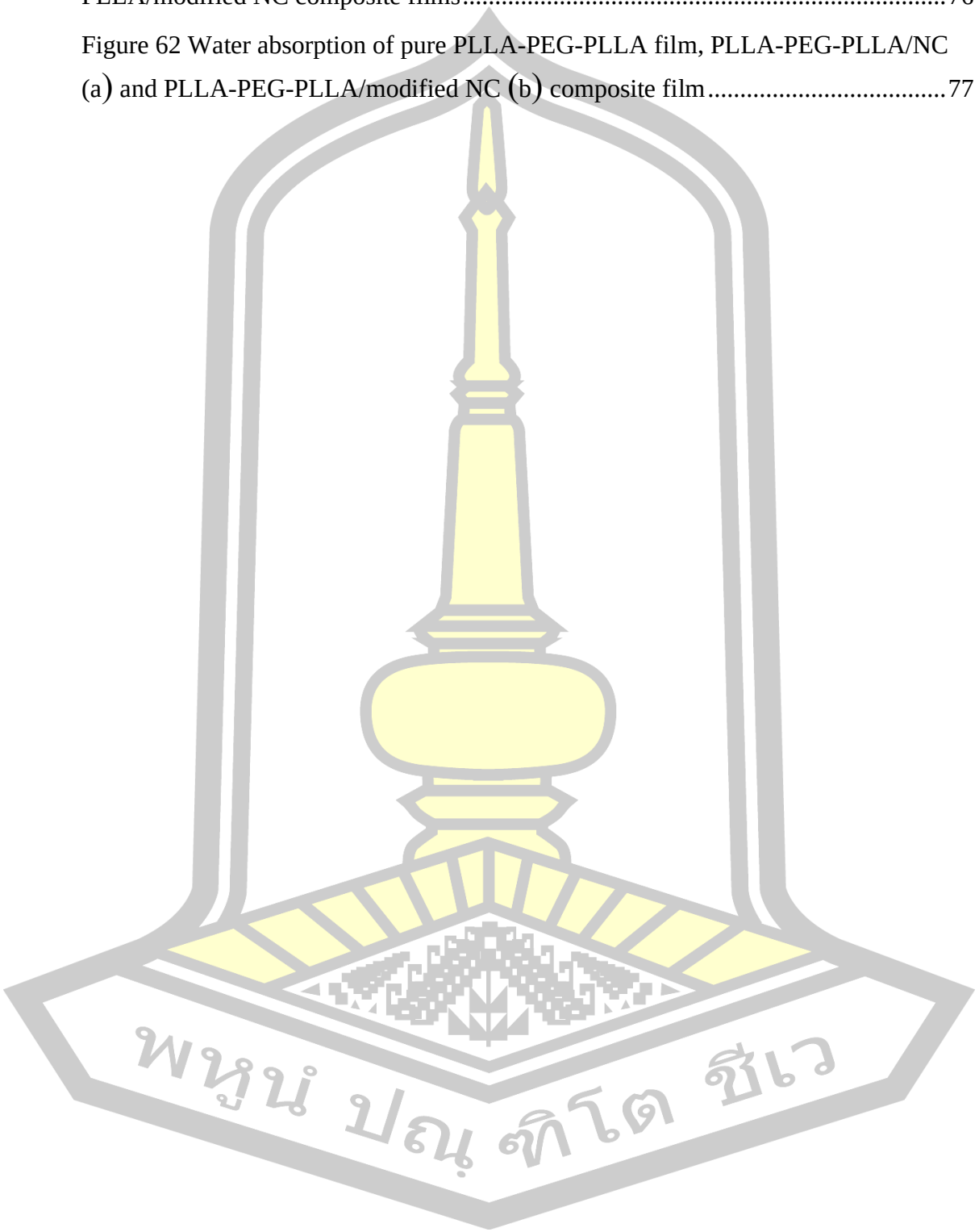

CHAPTER 1
INTRODUCTION

1.1 Background

Nowadays, plastics are used in the daily life of a human. The plastics used mostly produced from petroleum. Because of the plastics are lightweight, inexpensive, and high strength. Plastics are generally non-biodegradable, or they may take centuries to degenerate caused environmental problems. In the last decades, researchers around the world have been trying to create materials that replace plastic from petroleum. Until they discovered biodegradable polymers and it can be divided into two types according to the source, which natural processes such as starch and chitosan *etc*.[1] and synthesis processes such as poly(lactic acid) (PLA), poly(glycolic acid) (PGA), and poly(caprolactone) (PCL) *etc*.[2]. The produced synthesis polymers are created from monomers for instance glycolic acid (GA), lactic acid (LA) and ϵ-caprolactone (CL), respectively. Biodegradable polymers from synthesis are widely used in many biomedical applications such as implantable devices [3], drug delivery systems [4] and tissue engineering [5]. Polylactic acid (PLA) is an aliphatic polyester produced from lactic acid (2-hydroxy propionic acid) as a basic building block. It is a compostable thermoplastic and biodegradable derived from renewable plant sources, such as starch or sugar. The process of PLA can be achieved in many ways through conventional techniques such as extrusion, injection, and spinning. The outstanding mechanical properties of PLA dependent on the optical purity, molecular weight, and degree of crystallinity. Generally, the PLA properties similar to polystyrene (PS) properties [6]. The disadvantages are many obvious of PLA, its degradation rate unresponsive a wide range of application-specific requirements, and there are no cell recognition sites that are important for tissue compatibility on the surface of PLA application on tissue engineering. On other side, in the case of using PLA directly as a packaging material, brittle breakage has often occurred. Therefore, this property must be modification PLA. The modification of PLA includes the copolymerizing of the lactide with other lactone-type monomers, hydrophilic macro initiators such as polyethylene glycol (PEG), or other monomers with functional groups (such as amino and carboxylic groups, *etc*.), and the blending PLA with other materials.

The PEG is a highly biocompatible, that is soluble in aqueous solutions and organic solvents, which supports to its excellent biocompatibility and processability, respectively. When PEG combined with PLA, it results in improved mechanical properties and hydrophilicity of PLA [4]. The low molecular-weight PEG was presented with good miscibility with the PLA matrices. However, it has fast migration from the matrices to surfaces on aging. While high molecular-weight PEG reduce the migration effect but phase separation of matrices [7].The poly(L-lactide)-block-polyethylene glycol-block-poly(L-lactide) or PLLA-PEG-PLLA was used extensively for use in the drug delivery system [4,6]. The outstanding properties of PLLA-PEG-PLLA were exhibited flexible and high hydrophilicity than PLA due to highly chain mobility of hydrophilic PEG blocks [8]. Good phase compatibility [9] was also

regarded on PLLA-PEG-PLLA matrix but the PLLA-PEG-PLLA has low mechanical strength not suitable for some applications.

Rice is the primary food staple and provides a significant portion of dietary intake. Thailand is not only one of the world's largest rice producers; it also remains the world's largest rice exporter. Therefore, the leftover rice straw to be harvested after harvesting large quantities of rice. Although rice straw is used for various such as animal feed, make compost, or use as a material for straw mushroom cultivation, but the amount of rice straw is still a lot. For this reason, some farmers were eliminated rice straw by burning method which results in environmental impacts. Nanocellulose are used to reinforce the polymer and improve mechanical properties such as pineapple leaves [10], banana fibers [11], wood flour [12], Agave tequilana Weber Waste[13], grape residue [14]. Thus, nanocellulose was extracted from rice straw to reduce environmental pollution and increase the value of rice straw. The properties of nanocellulose exhibit low density [10], high strength [15] and high thermal property [16].The composite films between poly(L-lactide)-*b*-poly (ethylene glycol)-*b*-poly(L-lactide) and nanocellulose were developed to improve their mechanical and thermal properties.

1.2 Purpose of research

To study the method of cellulose nanocrystal synthesis from rice straw

To modify cellulose nanocrystals with 3-[(2,3-Epoxypropoxy)-propyl]-trimethoxysilane

To study the effect of addition of nanocellulose and modified nanocellulose on the properties of PLLA and PLLA-PEG-PLLA films in the weight ratios 1%, 3% and 5%

1.3 Scope of research

1.3.1 The nanocellulose was synthesized from rice straw.

1.3.2 The modified nanocellulose was prepared from nanocellulose by reacting with 3-[(2,3-Epoxypropoxy)-propyl]-trimethoxysilane.

1.3.3 The nanocellulose and modified nanocellulose were characterized by particle size analysis, fourier transform infrared spectroscopy, X-ray photoelectron spectrometry, X-ray diffractometry, thermogravimetric analysis, differential scanning calorimetry, scanning electron microscopy and transmission electron microscopy.

1.3.4 The PLLA/nanocellulose and PLLA/modified nanocellulose composites were prepared through the casting method.

1.3.5 The PLLA-PEG-PLLA/nanocellulose and PLLA-PEG-PLLA/modified nanocellulose composite films were made through the casting method.

1.3.6 The PLLA/nanocellulose and PLLA/ modified nanocellulose composite films were characterized by UV-Vis spectrophotometry, fourier transform infrared spectroscopy, thermogravimetric analysis, differential scanning calorimetry, X-ray diffractometry, scanning electron microscopy and tensile testing.

1.3.8 The PLLA-PEG-PLLA/nanocellulose and PLLA-PEG-PLLA/modified nanocellulose composite films were characterized by UV-Vis spectrophotometry, fourier transform infrared spectroscopy, thermogravimetric analysis, differential

scanning calorimetry, X-ray diffractometry, scanning electron microscopy and tensile testing.

1.4 Expected results

1.4.1 The nanocellulose and modified nanocellulose have successfully synthesized from rice straw.

1.4.2 The modified nanocellulose have accomplished prepared from nanocellulose.

1.4.3 The nanocellulose and modified nanocellulose can be used reinforcing fillers for PLLA and PLLA-PEG-PLLA.

1.4.4 The PLLA and PLLA-PEG-PLLA composite films can be used to replace petroleum-based plastics.

1.4.5 The composite films prepared with modified nanocellulose show better properties than nanocellulose.

1.5 Location of the study

Room SC1-406, Department of Chemistry, Faculty of Science, Mahasarakham University.

CHAPTER 2
LITERATURE REVIEW

2.1 Biodegradable polymers

Biodegradable polymers are deemed environmentally friendly because of their biodegradability. The molecular chains of the polymers can be digested down either through hydrolytic degradation or by enzymatic means [17]. Moreover, some biodegradable polymers are straight manufactured from renewable feedstocks. In contrast, biodegradable polymers (BPs) disposed in bioactive environments degrade by the enzymatic action of microorganisms such as bacteria, fungi, and algae [18]. Their polymer chains may also be broken down by non-enzymatic processes such as chemical hydrolysis. The biodegradation transforms them to CO_2, CH_4, water, biomass, humic matter, and other natural substances. The biodegradable polymers are thus naturally recycled by biological processes [19] (Figure 1).

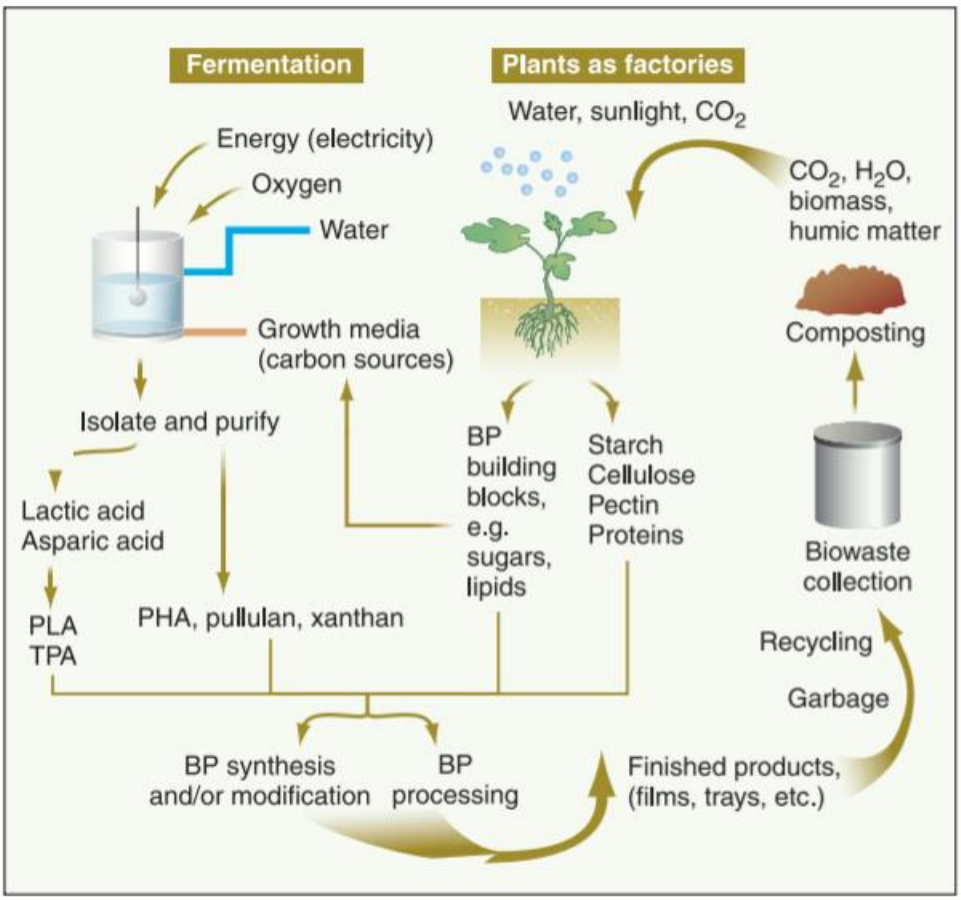

Figure 1 Cyclic process by which agricultural products and fermentative routes can yield biodegradable polymers [19]

2.2 Type of biodegradable polymers

The biodegradable polymers can be divided according to their origin, chemical composition, synthesis method, economic importance, application and processing method *etc*.[20]. The biodegradable polymers can be classified according to their source in three types:[21] Natural polymers were obtained from natural resources. Synthetic polymers based on raw obtained from petroleum derivatives (poly(ε-caprolactone) (PCL)) or from biomass (polylactic acid (PLA)) and produced by microorganisms (polyhydroxyalkanoates (PHAs)) [22]. An overview of these categories are shown in Figure 2 the carbohydrates, such as chitin, cellulose, and starch, and protein-based polymers, namely zein or soy protein. Among others are the most common type of biodegradable polymers for packaging application [23].

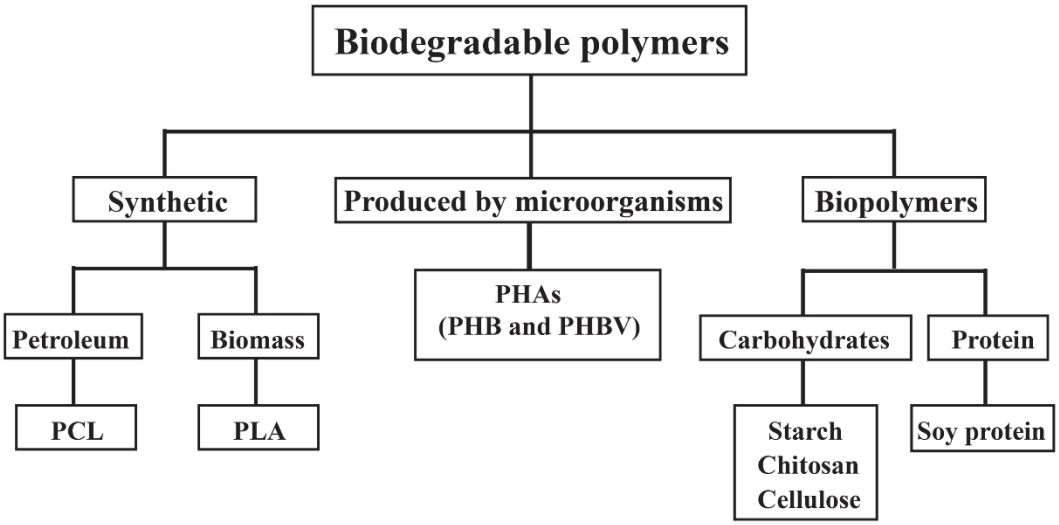

Figure 2 Schematic presentation type of biodegradable polymers based on their source [16,17]

2.3 Polylactide

Polylactide (PLA) is one of the most popular biodegradable polymers. PLA has transported important consideration as a candidate for non-petroleum based biodegradable polymeric materials. Because PLA is a semi-crystalline nature with good processing properties, biocompatible polymer with thermal plasticity, and mechanical properties similar to those of polystyrene [24]. PLA is one of the most encouraging competitors of replacing petrochemical polymers [25] but it has natural low toughness, and brittleness which limit the range of applications [26]. PLA can be applied in biomedical, industrial, environmental and pharmaceutical [27], and also in other fields, such as food packaging, furnishings, and agriculture[24, 28, 29]. It is widely used in many processing applications, including cast and thermoforming blown films, as well as blown films, injection moldings, and extrusion [30]. In addition, PLA has a wide range of applications in medical fields, such as drug delivery systems, screws for bone fractures, and sutures because of its high mechanical strength, good biocompatibility, excellent shaping and moulding properties.

2.3.1 The stereoisomeric forms

PLA belongs to the family of aliphatic polyesters derived from α-hydroxy acids. The building block of PLA, lactic acid (2-hydroxy propionic acid), can exist in optically active D-/L-enantiomers. The petrochemical synthesis yields an optically inactive 50:50 mixture of D- and L-forms of lactic acid, whereas the bacterial fermentation derived lactic acid exists almost exclusively in the L-form [31]. The structures of three stereoisomeric forms, L,L-lactide, D,D-lactide, and meso-lactide (D,L -lactide), as shown in Figure 3. PLA is usually obtained via the ring opening polymerization (ROP) of lactides or the polycondensation of lactic acid are shown in Figure 4 [3, 25, 27]. Depending on the proportion of the enantiomers, PLA with variable material properties can be obtained. This approach enables the production of a wide spectrum of PLA polymers to match performance requirements [30].

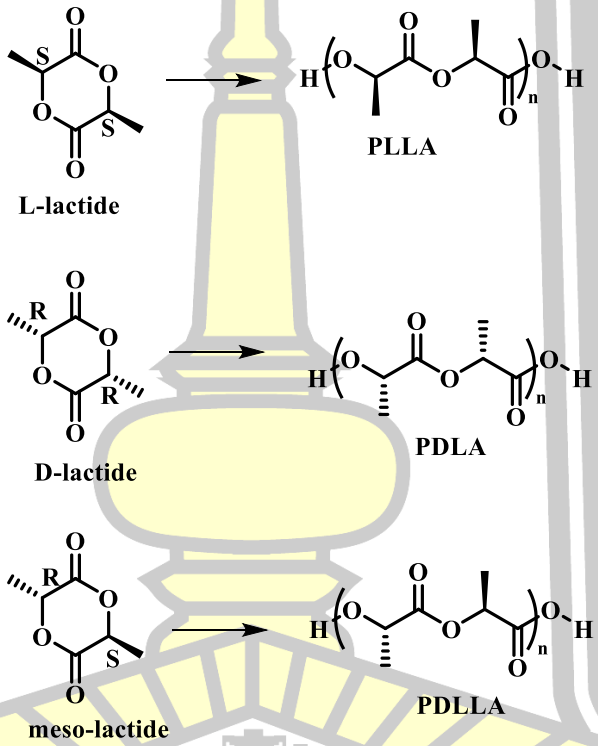

Figure 3 The structures of three stereoisomeric forms, L,L-lactide, D,D-lactide, and meso-lactide [34]

2.3.2 The synthesis methods

PLA can be synthesized by different polymerization process [34] from lactic acid including: polycondensation, ring-opening polymerization and by direct methods like azeotropic dehydration and enzymatic polymerization (Figure 4). Currently, direct polymerization and ring-opening polymerization are the most used production techniques. Lactide can be made through a decompression method in which the water is separated from the system, and then, some catalysts are added into the reactor. After reacting for several hours, lactide is concerned. Then, the lactide opens its ring to polymerize. Compared with ring-opening polymerization, direct condensation polymerization has fewer manufacturing steps and lower cost and is easier to

manipulate and commercialize. The primary disadvantage of this method is the low molecular weight [25] of the resultant polymer, which is due to the equilibrium among the free acid, the oligomers, and the water produced during the reaction or some special treatment. Thus, some traditional method-ring opening polymerization was developed. Catalytic ring-opening polymerization of the lactide intermediate results in PLA with controlled molecular weight by controlling residence time and temperatures in combination with catalyst type and concentration, it is possible to control the ratio and sequence of D- and L-lactic acid units in the final polymer. The ring-opening polymerization of lactide can be shipped out in melt, bulk, or in solution and by cationic, anionic, and coordination-insertion mechanisms depending on the catalyst [34]. Various types of initiators have been successfully tested, but among them, stannous octoate is usually preferred because it provides high reaction rate, high conversion rate, and high molecular weights, even under rather mild polymerization conditions.

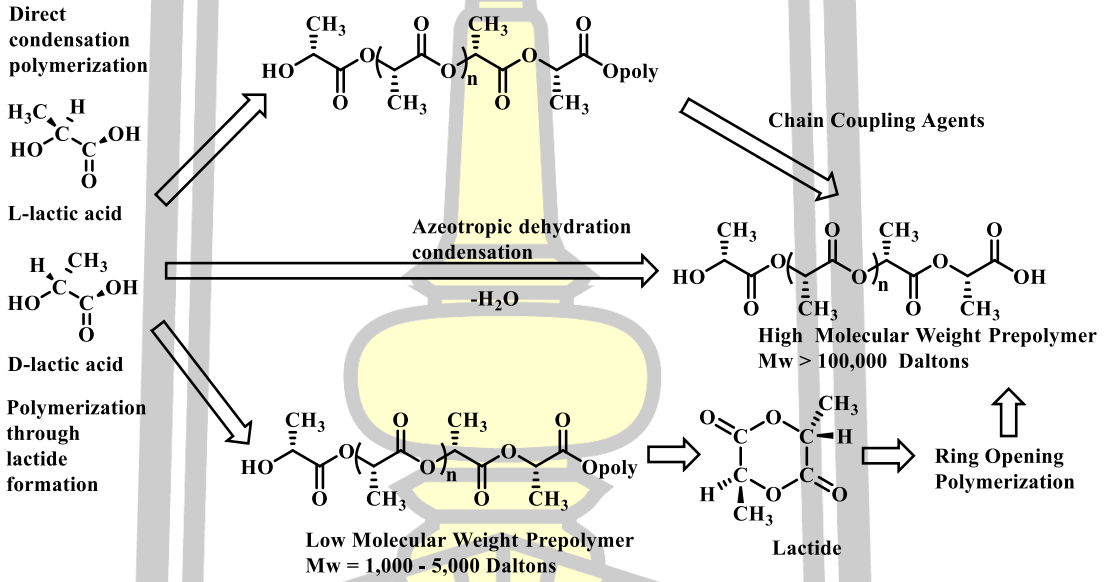

Figure 4 Synthesis methods for obtaining high molecular weight PLA [3, 25, 35]

2.3.3 The properties

The properties of poly(L-lactide) (PLLA) depend on the component isomers, processing temperature, annealing time, and molecular weight. The PLLA is the product resulting from the polymerization of L-lactide. The PLLA has a crystallinity of around 37% [36], a glass transition temperature (T_g) between 50-80 ºC [37] and a melting temperature (T_m) between 173-178 ºC [37]. Because of the stereo regular chain microstructure, optically pure polylactides, poly (L-lactide) (PLLA) and poly (D-lactide) (PDLA), are semi-crystalline. The crystallization ability of polylactides decreases with chain stereoregularity and below 43% optical purity crystallization is no longer possible [28].

Table 1 PLA mechanical properties source: physical and mechanical properties of PLA, and their functions in widespread applications: a comprehensive review

		PLLA	PDLA	PDLLA
Tensile strength	MPa	59	66	44
Modulus of elasticity	MPa	3750	4150	3900
Elongation at break	(%)	7	4	5.4
Yield strength	MPa	70	70	53
T_m	°C	170-190	180	-
T_g	°C	50-60	50-60	-
Half-life in 37°C normal saline	months	4-6	4-6	2-3

2.4 Poly(ethylene glycol)

Poly(ethylene glycol) (PEG), also called poly (ethylene oxide) (PEO) are synthetic, highly water soluble, inert polymers that are produced in a large range of molecular weights. The PEG of various molecular weights has been used widely in consumer care products such as laxatives, toothpaste, and hair shampoos, and for the past 20 years, also in biopharmaceuticals. Chemical modification with PEG is used to improve pharmaceutical [33] properties of both small molecule and biotherapeutic drugs. PEG is a linear polyether of ethylene glycol (ethane-1,2-diol) of the general structure [38] shown in Figure 5.

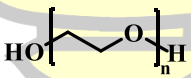

Figure 5 Structure of a single PEG chain [33]

2.5 Poly(L-lactide)-*b*-poly(ethylene glycol)-*b*-poly (L- lactide)

PLLA-PEG-PLLA copolymer was synthesized using the ring-opening polymerization of lactide in the presence of PEG, whose hydroxyl end groups initiate the ring opening (Figure 6) [7]. In fact, the amphiphilic nature of the PLLA–PEG–PLLA copolymers, with hydrophilic PEG and hydrophobic PLA segments, provides an opportunity to form polymersomes in water due to its hydrophilicity [39].

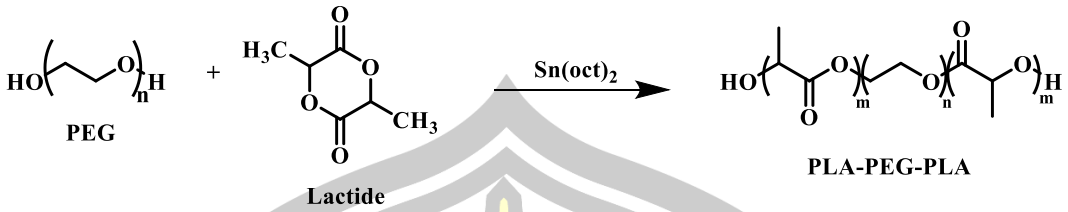

Figure 6 Synthesis route of PLLA-PEG-PLLA copolymer [7, 9]

2.5.1 Characterization of poly(L-lactide)-*b*-poly(ethylene glycol)-*b*-poly (L-lactide)

PLLA-PEG-PLLA oligomer was synthesized and characterized by ^{1}H NMR. As shown in Figure 7 the presence of methine (CH) and methyl (CH_3) protons in PLA were observed at around 5.20 ppm (c) and 1.58 ppm (a) respectively. The methylene protons in CH_2 group of PEG were around 3.64 ppm (b). Based on these assignments, the calculated the LA/EG ratio using the integration ratio of resonances due to PEG blocks.

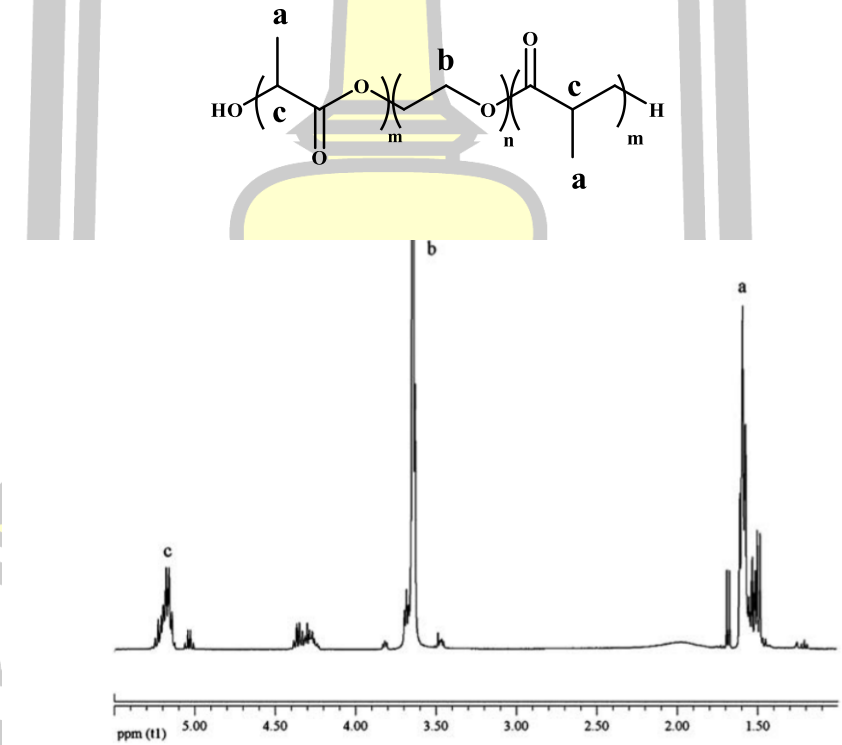

Figure 7 ^{1}H NMR spectrum of the PLA-PEG-PLA triblock [40]

FT-IR spectra of PLLA-PEG-PLLA copolymer was shown in Figure 8. In the spectrum shown, the sharp and intense bands at 1727 cm^{-1} and 1103 cm^{-1} were awardable to the presence of carboxylic ester (C=O) and ether (C–O) groups, which indicate that the formation of PLLA-PEG-PLLA copolymer has occurred successfully.

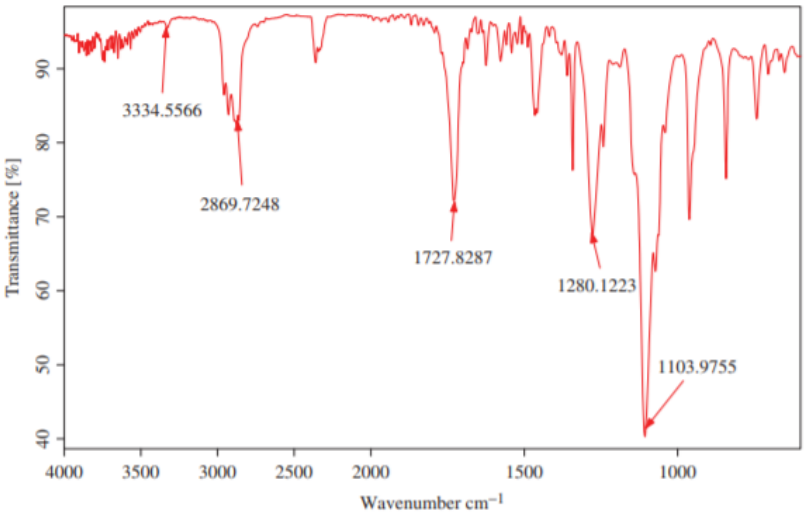

Figure 8 FTIR spectrum of PLA-PEG-PLA copolymer [41]

The microparticles of PLLA-PEG-PLLA copolymer for drug delivery (Figure 9) have a relatively spherical shape with a mean diameter of about 2.2 μm.

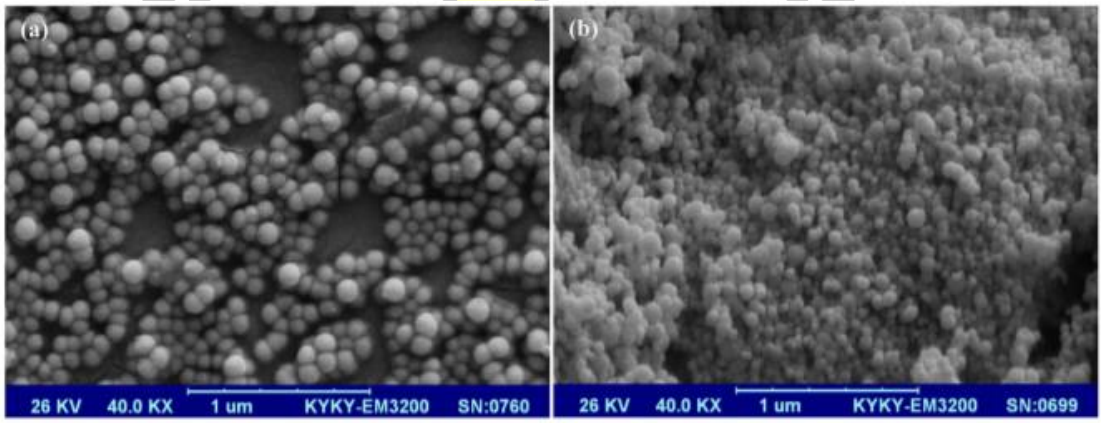

Figure 9 SEM photograph of mPEG-PLA (a) and PLA-PEG-PLA (b) microparticles [42]

The molecular weights (M_w and M_n) and polydispersity (M_w/M_n) of the produced PLLA-PEG-PLLA copolymers determined by gel permeation chromatography (GPC) was listed in Table 2. Data from the table indicate that relatively high molecular weight can be obtained by copolymerizing LA and PEG under controlled conditions. It can also be seen from the table that the concentration of PEG affects the molecular weight significantly, where M_n decreases with higher PEG content. This might be attributed to the fact that the -OH groups in PEG are involved in chain transfer reactions. With higher PEG content, the content of -OH groups in polymerization system is higher, giving more chance for chain transfer reaction [43].

Table 2 Polymers characterization by ^{1}H NMR, DSC and GPC [41]

Copolymer	M_n[a] (KDa)	M_w[a] (KDa)	PDI[b]	PEG (%)	T_m (°C)[c]
PLA_{12}–PEG_6–PLA_{12}	29	30	1.02	20	166.97

[a] Determined by GPC analysis using narrow molecular weight polystyrene standards
[b] Polydispersity index of the polymers (PDI = Mw/Mn)
[c] Calculated from the first run of DSC

Water contact angles were measured for the PLLA-PEG-PLLA triblock copolymer films with different PEG contents, as shown in Figure 10. PLA film showed characteristically high water contact angles (79º±2º), as expected, while the water contact angle decreases with higher PEG content in the PLLA-PEG-PLLA copolymer films. This result is similar to that of many studies using PEG as a surface modifier [43]. It is interesting to note that the water contact angle of PLA/PEG physical blend film with PEG content of 50% (w/w) is 33.5º±2º [44]; while the PLLA-PEG-PLLA triblock films had a relatively high initial water contact angle of 55º±5º (measured at 10 sec after water-film contact), which gradually dropped to 0º in less than 2 min, indicating total wettability of the material. The results suggest that PLLA-PEG-PLLA triblock better hydrophilicity than physical blends, at least in the form of film.

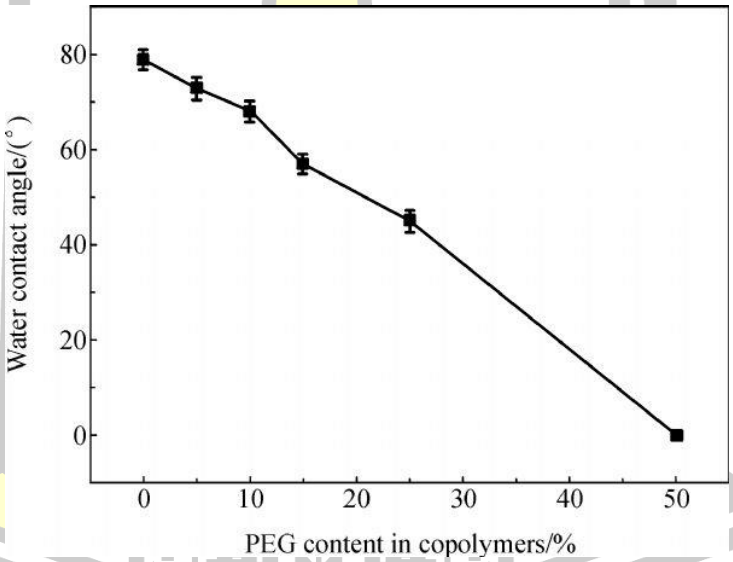

Figure 10 Dependency of the water contact angle with the PEG content for the PLLA-PEG-PLLA triblock films [44]

The characteristic high-intensity diffraction peak [7] of 16° was attributed to the PLA block, and the peaks of 18.9°and 23.2° were attributed to the PEG block, which revealed the existence of a natural crystalline form of PLLA-PEG-PLLA triblock before supercritical processing as show Figure 11.

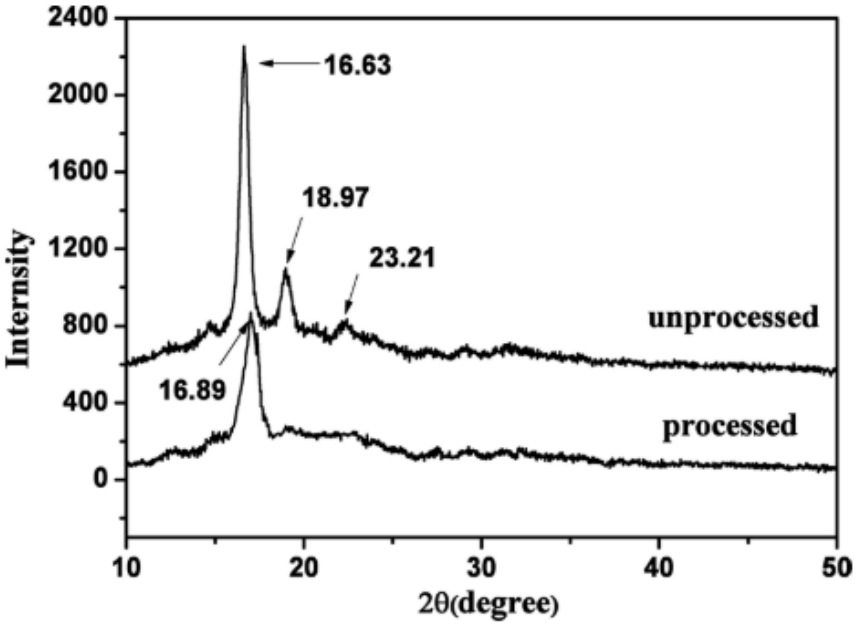

Figure 11 XRD patterns of the PLA–PEG–PLA copolymer [45]

The thermal characteristics were measured by using DSC (Figure 12). The T_m peaks of PLLA and PLLA-PEG-PLLA were in the ranges 174-175 °C [7] and 169-171 °C [7], respectively. The T_{cc} peaks of the PLLA-PEG-PLLA were lower than those of the PLLA. The T_{cc} peaks of PLLA and PLLA-PEG-PLLA were in the ranges 92-97 °C and 72-78 °C [39], respectively.

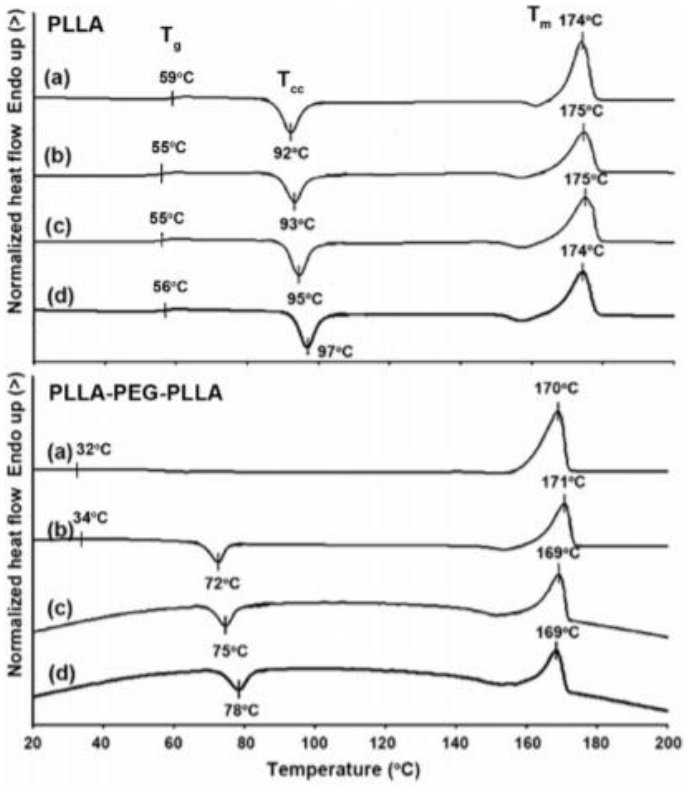

Figure 12 Heating DSC curves of (above) PLLA and (below) PLLA-PEG-PLLA (a) without chain extender and with chain extender contents of (b) 1.0, (c) 2.0 as well as (d) 4.0 phr (T_g, T_{cc} and T_m as shown) [7]

The averaged results of tensile properties including stress at break, strain at break and Young's modulus are clearly compared in Figure 13. It was found that the PLLA films with and without chain extension showed similar stress at break, strain at break and Young's modulus values in the ranges 42–48 MPa, 5–6% and 1642–1757 MPa [7], respectively. Chain extension did not significantly change the mechanical properties of PLLA films. This could be due to all the PLLA films having glassy rigid characteristics because of their high T_g.

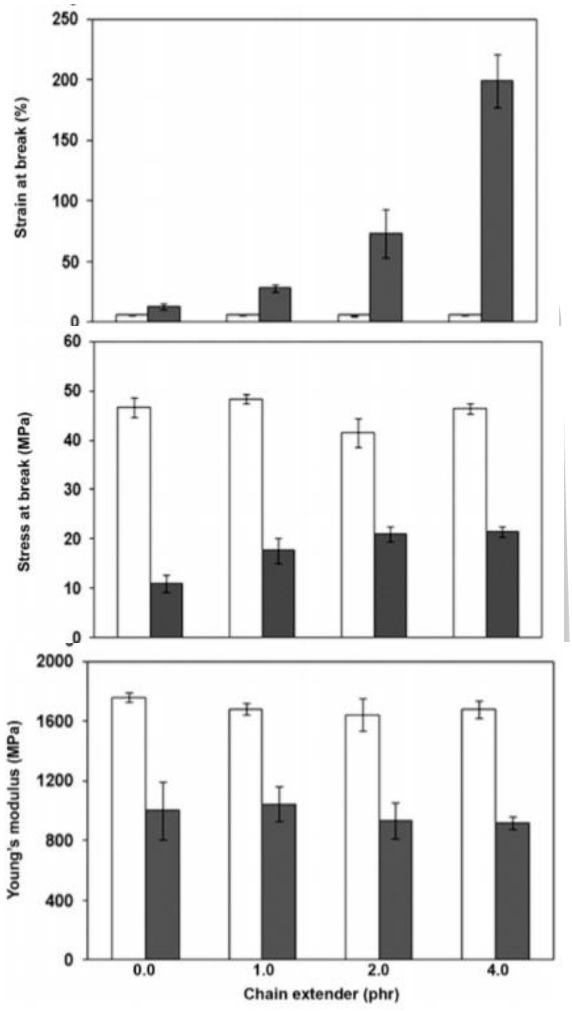

Figure 13 Tensile properties of (□) PLLA and (■) PLLA-PEG-PLLA films with various chain extender contents [7]

2.6 Rice straw

Rice straw is the vegetative part of the rice plant cut at grain harvest or after. It may be burned and left on the field before the next ploughing, ploughed down as a soil improver or used as a feed for livestock [46]. Spatial and temporal distribution of paddy harvested area in Thailand during the crop season of 2015/2016 show in Figure 14 [47] and affect the amount of rice straw as shown Figure 15. It divided by the amount of water.

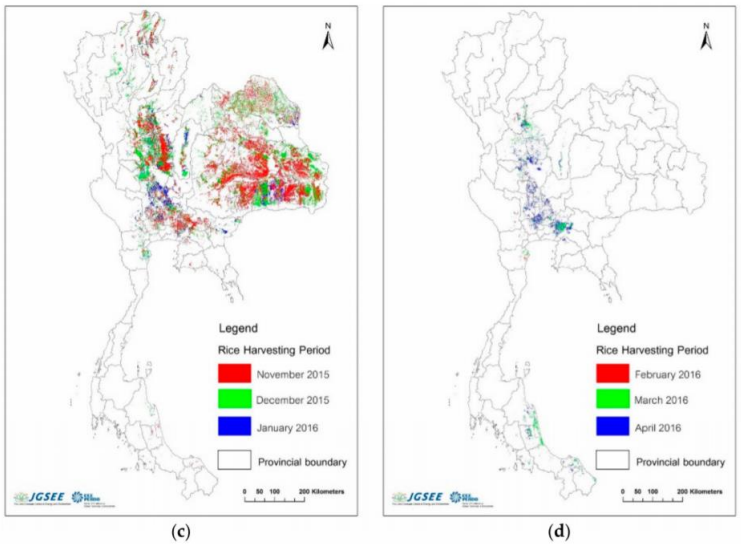

Figure 14 The temporal distribution of paddy reaped area in Thailand during the crop season of 2015/2016: (a) May–July 2015, (b) August–October 2015, (c) November 2015–January 2016, and (d) February–April 2016

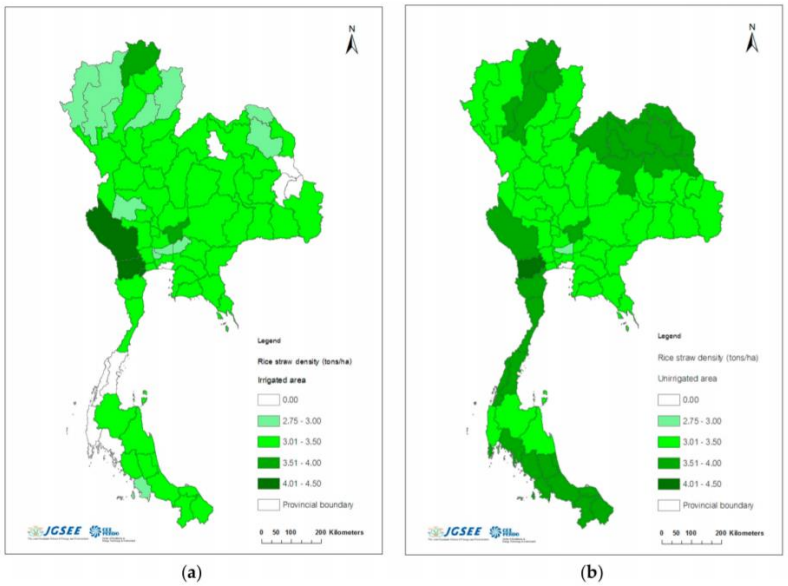

Figure 15 Rice straw density in each province classified by water resource system: (a) irrigated area; (b) rain-fed area

The pattern of rice straw management in each field is presented in Table 3. For the irrigated paddy fields, nearly half of the rice residue (47.2%) was for off-field utilization, whether for personal use or for sales as compost, animal feeding, and mushroom planting. Moreover, approximately 29.7% of the rice residue was open-burned in the field, and about 23.2% was left in the field. The reason for open-burning was to eliminate rice residue in order to prepare the area for the next cultivation. In addition, it was evident that the field with rice residue burning had a lower tillage cost

than the field without rice residue burning by about $19–57 USD/ha, which was primarily due to the difficulty and time consumption of tillage.

Table 3 Percentage share of rice straw management derived from the questionnaire survey [47]

Rice Straw Management	Percent Share of Rice Straw Management (%)									
	Northern		Northeastern		Central		Southern		Whole Country	
Fermentation	21.6	(20.1)	6.9	(11.9)	13.9	(5.4)	31.0	(13.0)	16.5	(12.9)
Animal feed	25.3	(21.3)	38.3	(31.1)	6.2	(13.2)	31.5	(30.2)	12.1	(22.1)
Mushroom plantation	6.5	(4.5)	5.7	(9.8)	0.8	(1.7)	17.1	(6.2)	3.3	(5.3)
Sold to baler operator	14.1	(5.5)	0	(1.7)	15.9	(32.9)	1.0	(3.2)	14.1	(12.5)
Baling and personal use	0.8	(0.9)	0.2	(6.8)	1.5	(2.2)	0.0	(0.0)	1.2	(3.1)
Open-burning	20.3	(26.2)	1.1	(21.2)	35.9	(18.3)	0.0	(2.1)	29.7	(21.4)
Left in the field	11.3	(21.5)	47.7	(17.6)	25.8	(26.4)	18.8	(45.4)	23.2	(22.6)

2.7 Cellulose

Plant (or lignocellulosic) fibers are cellular, complex hierarchical biocomposites designed by nature. Majority of cell walls in plants consists of cellulose, hemicelluloses and lignin (Figure 16, Figure 17) where lignin presents at about 10-25% by dry weight and acts as a binder between cellulose and hemicelluloses components. It is the lignin, which confers the stiffness and strength with its binding function and gives protection to the cell wall. Another two major components of plant cell wall i.e. cellulose and hemicelluloses represents about 35-50% and 20-35% of dry weight of lignocellulosic biomass, respectively. The compositions of different lignocellulosic biomasses are briefly described in Table 4.

Cellulose is the most abundant renewable polymer on earth, and it can be found in plants, algae [48], tunicates [49] and some bacteria. Cellulose is a linear homopolysaccharide (monosaccharides (sugar) monomer) with highly ordered structure of β-1.4-linked anhydro-D-glucose units are shown Figure 18. The quantity, as well as characteristics of cellulose, can vary with the characteristics of sources (e.g. wood contained around 40 to 50% cellulose, and cotton which is 90% cellulose). Tasteless, odourless, as well as hydrophilicity with contact angle 20-300°, are the principal characteristics of cellulose. The crystallinity together with amorphous transition temperature allows it to differ from starch. Cellulose displays higher crystallinity compared to starch, and also amorphous transition temperature is noticed around 320 °C [15] in water because of the crystalline character of cellulose, another hand, starch possesses solely a transition temperature above the 60-70 °C [50] in water. Cellulose exhibits kind of chirality and hydrogen bonds with water, however because of the larger size; it is partially soluble in water and insoluble in the majority of organic solvents.

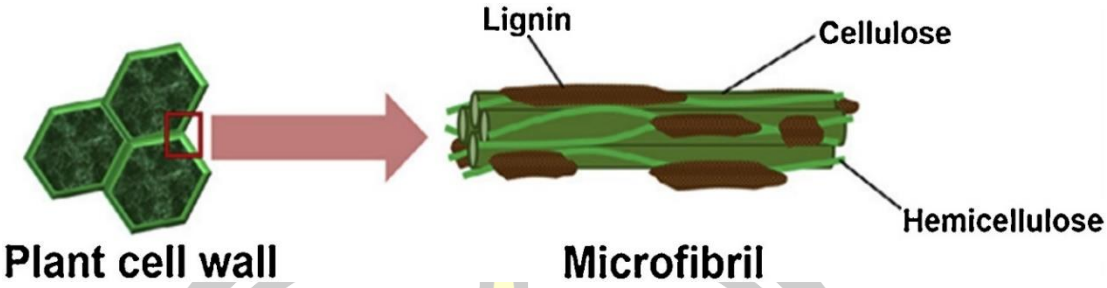

Figure 16 Structure of plant cell wall in lignocellulosic biomass which is consisted of lignin, hemicellulose and cellulose [51]

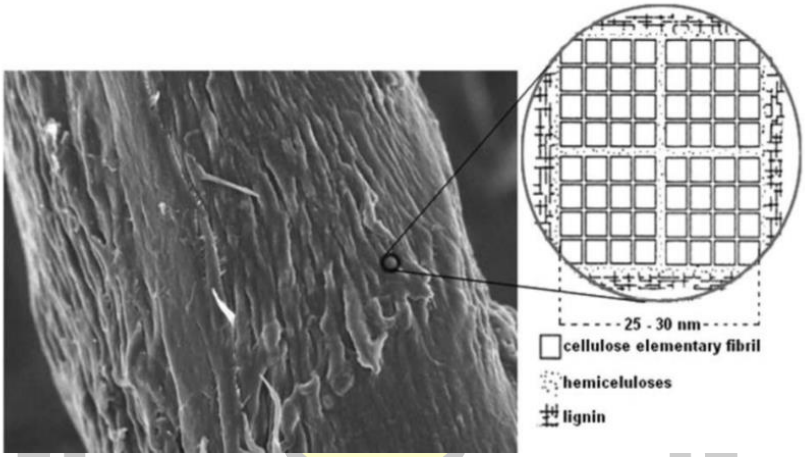

Figure 17 Scanning electron micrograph of a sisal fiber and its organization [52]

Table 4 Chemical composition of lignocellulosic materials from different source[53]

Source	Composition			
	Cellulose	Hemicellulose	Lignin	Extracts, pectin, and waxes
Hardwood	43–47	25–35	16–24	2–8
Softwood	40–44	25–29	25–31	1–5
Pinecone biomass	42–46	27	20–23	4–11
Coconut fiber	31–32	25–26	33–37	5–11
Cotton stalk	48–52	25–27	24–26	2– 4
Sugarcane bagasse	45	30	20–22	3–5
Corncob	28–34	39–47	21–29	5–12
Jute	60	23	16	1
Pineapple leaf	34–40	21–25	25–29	8–10
Wheat straw	37–43	31–37	18–22	2–14

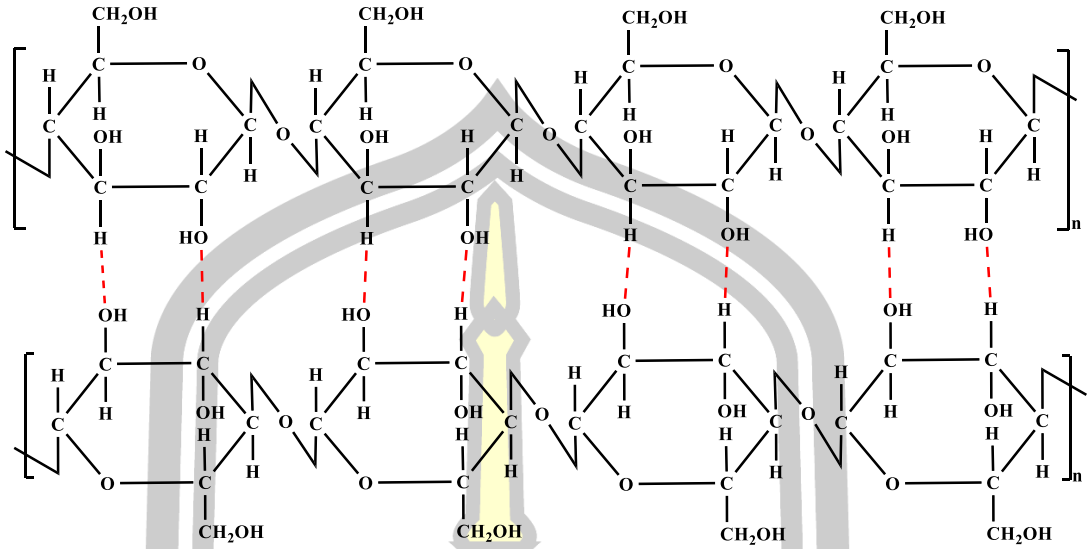

Figure 18 Schematic representation of cellulose [53]

2.8 Nanocellulose

The expression nanocellulose describes the cellulose fibril or crystallite containing at least one dimension in the nanoscale range, and it can be received by means of chemical or mechanical treatment of the wood pulp or plant cellulose and so on [15]. The use of nanocellulose is actually reliant on the structural-properties relationship. To render themselves for the specific application of nanocellulose, they are widely categorized in various sorts including cellulose Microcrystalline cellulose (MCC), Microfibrillated cellulose (MFC), Nanofibrillated cellulose (NFC) [54], cellulose nanocrystals (CNC), nanorods or cellulose whiskers [55] and so on. These types of nanocellulose are obtained by changing their source like as vegetable, lignocellulosic materials, bacterial cellulose, tunicate cellulose, algae cellulose and so forth [56] A summary of the dimension of nanocellulose materials is outlined in Table 5.

Table 5 Dimension of various types of nanocellulose

Cellulose structure	Diameter (nm)	Length (nm)	Aspect ratio (L/d)	Ref.
Microfibrillated cellulose (MFC)	10–40	>1000	100–150	[57]
Microcrystalline cellulose (MCC)	>1,000	>1000	~1	[58]
Cellulose nanofibrillated (NFC)	4–20	>1000	-	[14]
Cellulose nanocrystals (CNC)	5–70	100–250	-	[59]

2.8.1 Nanofibrillated cellulose

Nanofibrillated cellulose (NFC) expression is employed to express fibrils with dimension in the range of nanometric scale that is primarily obtained from wood by means of mechano-chemical treatment of wood pulp. NFC comprises of both individuals as well as aggregated nanofibrils [54] The primary fibril is identified as 3-5 nm in diameter and around 500-1000 nm long, although the aggregated NFC is in the range of 20-50 nm in diameter. Both amorphous and crystalline regions are equally noticed in the NFC. The fundamental dissimilarity between microfibrils and nanofibrils is the fact that, nanofibrillated possess finer diameter in comparison with micro-fibrillated cellulose[60] as shown in Figure 19.

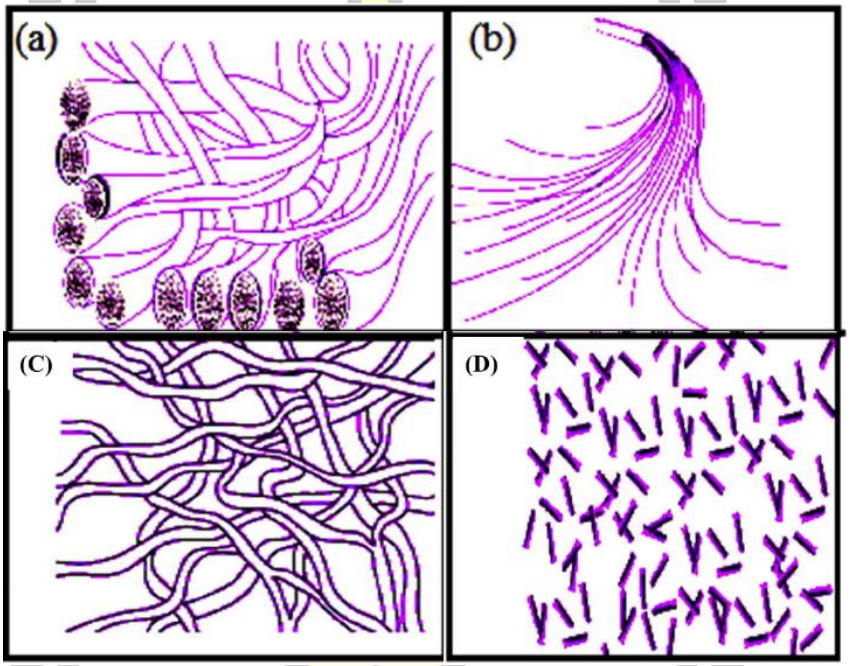

Figure 19 Various types of nanocellulose, a) cellulose fibre, b) microfirbrillated cellulose, c) nanocrystalline cellulose, d) cellulose nanofibrils [61]

2.8.2 Cellulose nanocrystals

The term cellulose nanocrystal describes the rod-like nanocrystal configuration. Acid hydrolysis method is used to eradicate the amorphous regions in the native cellulose, and the remarkably crystalline region in native cellulose is commonly unaltered by acid treatment method producing a rod-like structure as cellulose nanocrystal (CNC) is achieved ultimately referred to as nanocrystalline cellulose or cellulose whiskers as demonstrated in Figure 20. Cellulose nanocrystal bears the wide range of properties including huge surface area, excellent stability, fascinating mechanical (higher specific strength as well as modulus), and also extraordinary optical properties. Cellulose nanocrystal exhibits the comparatively high level of crystallinity around (54-88%) [62]. The dimension of cellulose nanocrystal is dependent upon the nature of the source, and normally, it possesses typical dimension 3-30 nm in diameter as well as 100 nm to 1-2 μm in length. It reveals that all dimensions of cellulose nanocrystalline are actually in the nanometer

size range. Cellulose nanocrystalline has been utilized in the role of mechanical strengthening agents, medicine delivery vehicles, templates in the synthesis of nanocomposite material as well as protein immobilization substrate.

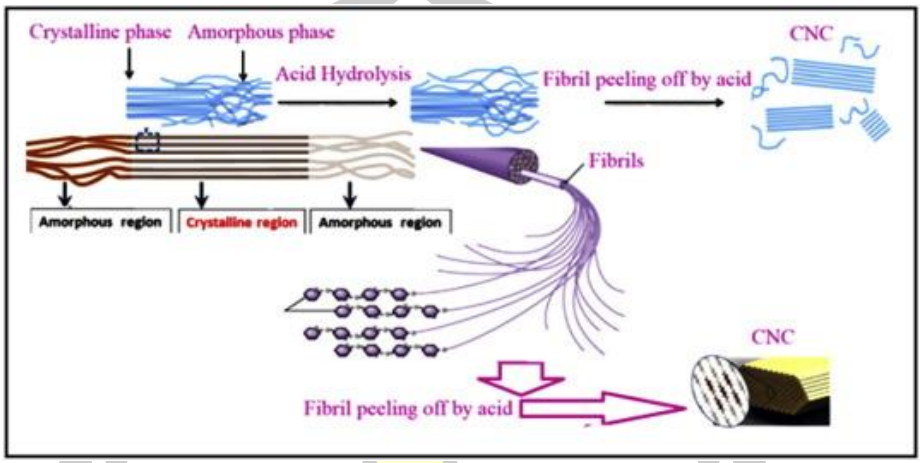

Figure 20 Extraction of cellulose nanocrystal [61]

2.8.3 Extracted from natural cellulose fibers.

The tightly packed cellulose fibrils of lignocellulosic biomass generally have some crystalline region, which gives the strength and stiffness and some amorphous region, which gives flexibility to the plant cells. Nanocellulose is nothing but cellulose in the form of fibers or crystals having length in few micrometers and diameter <100 nm and, which can be extracted from natural cellulose fibers (Figure 21). It is biodegradable, light in weight having density around 1.6 gm/cc with 10 GPa of high tensile strength, which is comparable to cast iron. It also possesses reactive hydroxyl groups which makes it suitable for surface functionalization for use in variety of applications.

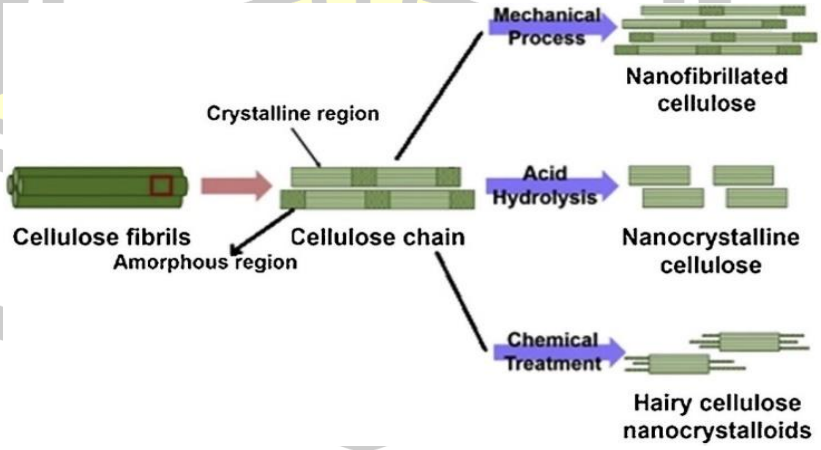

Figure 21 Schematic representation of extraction of nanocellulose from lignocellulosic biomass [51]

2.8.4 Processes for nanocellulose extraction

2.8.4.1 Pretreatment extraction of nanocellulose

The preliminary step for nanocellulose extraction is the pretreatment of lignocellulosic biomass to remove the hemicelluloses and lignin from main cellulosic component. There are two major approaches for biomass pretreatment like alkali treatment and acid-chlorite treatment [10], [51]. Although cellulose is highly abundant in nature, lignocellulosic wastes like agricultural waste and residues are now-a-days the most cited and chosen substrate for nanocellulose extraction to solve the dual purpose of valorization of wastes as well as environmental protection.

2.8.4.2 Alkali treatment

The biomass is treated mostly with sodium hydroxide or potassium hydroide as alkali to remove the amorphous region of hemicelluloses and lignin from the cellulosic fibres. Then the filtrate is washed with water to neutrality and the obtained solid contains mostly the cellulosic part. This pretreatment procedure was described in detail by several researchers and also reported in our earlier publication [51]. The rice straw was soaked in different concentrations of NaOH (8-16%) and then heated to 90°-160 °C for 1-2 h for removal of hemicelluloses and some portions of lignin.

2.8.4.3 Acid-chlorite treatment

The removal of most of the lignin from lignocellulosic biomass is done by combined treatment of sodium chlorite acidified with glacial acetic acid. This process is mostly called as bleaching or delignification process. It is performed with the mixing of distilled water, sodium chlorite, and acetic acid with lignocellulosic biomass at 70-80 °C for 4-12 h. [51, 52]. From that point onward, the blend is continued stirring overnight, followed by washing with distilled water until coming to the neutral pH. The obtained white coloured residues are collected and dried in oven at 50 °C, which is characterized as holocellulose free of lignin. The crystallinity index of nanocrytalline cellulose by used different processes as shown in Table 6.

Table 6 Crystallinity index of nanocrytalline cellulose

	Pre-treatment	Bleaching	Hydrolysis	Crystallinity index (%)	Ref.
2:1 v/v toluene/ ethanol	5%KOH	1.4% NaClO	64–65 wt%H_2SO_4	91.2	[59]
Tap water	10%NaOH	H_2O_2	50wt%H_2SO_4	76.1	[64]
Tap water	12%NaOH	3% $NaClO_2$	10wt%HCl	89.97	[65]
2:1 v/v benzene / ethanol	10%NaOH	1% NaClO	58wt%H_2SO_4	76.99	[66]

2.8.5 The properties of nanocellulose

2.8.5.1 Mechanical properties of nanocellulose

The mechanical properties are tailored via altering the microstructure of micro or nanocellulose as show in Table 7.

Table 7 Mechanical properties of nanocellulose[67]

Type of nanocellulose	Young's modulus (GPa)	Characterization method	Ref.
Cellulose nanofibril	81 ± 12	AFM	[68]
Cellulose nanofibril	100	Tensile testing	[69]
Bacterial Cellulose	114	Raman spectroscopy	[70]
Cellulose nanocrystalline	139.5 ± 3.5	Nono indentation	[71]
Cellulose nanocrystalline	206	Atomic structure model	[72]

2.8.5.2 Thermal properties of nanocellulose

The thermal degradation of lignocellulosic materials starts with an initial decomposition of hemicelluloses, accompanied by an initial phase of pyrolysis of lignin, depolymerization, effective flaming combustion, as well as char oxidation. Additionally, cellulose nanofibrils consist of a very high degradation temperature onset (350 °C) and also much better thermal performance compared to hemicellulose, pectin, and lignin. On the other hand, the onset of the thermal degradation of nanocrystals usually takes place at 200-300 °C [11]. Cellulose nanocrystals with lesser sulfate amount possess more beneficial thermal stability. Alternatively, banana

cellulose nanofibrils displayed three primary weight loss zones. The preliminary weight is a result of moisture evaporation and then thermal depolymerization of hemicellulose additionally the cleavage of glycosidic linkages of cellulose [73]. The broad peak in the part from 200 °C to 500 °C is because of residual lignin components. A convection drying of cellulose nanofibrils eliminates water, gradually leading to the creation of aggregates. As a result, the dried cellulose nanofibrils offer the lesser level of thermal stability in comparison with the original fibres as show in Figure 22 [74].

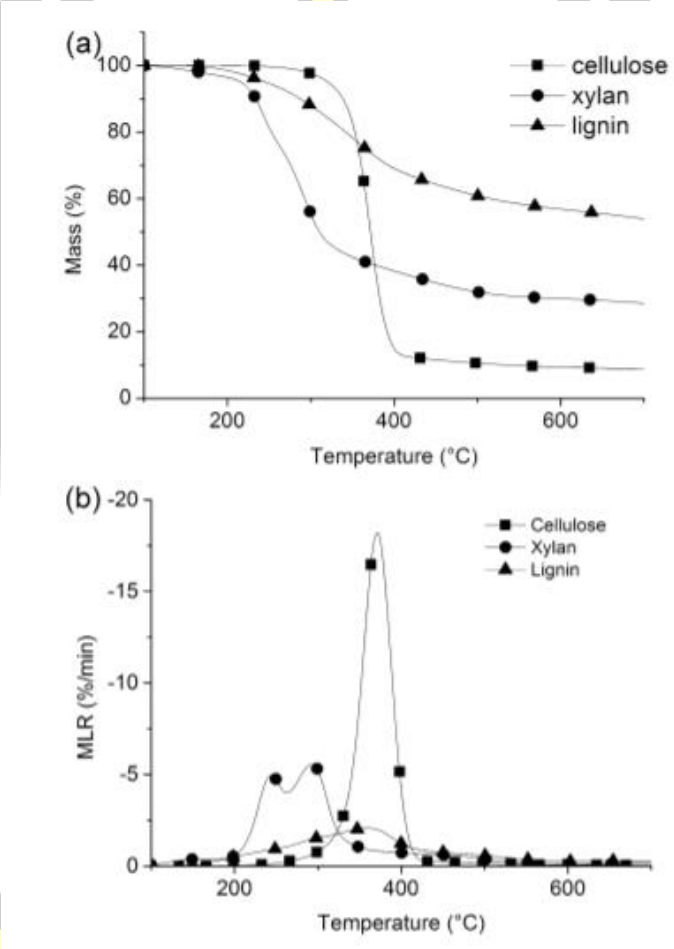

Figure 22 Thermogravimetric analysis: (a) mass and (b) mass loss rate (MLR) versus temperature curves of cellulose, xylan and lignin [75]

2.8.5.3 The crystallinity of nanocellulose

Crystallinity is incredibly influenced by the lignocellulosic source. For example, crystallinity of flax, rutabaga, as well as wood cellulose nanofibres are 59%, 64%, and 54%, respectively, however, a crystallinity of 85.9%, 76%, 84.9%, 94%, 80 .6%, and 81.7% had been basically noticed for cellulose nanocrystals achieved from sisal, rice husk, flax, cotton, corn stover, and commercial microcrystalline cellulose, respectively [16]. Alternatively, degrees of crystallinity of 78% and also 70% have been found for wheat straw and soy hull cellulose nanofibrils, respectively. In-depth, really low values have been seen for beet pulp ~ 30–40% [50]. The degree

of crystallinity levels in the sequence: pineapple > banana > jute, which order confirms with the values of cellulose content identified through these samples. Generally, cellulose nanocrystal that is made from H_2SO_4 possesses lesser crystalline values compared to those made from HCl. Also, the increase in hydrolysis time period improves crystallinity a result of the removal of amorphous regions [52].

2.9 Nanocellulose-based polymer composites

Polymer composites are hybrid materials with one or more particle components (fillers) within a polymer matrix [76]. The addition of micro size filler as reinforcement was heralded in the 60s as a way to prepare polymer materials with improved properties similar tendency using “nano” reinforcement has been observed. Currently, several nanomaterials with different sizes and shapes have been used as reinforcement [68] such as carbon nanotube, graphene, graphene oxide, layeredouble hydroxides , carbon nanofiber and CNCs. Among these nanofillers, the use of CNC as reinforcement in different biodegradable polymeric matrices is a growing area of nanomaterials. This growth stems from the possibility to prepare nanocomposites with improved properties maintaining the biodegradability of the matrix. Nanocellulose-based composites have been prepared mainly by solvent casting, melt mixing and in-situ polymerization.

2.9.1 Thermal properties of nanocellulose-based polymer composites

The effect of nanocellulose on the crystallization and the spherulite growth of biodegradable polymers from the melt have been intensively investigated by differential scanning calorimetry (DSC). Several authors reported that nanocellulose act as nucleating agent, increasing especially the melting temperature (T_m), crystallization temperature (T_c) and degree of crystallinity (X_c) of the polymer. An increase in T_m can be related to the presence of thicker polymer crystalline lamellae. While the decrease of this temperature can result from the crystallization of slightly less perfect polymer crystals. When a nanofiller acts as nucleating agent, usually T_c of the nanocomposite is shifted to a temperature slightly higher than that of the neat polymer, which is directly related to an increased number of heterogeneous nuclei for crystallization [77, 78].

Table 8 Thermal properties improvements for nanocellulose-based polymer composites

Polymer matrix	Filler		T_g	T_m	T_{cc}	X_c	Year	Ref.
PLLA	-		-	171.4	-	14.3	2010	[80]
	CNCs		-	171.8	-	15.0		
	n-docecyldimethylchlorosilane	2	-	171.4	-	20.7		
PLLA	-		43	145.2	-	20.1	2011	[52]
	Acetic anhydride	2	45.3	146.1	-	27.8		
PLLA	-		61	152.6	-	2.9	2013	[81]
	CNCs	2.5	59	152.2	127.7	12.4		
	n-octadecyl-isocyanate		60	149.1	113.1	2.5		
PLLA	-		63.22	175.66	97.54	39.32	2015	[82]
	CNCs		62.35	174.45	94.51	39.33		
	Dodecanoyl (DDC)		63.02	176.14	92.78	39.35		
PLLA	-		55.6	166.1		0.1	2018	[83]
	CNCs		51.7	166.0		3.7		
	3-aminopropyltrimetroxylsilane (APTMS)	5	51.2	167.2		15.4		

2.9.2 Mechanical properties of nanocellulose-based polymer composites

The use of nanocellulose in different polymer matrices to achieve nanocomposites with adequate mechanical properties is important for the better employment of these materials in the different fields where they are used. Several authors studied theoretically the effect of nanocellulose on the mechanical properties of polymer nanocomposites. as show in Table 9

Table 9 Mechanical property improvements for nanocellulose-based polymer nanocomposites.

Polymer matrix	Filler		Tensile modulus (GPa)	Tensile strength (MPa)	Elongation at break (%)	Year	Ref.
PLLA	-		1.1±0.01	48.3±2.9	31.1±3.0	2010	[80]
	CNCs		1.2±0.03	48.3±0.4	12.2±0.2		
	n-docecyldimethylchlorosilane	2	1.4±0.04	53.8±2.1	7.1±1.8		
PLLA	-		2.5	55	4.1	2012	[84]
	CNCs		2.6	40	2.2		
	3-aminopropyltriethoxylsilane (ATS)	15	3.1	45	2.0		
PLLA	-		-	40±1	4.3±0.3	2013	[81]
	CNCs		-	40±1	5.3±0.6		
	n-octadecyl-isocyanate	2.5	-	51±2	5.6±1.2		
PLLA	-		1.2±0.2	33.3±5	-	2015	[85]
	CNCs		2.8±0.3	38.1±1	-		
	3-aminopropyltrimetroxylsilane (APTMS)	5	2.9±0.3	40.3±2	-		
PLLA	-		2.69±3.05	45±2.31	11±8.81	2015	[82]
	CNCs		1.87±2.52	43±3.90	14±1.52		
	3-aminopropyltriethoxylsilane (ATS)	0.5	2.81±0.93	42±2.71	9±6.08		
	Dodecanoyl Chloride (DDC)		1.93±9.87	43±5.48	13±5.87		
PLLA		5	1.8±0.1	57±1	3.3±0.2	2016	[86]

Acetic anhydride	2.1±0.1	62±4	4.3±0.5

2.10 Related research

In 2003, [8] reported that crystallization and phase separation in blends of high stereoregular poly(lactide) with poly(ethylene glycol) The effect of cooling rate on crystallization and subsequent aging of high stereoregular poly(lactide) (PLA) blended with poly(ethyleneglycol) (PEG) was studied by thermal analysis and by direct observation of the solid state structure with atomic force microscopy (AFM). The blend was not stable at ambient temperature. With time, epitaxial crystallization of PEG on the edges of the spherulites depleted the surrounding region of PEG, which created a vitrified region surrounding the spherulites. Further from the spherulites, the homogeneous amorphous phase underwent phase separation with formation of a more rigid PLA-rich phase and a less-rigid PEG-rich phase. Decreasing the amount of PEG in the blend decreased the crystallization rate of PLA and increased the nucleation density.

In 2013, [87] studied the effect of poly(ethylene glycol) (PEG) on the preparation of Poly(lactic acid) (PLA)/PEG blend and its nanocomposites by melt intercalation method .The incorporation of PEG into PLA the tensile strength and modulus decreases, whereas the percentage elongation and impact strength increase predominantly. Further, the PLA/PEG blend nanocomposites showed improved tensile strength and modulus with the addition of oraganoclays into the blend. The addition of PEG into PLA matrix reduces the T_g as well as T_c, which is primarily due to plasticizing effect of the PEG.

In 2016, [62] synthesized CNC-PLLA nanomaterials via in-situ ring-opening polymerization of l-lactide in a suitable organic solvent (DMSO) in the presence of cellulose nanocrystals. The resulting homogeneous nanomaterial consists of CNC with grafted PLLA and low molecular weight free PLLA homopolymer. The CNC-PLA nanocomposite films were transparent and had significantly improved barrier properties relative to neat PLA. Nanocomposite films with only 1 wt.% CNC could improve WVTR and OTR by 81% and 87%, respectively, compared to neat PLA films. This brings the oxygen and moisture barrier performance of CNC-PLA nanocomposite films closer to those of PET, PVC, LDPE and HDPE. Moreover, the crystallinity of CNC-PLA nanocomposites could be tuned by selecting and controlling the processing method. This difference was evident in the improvements gained in the dynamic mechanical properties of CNC-PLA nanocomposites films. The storage moduli for solution-cast and compression-molded nanocomposite films, at the same CNC loading of 2 wt.%, increased by 100 and 29%, respectively The modulus increased by 12% when CNC loading was increased to 5 wt.%, from 40 MPa for solution-cast neat PLA to 480 MPa The schematic synthesis route of CNC-PLA copolymer as shown Figure 23.

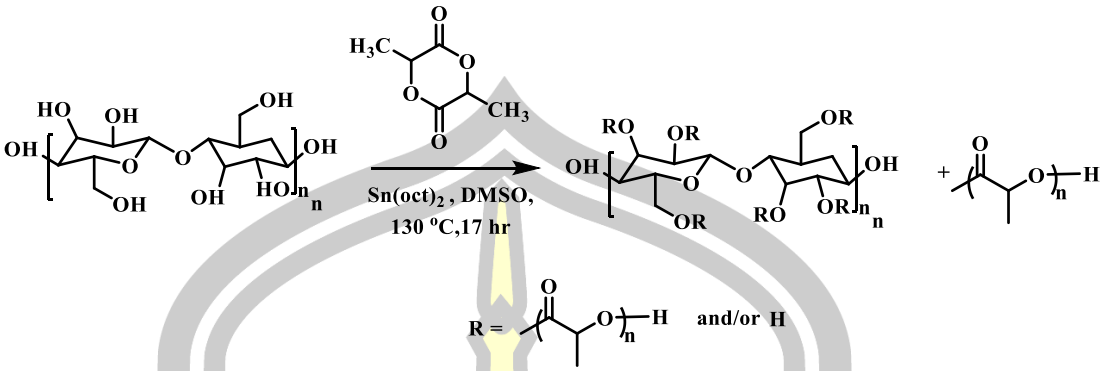

Figure 23 Schematic synthesis route of CNC-PLA copolymer [62]

In 2016, [85] studied the effect of polylactide-graft-cellulose nanocrystals on the thermal and mechanical properties of poly(l-lactide) matrices. Cellulose nanocrystals (CNCs) were grafted with polylactide chains via a solvent-free process by ring-opening polymerization of l-lactide using magnesium hydride as a catalyst. Nanocomposites based on poly(l-lactide) matrix containing ungrafted nanocrystals (PLLA/CNCs) and grafted nanocrystals (PLLA/PLLA-g-CNCs) were investigated. DSC revealed that the grafted nanocrystals exhibited a strong influence on the crystallinity of the nanocomposites, inducing a significant enhancement of the mechanical properties of PLLA/PLLA-g-CNCs compared with PLLA/CNCs material. The role played by the polylactide grafted layer on the interaction between the CNCs and PLLA matrix was revealed by mechanical analyses in the solid and molten states.

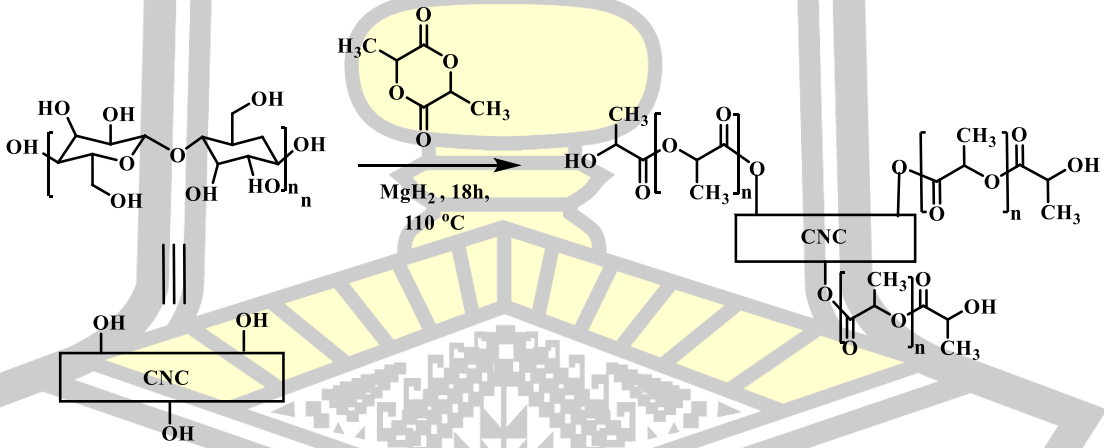

Figure 24 Schematic synthesis route of PLLA-g-CNCs [85]

In 2016, [88] studied CNC nanoparticle which has been successfully grafted with low molecular weight PDLA chains via in situ ring-opening polymerization of the D-lactide monomer. Thus, synthesized CNC-g-PDLA could be dispersed stably in chloroform so that the PLLA/CNC-g-PDLA nanocomposite can be easily prepared via solution casting. The PLLA/CNC-g-PDLA nanocomposites exhibit much faster matrix crystallization rate and enhanced storage modulus above the T_g because the stereocomplex between grafted PDLA and PLLA matrix can serve as not only nucleating agents but also effective interfacial enhancers. More important, the heat distortion resistance of nanocomposite is evident improved due to the stable

interaction between CNC and PLLA, which provide a new way to fabricate advanced PLA-based nanocomposites with optimized properties.

In 2018, [7] poly(L-lactide) or (PLLA) is a biodegradable bioplastic that has been widely investigated for use instead of petroleum-based plastics. However, its practical applications have been limited by its brittleness. Herein, a high molecular weight triblock copolymer of poly(L-lactide)-*b*-poly(ethylene glycol)-*b*-poly(L-lactide) (PLLA-PEG-PLLA) was synthesized by ring-opening polymerization of L-lactide using stannous octoate and PEG as the initiating system. The effect of an epoxy-based chain extender on the thermal properties, melt flow index (MFI), phase morphology and tensile properties of the PLLA-PEG-PLLA were investigated and compared to PLLA homopolymer. Chain-extended PLLA-PEG-PLLA and its films were prepared by reactive melt blending and compression molding, respectively. The flexible PEG blocks significantly improved both crystallization of PLLA blocks and strain at break of PLLA-PEG-PLLA films. The chain extension can decrease MFI of both the PLLA and PLLA-PEG-PLLA but their crystallizabilities were suppressed. All the PLLA-PEG-PLLA films with and without chain extension had no phase separation. The tensile properties of PLLA-PEG-PLLA films increased by the chain extension. The results showed that the chain-extended PLLA-PEG-PLLA have potential for use as highly flexible bioplastics.

CHAPTER 3
RESEARCH METHODOLOGY

3.1 Chemicals and instruments

3.1.1 Chemicals

The chemicals in this research were shown in Table 10.

Table 10 Chemicals

Chemicals	Grade (%)	Supplier
Sodium hydroxide (NaOH)	AR grade	Ajax Finechem
Hydrogen peroxide (H_2O_2)	30-32%	ANaPURE
Sulfuric acid (H_2SO_4)	98%	ANaPURE
Dichloromethane (CH_2Cl_2)	AR grade	Fisher chemical
3-[(2,3-Epoxypropoxy)-propyl]-trimethoxysilane	AR grade	Merck
poly(L-lactide)-*b*-polyethylene glycol-*b*-poly(L-lactide) or PLLA-PEG-PLLA	M_n = 89,900 g/mol [7]	Biodegradable Polymer Research Unit, Depart of Chemistry, Mahasarakham University
poly(L-lactide) or PLLA	M_n =88,400 g/mol [7]	
Rice straw	jasmine rice	Mahasarakham province

3.1.2 Instruments

The instruments in this research were shown in Table 11.

Table 11 Instruments

Instruments	Company	Model
pH Meter	Metrohm	713pH Meter
Sonicator bath	BANDELIN	BN/DT100
Vacuum oven	MMM Group	vacucell
Centrifuge	Sigma	Sigma 6-16 K
Particle size analyzer	Malvern	Zetasizer Nano S9
Attenuated total reflectance fourier	Bruker	TENSOR 27

transform infrared spectrometer (ATR-FTIR)		
Fourier transform infrared spectrometer (FT-IR)	Perkin-Elmer	Spectrum GX
X-ray photoelectron spectrometer (XPS)	Kratos Analytical	AXIS ULTRA DLD
UV-VIS Spectrophotometer	Agilent Technologies	Cary 60
Scanning electron microscope (SEM)	JEOL	JSM-64606V
Transmission electron microscope (TEM)	FEI	Tecnai G2 20
Thermogravimetric analyzer (TGA)	TA-Instruments	TG SDT Q600
Tensile testing machine	Dongguan Liyi Environmental Technology	LY-1066B
Differential scanning calorimeter (DSC)	Perkin-Elmer	Pyris Diamond

3.2 Experiment

3.2.1 Preparation of nanocellulose from rice straw

3.2.1.1 Alkali treatment

Rice straw was cut in length of 1-2 cm, washed 3-4 times with tap water for removing dust before drying at 100 ˚C for 24 h. The ground rice straw (1g/20 ml) was treated with an alkali solution (2M NaOH) [89] under stirring for 1 h. at 80 ˚C. After that, the product was filtered and washed with water until neutral.

3.2.1.2 Bleaching process

After the alkaline treatment process, the product (1g/200 ml) was mixed with 18.5% H_2O_2 for 3 h., then filtered and washed with water until neutral.

3.2.1.3 Acid hydrolysis

The cellulose fibers (1g/10 ml) were hydrolyzed using 64 %H_2SO_4 (v/v) at 45˚C for 0.5 h. according to a previously reported method [59, 90] under constant stirring. The acid hydrolysis product was diluted with cold water to stop the hydrolysis reaction. The suspension was washed 5 times with distilled water by centrifugation (10,000 rpm, 4 ˚C, 15 min) [90, 91] in order to remove the excess of sulfuric acid. The suspension was then dialyzed against distilled water using cellulose membranes with a molecular weight of 12–14 kDa [92] until a constant pH was reached and finally the resulting suspension was sonicated using sonicator (at 45 ˚C, 0.5 h.) to correctly disperse suspended nanocrystals.

The suspension cellulose samples were divided into 2 types for remove water.

1. The suspension cellulose was evaporated oven at 60 ˚C for 12 h. Then, the sample was powdered by grinding.
2. The suspension cellulose was dried by a freeze-dry machine and then the cellulose samples were stored in a desiccator.

3.2.1.4 Modified nanocellulose

The step I, In the process of preparation silanols, the silanols was prepared by adding water to [3-(2,3-Epoxypropoxy)-propyl]-trimethoxysilane [12] and then adding 95% ethanol under stirring for 30 minutes. The step II, coupling agents were prepared by reaction of silanol (2%v/v) and nanocellulose (1 g) under stirring for 2 h. and then oven at 120 ˚C for 2 h., The suspension was washed with distilled water using centrifuge at 3,500 rpm for 30 min (5 times) and oven at 105 ˚C for 12 h. The modified nanocellulose powder was stored in a desiccator. These two steps are in Figure 25.

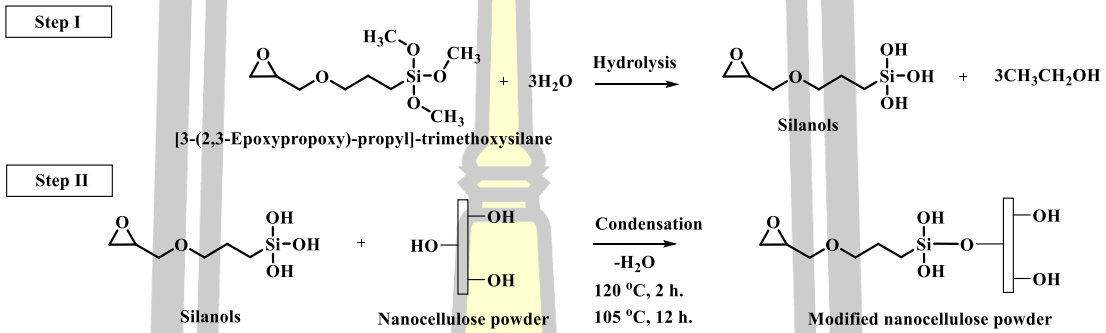

Figure 25 the schematic method for modified nanocellulose [12]

3.2.2 Fabrication of PLLA/nanocellulose, PLLA/modified nanocellulose, PLLA-PEG-PLLA/nanocellulose and PLLA-PEG-PLLA/modified nanocellulose composite films

The polymer matrix (PLLA and PLLA-PEG-PLLA) was dissolved in 10 ml, dichloromethane before mixing nanocellulose and modified nanocellulose for 0.5 h. under stirring. The suspension was poured on the petri before drying room temperature, 12 h. After that, composite films were perfumed by vacuum oven at room temperature for 24 h. The ratio of composite films in this research were 1, 3, and 5 %wt.

3.3 Characterization of nanocellulose and modified nanocellulose

3.3.1 Particle size analyzer

The average particle size and size distribution of the nanocellulose and modified nanocellulose were evaluated by a particle size analyzer in water medium.

3.3.2 Attenuated total reflectance fourier transform infrared spectrometer

Fourier transform infrared spectroscopy (FTIR) spectra were recorded over the 600 cm^{-1} - 4000 cm^{-1} range, at room temperature, employing a diamond attenuated total reflection (ATR) crystal.

3.3.3 Fourier transform infrared spectrometer

Fourier transform infrared spectroscopy (FTIR) spectra were recorded over the 400 cm^{-1} - 4000 cm^{-1} range, at room temperature. The nanocellulose and modified nanocellulose were mixed with KBr powder and then pressed into thin pellets.

3.3.4 X-ray photoelectron spectrometer

The X-ray photoelectron spectrometer (XPS) measurements were analyzed to investigate the surface chemical changes of the nanocellulose and modified nanocellulose, was excited with X-ray hybrid mode 700 × 300 µm spot area with a Mono (Al (Mono)) (150 W).

3.3.5 X-Ray diffractometer

The study of the crystallinity of the nanocellulose and modified nanocellulose were measured using X-ray diffractometer (XRD) at room temperature using CuKα radiation at 40 kV and 40 mA. For XRD, the scanning angle range of 2θ = 5°– 40° at a scan speed of rate 0.2 degrees/sec was used to determine the crystalline structures.

The crystallinity index, CrI was determined using Segal's formula as given below [93, 94].

$$CrI(\%) = \frac{I_{002} - I_{am}}{I_{002}} x100 \quad (1)$$

Where I_{002} is the overall intensity of the peak at 2-theta about 22.5°, I_{am} is the intensity of the baseline at 2-theta about 15.7°

3.3.6 Scanning electron microscope

The morphology of nanocellulose and modified nanocellulose were analyzed using scanning electron microscope (SEM). The nanocellulose and modified nanocellulose coated with gold to enhance conductivity before scanning.

3.3.7 Transmission electron microscope

The morphological and structural of nanocellulose and modified nanocellulose were studied using transmission electron microscope (TEM). For prepared, the nanocellulose and modified nanocellulose (20 µL) were dropped on parafilm. then, formvar/carbon mesh grid 300 mesh dully side was on the nanocellulose and modified nanocellulose for 5 min. The grid was moped using a triangle filter paper, washed the grid (2 drops of distilled water), and then adding 2% Uranyl acetate on the grid for 1 min. After that, the grid was stored in desiccator cabinet for 24 h. and was studied with TEM at a potential of 200 KeV.

3.3.8 Thermogravimetric analyzer

The thermal properties of nanocellulose and modified nanocellulose were carried out using thermogravimetric analyzer (TGA). The sample was heated from 50 ˚C to 800 ˚C at a rate of 20 ˚C /min under a nitrogen gas purge.

3.3.9 Differential scanning calorimeter

Thermal properties of nanocellulose and modified nanocellulose were determined with differential scanning calorimeter (DSC) under a nitrogen gas flow. The nanocellulose and modified nanocellulose were weighed about 3-5 mg and were held at 200 °C for 2 min to remove thermal history. For heating DSC thermograms, the nanocellulose and modified nanocellulose were heated from -10 to 205 °C at a rate of 10 °C/min. and cooling DSC thermograms, the sample was held at 205 °C for 1 min to remove thermal history before cooling to -10 °C at a rate of 10 °C/min.

3.4 Characterization of PLLA/nanocellulose, PLLA/modified nanocellulose, PLLA-PEG-PLLA / nanocellulose and PLLA-PEG-PLLA/modified nanocellulose composite films

3.4.1 UV-Vis spectrophotometer

The transmittance of composites films (according to ASTM D1746 - 03) were measured using UV-Vis spectrophotometer. The spectral wave range was analyzed from 200 nm to 800 nm [86,87].

3.4.2 Fourier transform infrared spectroscope

The composite films were performed using a fourier transform infrared spectroscopy (FTIR) spectra were recorded over the 600 cm^{-1} - 4000 cm^{-1} range, at room temperature, employing a diamond attenuated total reflection (ATR) crystal.

3.4.3 X-ray diffractometer

The study of the crystallinity of the composite films was measured using X-ray diffractometer (XRD) at room temperature using CuKα radiation at 40 kV and 40 mA. For XRD, the scanning angle range of $2\theta = 5° – 40°$ at a scan speed of rate 0.2 degrees/sec. was used to determine the crystalline structures.

3.4.4 Scanning electron microscope

Scanning electron microscope (SEM) was used to study surface and morphology (shape, pattern, size) of the composite films. For the surface of composite films were cut 1x1 cm. While the cross-section of the composite films was immersed in liquid nitrogen for 30 min. and deducted. Then, the composite films were coated gold for 15 min.

3.4.5 Differential scanning calorimeter

Thermal properties of composite films were determined with differential scanning calorimeter (DSC) under a nitrogen gas flow. The composite films were weighed about 3-5 mg and were held at 200 °C for 2 min to remove thermal history. For heating DSC thermograms, the composite films were heated from -10 to 205 °C at a rate of 10°C/min. and cooling DSC thermograms, the sample was held at 205 °C for 1 min to remove thermal history before cooling to -10 °C at a rate of 10 °C/min. The degree of crystallinity from DSC (X_c, DSC) of the PLLA blocks was determined from the enthalpies of melting (ΔH_m) and cold crystallization (ΔH_{cc}) using Eq. (2).

$$X_c,\text{DSC } (\%) = [\Delta H_m - \Delta H_{cc}]/[93.7 \times W_{PLLA}]x100 \quad (2)$$

where the enthalpy of melting for X_c, DSC = 100% of the PLLA was 93.7 J/g [7]. The W_{PLLA} was the weight fraction of the PLLA obtained from 1H NMR that was 1.0 and 0.83 for the PLLA and PLLA-PEG-PLLA respectively.

3.4.6 Thermogravimetric analyzer

The thermal properties of composite films were carried out using thermogravimetric analyzer (TGA) and heated from 50 °C to 800 °C at a rate of 20 °C /min. under a nitrogen gas purge.

3.4.7 Tensile testing

The mechanical properties of the composite films were made on a universal testing machine (ASTM D882) at room temperature. The sizes of the composite films were 1 × 8 cm., gauge length 25 mm and cross-head speed 50 mm/min. (repeat 5 times).

3.4.8 Water absorption

The water absorption tests were to ASTM D570. The composite films were dried in an oven at 50 ˚C for 24 h until constant weight. The composite films were immersed in distilled water at 25 ˚C. after absorbing for a specific period, the absorption water on the surface of the specimen was removed with filter paper, weighed again and the water absorption was calculated using the equation [97, 98]:

$$\text{Water absorption (w/w)} = \frac{W_2 - W_1}{W_1} \quad (3)$$

Where W_1 is weight of the dry film before immersion and W_2 is weight of the film after immersion.

3.5 Data analysis

The data from characterization composite films analysis tensile testing were carried out in n = 5. The data was analyzed using descriptive statistics (mean, standard deviation).

3.6 Abbreviation

Table 12 abbreviation in this research

Name	Abbreviation
Nanocellulose	NC
Modified nanocellulose	modified NC
Poly(L-lactide)	PLLA
Poly(L-lactide)-*b*-poly(ethylene glycol)-*b*-poly (L-lactide)	PLLA-PEG-PLLA

CHAPTER 4
RESULTS AND DISCUSSION

4.1 Characterization of nanocellulose and modified nanocellulose

4.1.1 Physical appearances

The physical appearances of the rice straw from jasmine rice in the Mahasarakham province are shown in Figure 26 including, alkali-treated rice straw, bleached rice straw, NC and modified NC. The physical characteristics of rice straw displayed large fibers and dark in color. The hemicellulose and lignin composition in rice straw were eliminated using sodium hydroxide and hydrogen peroxide that changed the texture of the powder and also changed the color to white (Figure 26 b, c) [59, 99] Figure 26 d presented small size of the fibers after adding sulfuric acid. The results might be attributed to sulfuric acid, which eliminated amorphous regions by (hemicellulose and lignin) [90]. The modified NC was modified using 3-[(2,3-Epoxypropoxy)-propyl]-trimethoxysilane [100] produced exhibited more white powder than NC are shown in Figure 26 e. Similar results were obtained by Chieng *et.al* [101] and Evans *et.al* [102] who studied the extraction and characterization of cellulose nanocrystals from oil palm mesocarp fiber and sugarcane bagasse. This study found that raw material changed its color when chemically treated especially with the bleaching agent.

Figure 26 Physical appearances of rice straw (a), alkali-treated rice straw (b), bleached rice straw (c), NC (d) and modified NC (e)

4.1.2 Attenuated total reflectance fourier transform infrared spectrometry analysis

The cellulose was successfully isolated from cleaned and dried rice straw powder through a straightforward three-step de-waxing, de-lignification and hemicellulose removing process. The brown color of the rice straw powder reduced with each step of delignification and hemicellulose removal to become pure white. The resultant white product was confirmed to be cellulose by ATR-FTIR spectra. Figure 27 and table 9 demonstrates the ATR-FTIR spectra for rice straw, alkali-treated rice straw, bleached rice straw, NC and modified NC obtained from rice straw cellulose. Figure 27 a, the broad peaks at 3100-3500 cm^{-1} indicate the O-H stretching

bonds while the peaks around 2800-2950 cm^{-1} indicate the C–H stretching, 1724 cm^{-1} corresponds to C=O bond which is normally found in the linkages of the esters in the hemicellulose and lignin. The peaks observed around 1600-1700 cm^{-1} indicates the aromatic ring found in the lignin. The peaks between 1200-1300 cm^{-1} depicts an out of plane C–O stretching in the aryl group of the lignin linked to the rice straw before chemical modification. The absorption band at around 1600-1700 cm^{-1} was attributed to hemicellulose and decreased in intensity in the spectrum of alkali treated rice straw Figure 27 b. The spectra also clearly verified the sequential and complete removal of lignin (1516 cm^{-1}, aromatic skeletal vibrations) in de-lignification (Figure 27 d).The peak at 700-1250 cm^{-1} was assigned to Si-O or Si-O-Si [103] high intensity, when addition filled with 3-(2,3-Epoxypropoxy) propyltrimethoxysilane.

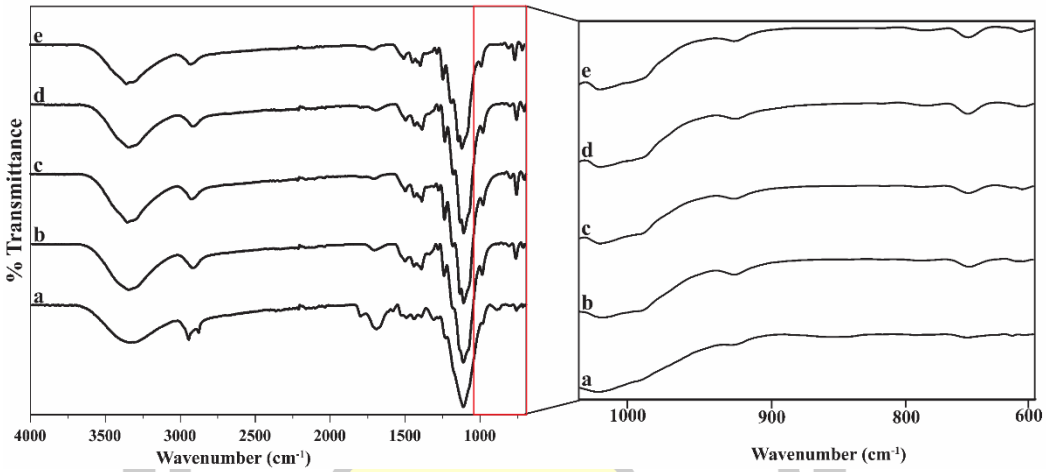

Figure 27 ATR-FTIR analysis of rice straw (a), alkali-treated rice straw (b), bleached rice straw (c), NC (d) and modified NC (e)

Table 13 ATR-FTIR wavenumber of rice straw, alkali-treated rice straw, bleached rice straw, NC and modified NC

Wavenumber (cm^{-1})	**Functional group**	
3327	OH stretching intramolelar hydrogen bonds	Cellulose
2918	C-H stretching	Cellulose
1724	C=O stretching of acetyl or carboxylic acid	Hemicellulose and Lignin
1627	C=C stretching of the aromatic ring	Lignin
1465	Asymmetric bending in CH_3	Lignin
1430	-CH_2 bending	Cellulose
1375	C-H bending	Cellulose
1315	-CH_2 wagging	Cellulose
1245	C–O stretching	Hemicellulose and Lignin
1158	C-O-C asymmetric stretching	Cellulose
1250-700	Si-O or Si-O-Si	3-(2,3-Epoxypropoxy) propyltrimethoxysilane

4.1.3 Fourier transform infrared spectroscopy analysis

The FTIR spectra of NC and modified NC are shown 28. The NC showed three dominant spectra at 3350 cm^{-1}, 2850 cm^{-1} and 1050 cm^{-1} (Figure 1(a)) which are associated with the stretching vibration of hydroxyl group (OH), alkyl chain (CH) and (C-O). The NC was modified by 3-(2,3-Epoxypropoxy) propyltrimethoxysilane, which displayed 3350 hydroxyl group (OH), 2850 alkyl chain (CH) and 1050 cm^{-1} (C-O) as well as NC. The new band 700-1250 cm^{-1} was assigned to Si-O or Si-O-Si thus, confirmed modified NC. The Si-O-C band observed in NC which might be impurities silica in the component of rice straw[104]. This result is consistent with previous research [11].

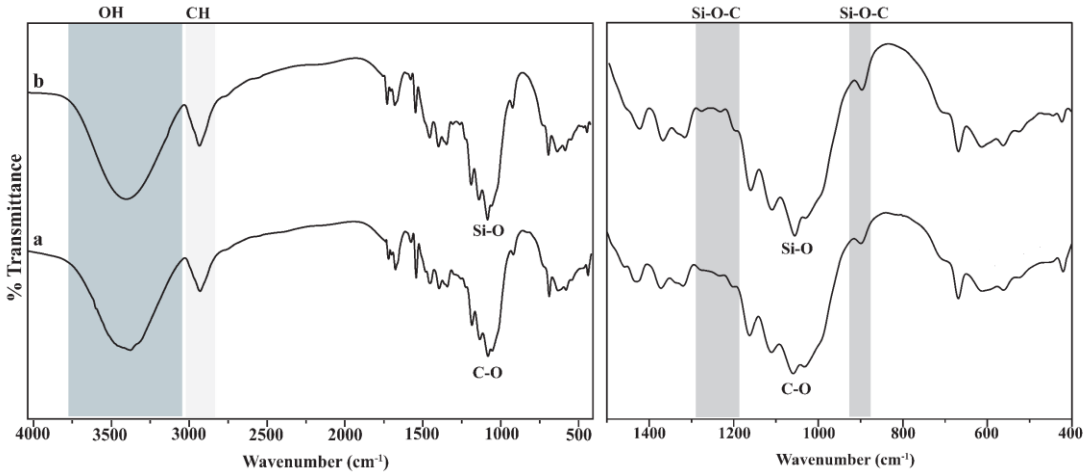

Figure 28 FTIR spectra of pure NC (a) and modified NC (b)

4.1.4 X-ray photoelectron spectroscopy analysis

The XPS analysis of NC and modified NC are shown in Figure 29 and Table 14. The Si 2p modified NC displayed two types of silicon bonds location at Si-O-Si (~103 eV) and SiO_3 (~104 eV), which was according to Figure 28. Thus, confirmed modified NC. The C1s XPS peak of NC was divided into three C peaks: C1 (~285 eV, 27.6%) associated with C-C/C-H linkages, C2 (~286 eV, 57.3%) associated with C–O of alcohols and ethers and C3 (~288 eV, 15.1%) associated with O-C-O. The C1s XPS peak of modified NC displayed three peaks C1 (~285 eV, 19.0%, C2 (~286 eV, 63.8%) and C3 (~288 eV, 17.1%), which increased C1 and C2 and decreased C1 [83, 100, 105].

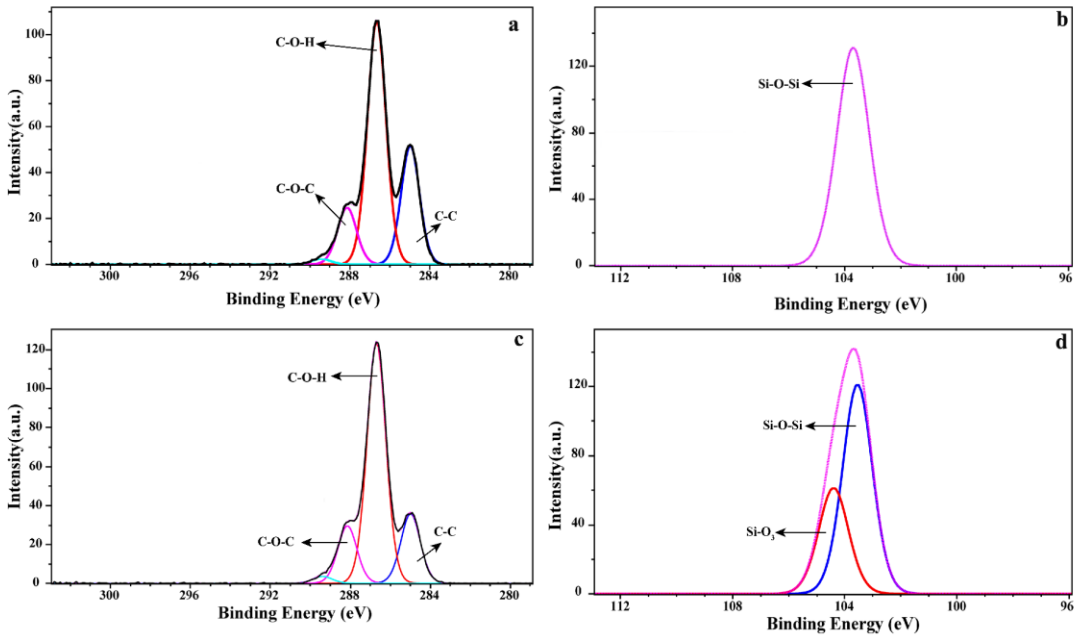

Figure 29 High-resolution XPS spectra of C1s, Si2p for NC (a,b) and modified NC (c,d)

Table 14 Surface group composition of NC and modified NC analyzed by C 1s XPS

Sample	C-C	C-O-H	C-O-C
BE (eV)	285	286.7	288.1
NC	27.6	57.3	15.1
modified NC	19.0	63.8	17.3

4.1.5 Scanning electron microscopy analysis

The surface morphologies of rice straw (a,f), alkali treatment (b,g), bleaching treatment (c,h), acid hydrolysis of cellulose (d,i) and modified NC (e,i) are shown in Figure 30. The morphology of the rice straw displayed large fibers (Figure 30a,f) [66]. When addition alkali into rice straw, could that the fiber appeared smoother on surface than the raw rice straw [59]. The results after bleaching treatment showed small and smooth fibers than the alkali-treated rice straw (Figure 30c,h). Figure 30 d,g exhibited small rod-like fiber and smooth on surface [106] when addition sulfuric acid. The modified NC (Figure 30e,j) showed smaller rod-like fiber and more organized than nanocellulose [13, 81].

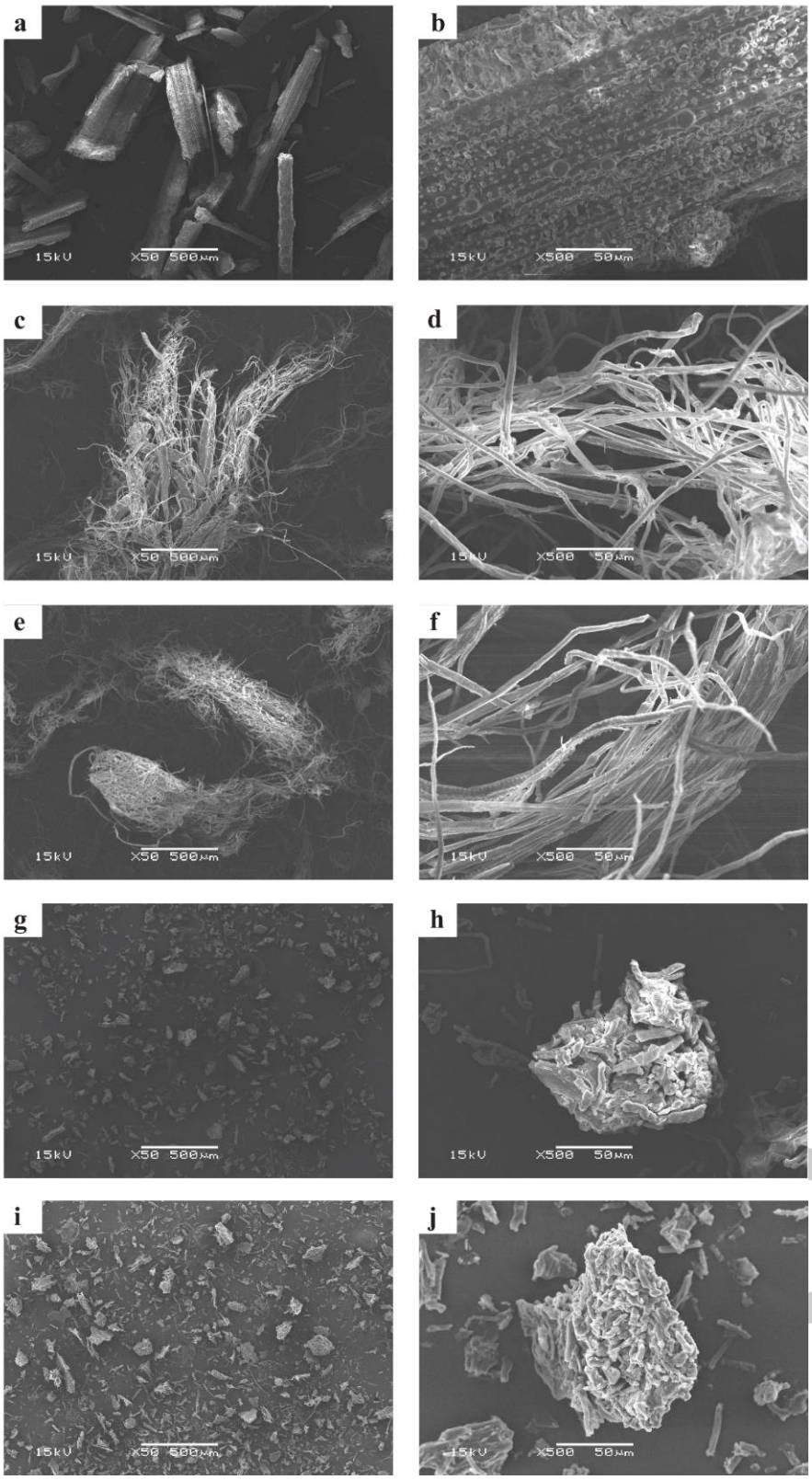

Figure 30 SEM images of rice straw (a,b), alkali-treated rice straw (c,d), bleached rice straw (e,f), NC (g,h) and modified NC (i,j)

4.1.6 Transmission electron microscopy analysis

TEM was used to observe the morphology of the NC and modified NC produced. The TEM of NC and modified NC are shown in Figure 31. The spherical NC by acid hydrolysis was displayed diameter 30.22±1.7 nm. While modification NC was showed spherical nanoparticle, diameter 35.53±1.6 nm and agglomeration of them. The high diameter of modified NC because 3-(2,3-Epoxypropoxy) propyltrimethoxysilane demonstrated coating on surface NC. The agglomeration of NC and modified NC occurred because the large amount of intermolecular hydrogen bonds of cellulose. The spherical NC by acid hydrolysis was previously reported [107, 108].

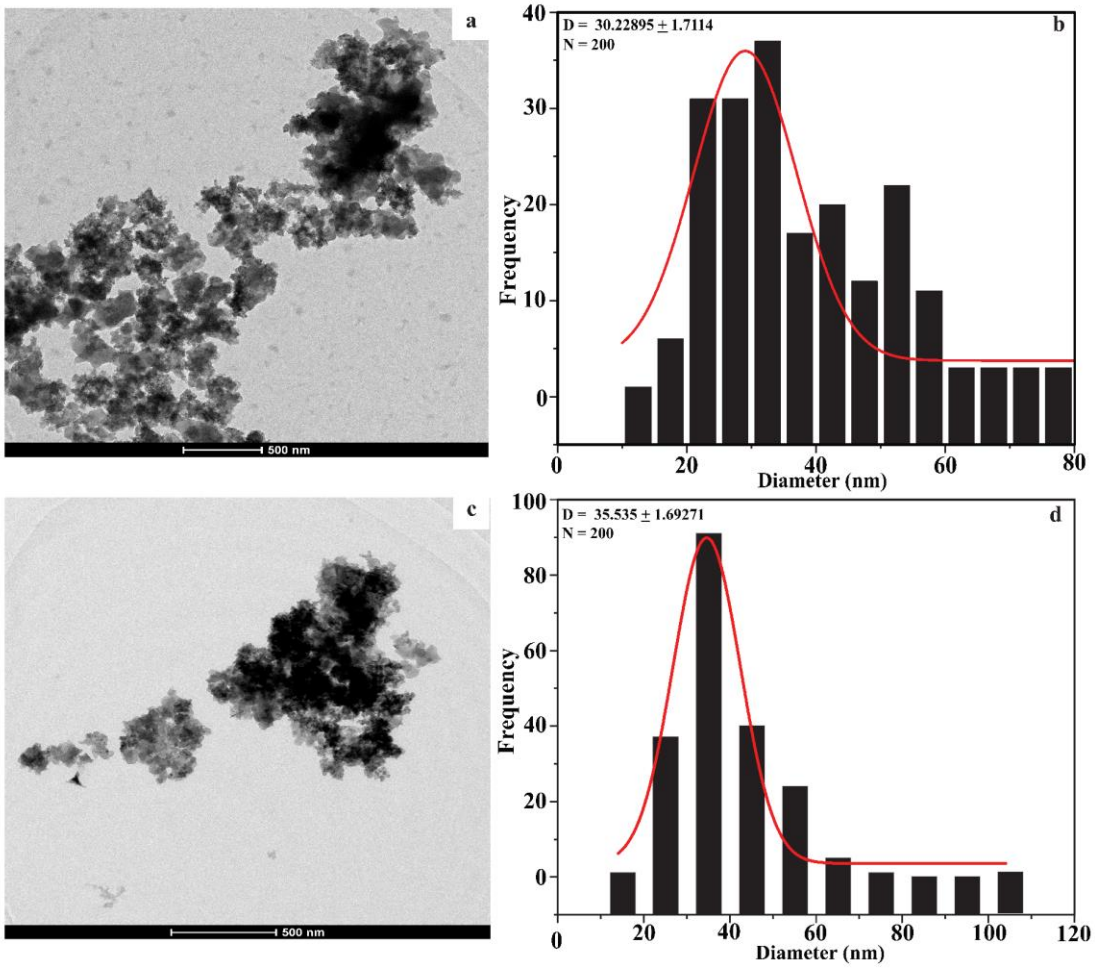

Figure 31 TEM images of NC (a,b) and modified NC (c,d)

4.1.7 X-ray diffractometry analysis

The XRD patterns of the bleached rice straw, NC and modified NC are shown below in Figure 32. The crystallinity index of bleached rice straw, NC and modified NC was calculated from the XRD. The bleached rice straw, NC and modified NC exhibited three main characteristic peaks around a 2θ value of 15.7°, 22.8°, and 34.7° respectively, which are characteristic of cellulose's crystal structures [59], [90], [94].

The degree of crystallinity of bleached rice straw, NC and modified NC are shown in Table 15. The NC and modified NC showed a higher degree of crystallinity than bleached rice straw due to the reduction and removal of amorphous non-cellulosic compounds, such as lignin and hemicellulose induced by bleaching, alkali and hydrolysis treatments conducted in the purification process. After acid hydrolysis the crystallinity index of NC and modified NC was observed 58.3% and 59.9%, respectively [59, 66, 94].

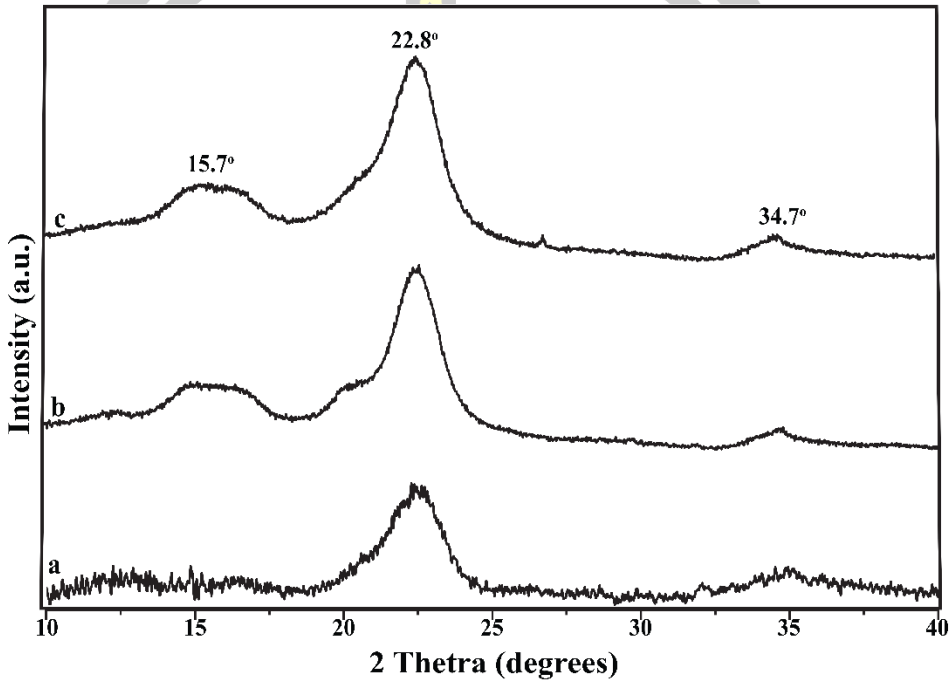

Figure 32 XRD analysis bleached rice straw (a), NC (b) and modified NC (c)

Table 15 Crystallinity of bleached rice straw, NC and modified NC

Sample	Intensity at 15.7° (I_{am})	Intensity at 22.8° (I_{002})	Crystallinity Index (CrI %)
bleached rice straw	412	559	26.9
NC	2229	5569	59.9
modified NC	2630	6309	58.3

4.1.8 Thermogravimetric analysis

TGA and DTG thermograms of rice straw, alkali-treated, bleached rice straw NC and modified NC are shown in Figure 33. The thermal degradation of rice straw showed a multi-stage process following different non-cellulosic and cellulosic components. The TGA of all samples exhibited small initial mass loss around 100 °C from evaporation of adsorbed moisture, followed by the most significant mass loss due to decomposition mass loss from burn. The following phase of degradation starts

at 250-290 °C [50] which is brought about by the thermal depolymerization of hemicelluloses and the breakdown of glycosidic linkages of cellulose. The third phase of degradation liable displayed with the lignin (250-420 °C) [91], which decomposes over a more extensive temperature range than cellulose and hemicellulose. The temperature where maximum weight loss occurs, as temperatures of maximum decomposition rate (Td_{max}) are shown in Table 16. The Td_{max} displayed 320 °C, 292 °C, 295 °C for rice straw, de-hemicellulose and lignin respectively, decreased thermal stability. While NC and modified NC showed higher thermal stability than de-hemicellulose(b), lignin(c) and rice straw(a) due to an increase in crystallinity and intermolecular hydrogen-bonded domains after the removal of amorphous components (hemicellulose and lignin). The results of this study correspond to the results of XRD.

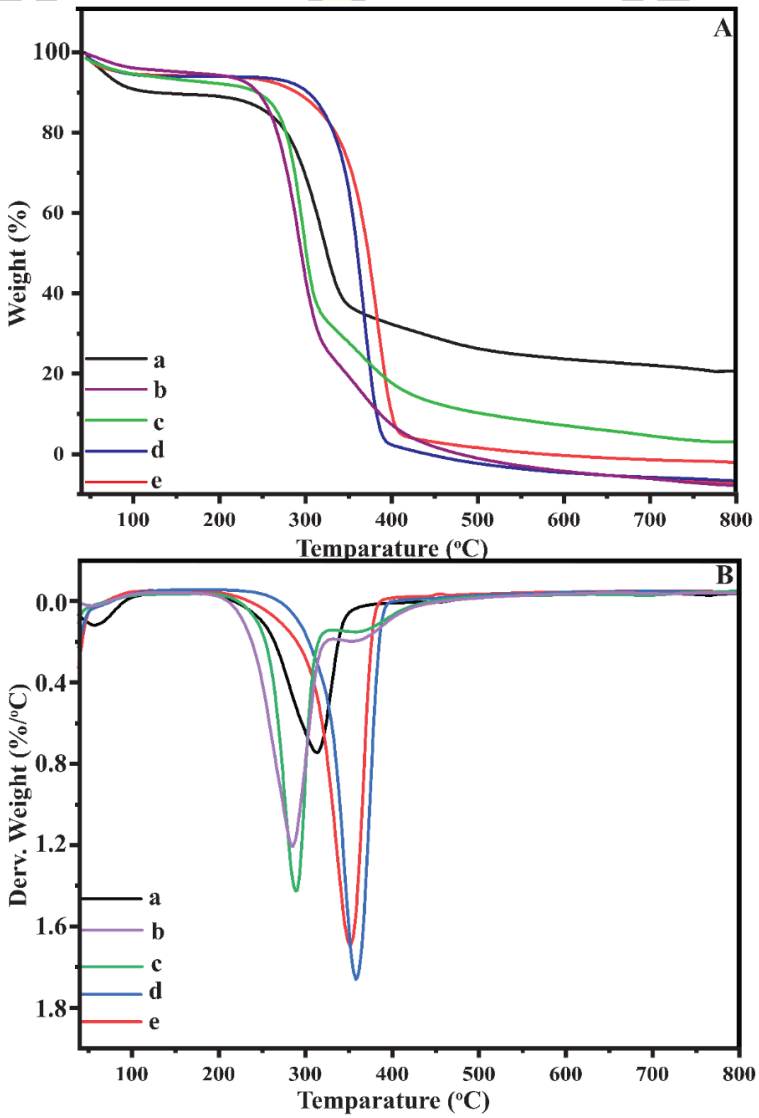

Figure 33 TGA(A) and DTG (B) curves of rice straw (a), alkali-treated rice straw (b), bleached rice straw (c), NC (d) and modified NC (e)

Table 16 TGA analysis of rice straw, alkali-treated rice straw, bleached rice straw, NC and modified NC

Samples	$T_{d, max}$ (^{o} C)	Residue at 600 ^{o}C (%)
rice straw	320	32.7
alkali-treated rice straw	292	10.1
bleached rice straw	295	11.8
NC	366	21.4
modified NC	360	22.4

4.1.9 Particle size analysis

The particle average size and distributions of NC and modified NC from two different materials are shown in Figure 34. Figure 34a displayed the particle average size of NC from rice straw 50-91 nm and 225-396 nm, respectively. While, modified NC (Figure 34b) showed a particle size in average 225-396 nm. as more uniformity than that of the NC. The single peak was observed in modified NC because of poor dispersion of them in the water medium (affected agglomeration) [94].

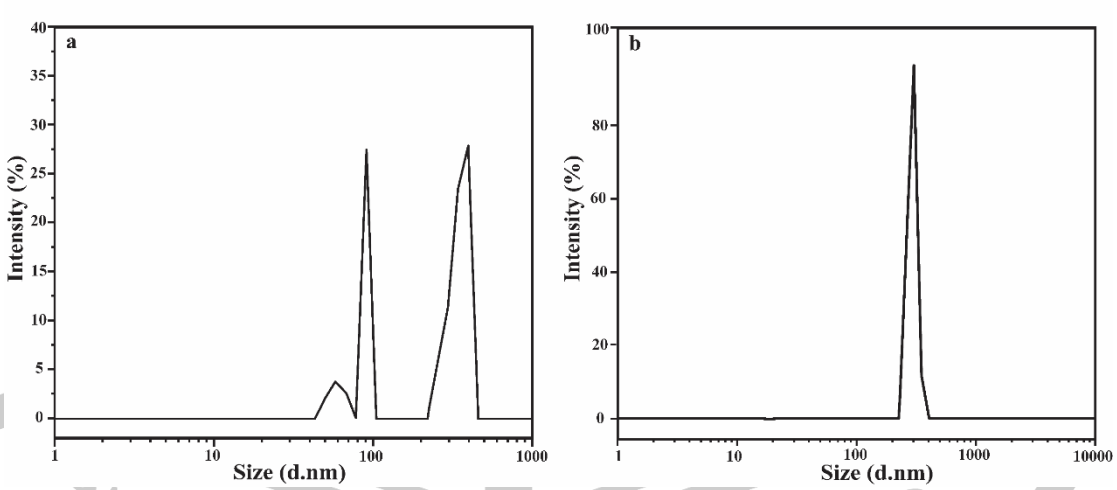

Figure 34 Particle size of NC (a) and modified NC (b)

4.2 Characterization of PLLA/NC and PLLA/modified NC composite films

4.2.1 Physical appearances

The effect of NC and modified NC composites on the film transparency was studied by varying the filler contents (1%, 3% and 5%wt) are shown Figure 35. Addition NC, the composite films exhibited decrease transparent while increasing modified NC the composite films displayed slightly decreasing transparent. Moreover, both composite film series appear with more opacity as a translucent material due to the light scattering effect of NC and modified NC in film matrixes. The findings of this research are consistent with previous [109].

Figure 35 Physical appearances of pure PLLA film (a), PLLA/NC composite films in the ratios 1%wt (b), 3%wt (c) and 5%wt (d) as well as PLLA/modified NC composite films in the ratios 1%wt (e), 3%wt (f) and 5%wt (g)

4.2.2 UV-Vis spectrophotometry analysis

The optical properties of pure PLLA film, PLLA/NC and PLLA /modified NC are show in Figure 36. The pure PLA film shows high transparency, consistent with previous research [110, 111]. The PLLA /NC composite films, the addition of large amounts of NC induced the transparency to degenerate. While PLLA/modified NC displayed good transparency indicating that the NC and modified NC influenced the light scattering originating from its aggregated state in the film are shown in Figure 36. The findings of this research are consistent with previous [112, 113].

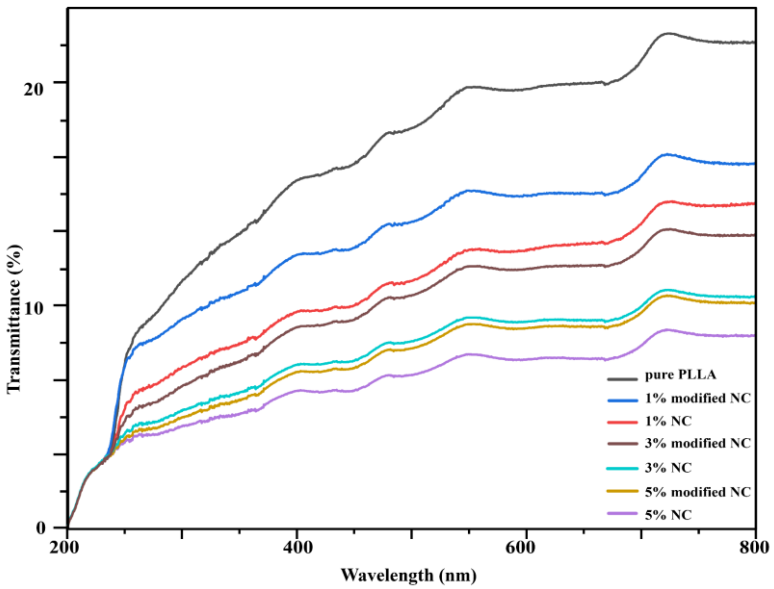

Figure 36 Transparency of pure PLLA film, PLLA/NC and PLLA/modified NC with 210 μm thickness

4.2.3 Fourier transform infrared spectroscopy analysis

The obtained ATR-FTIR spectra of NC, modified NC, pure PLLA film, PLLA/NC films and PLLA/modified NC in the composite film are shown in Figure 37. The dominant function of NC and modified NC the 3500-3000 cm^{-1} exhibited broad band and high intensity of OH stretching, 1450-1420 cm^{-1} (C-H stretching) and 950 cm^{-1} (C-O-C glycosidic ether). For modified NC, the dominant function was assigned to Si-O or Si-O-Si (700- 1150 cm^{-1}) [100]. The spectrum of pure PLLA film showed shape peaks at 1750 cm^{-1} (C=O) and 1450-1420 cm^{-1} (C-H stretching). For spectra of PLLA/NC and PLLA/modified NC composite film, demonstrated the broad peak at 3500 - 3000 cm^{-1} (OH stretching) and displayed shape peaks at 1750 cm^{-1} (C=O). When increasing NC and modified NC content presented high intensity of broad peak at 3500 - 3000 cm^{-1} (OH stretching) and the peak appeared at a higher wavenumber of 1750 cm^{-1} (C=O). These results confirmed the presence of NC and modified NC on PLLA matrixes [114].

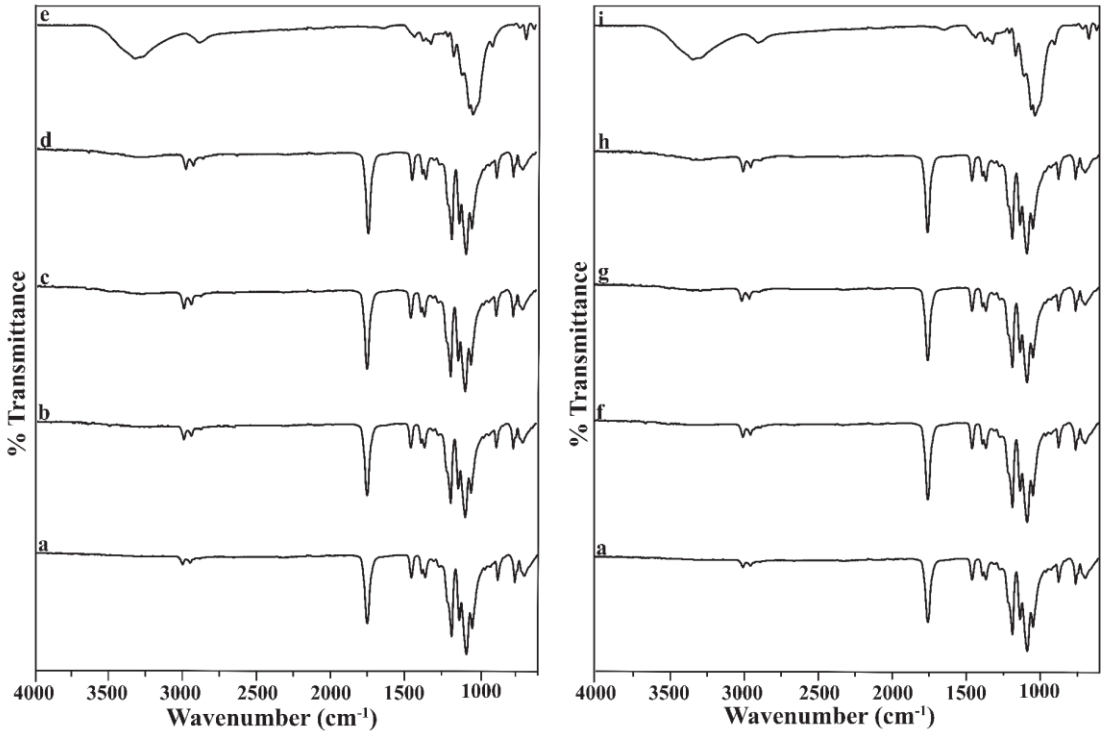

Figure 37 ATR-FTIR analysis of pure PLLA film (a), PLLA/NC composite films in the ratios 1%wt (b), 3%wt (c) 5%wt (d) and pure NC (e) as well as PLLA/modified NC composite films in the ratios 1%wt (f), 3%wt (g), 5%wt (h) and pure modified NC (e)

4.2.4 X-ray diffractometry analysis

The XRD analysis of pure film, PLLA/NC and PLLA/modified NC composite films were studied for crystallinity are shown in Figure 38. The NC and modified NC presented a small and broad peak at 2θ = 15.7°, 22.8°, and 34°. The peaks around 2θ=16°, 19°, and 22.7° correspond to the crystalline structure of PLLA and the peak positions are in accordance with those reported by Vestena *et al*, 2016 [114]. It can be considered as semi-crystalline in nature. The addition of NC is shown in Figure 38 (left) observed slightly increasing intensity according NC content. While the PLLA/modified NC composite films (Figure 38 (right)) displayed higher intensity than pure PLLA films. However, PLLA/modified NC composite films showed higher intensity than PLLA/NC due to interaction between PLLA and modified NC [115, 116].

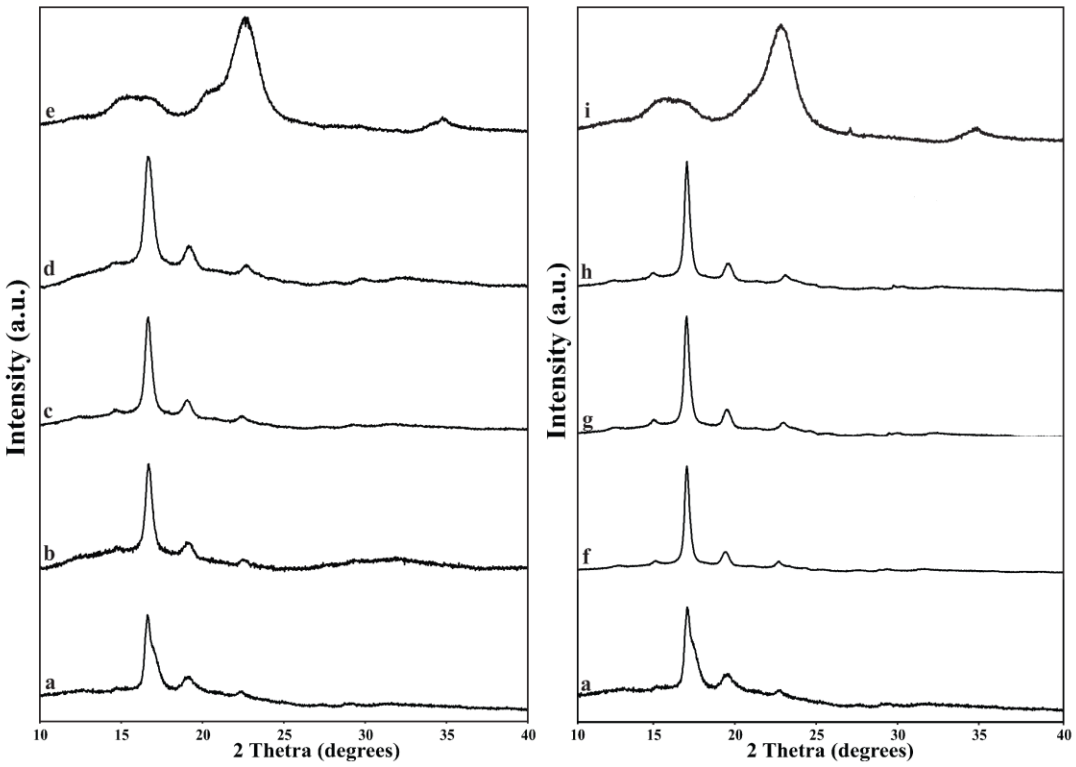

Figure 38 XRD patterns of pure PLLA film (a), PLLA/NC composite films in the ratios 1%wt (b), 3%wt (c), 5%wt (d) and pure NC (e) as well as PLLA/modified NC composite films in the ratios 1%wt (f), 3%wt (g), 5%wt (h) and pure modified NC (i)

4.2.5 Scanning electron microscopy analysis

4.2.5.1 Surface morphology of PLLA/NC and PLLA/modified NC composite films

The study morphology of composite films can be divided 2 types; Surface and Cross-Section. The surfaces of pure PLLA film and PLLA/NC composite films are shown Figure 39. The pure PLLA film (a,b) presented smooth and uniform. The addition of NC (1-5 %wt) into the PLLA surface displayed higher irregular than pure PLLA film. While the PLLA/ modified NC composite films are shown in Figure 40. The results showed that when to increasing modified NC into PLLA observed slightly irregular compare pure PLLA films. The PLLA/modified NC composite films showed smooth and uniform than PLLA/NC because of the modified NC displayed less hydrophilicity properties than NC [117, 118].

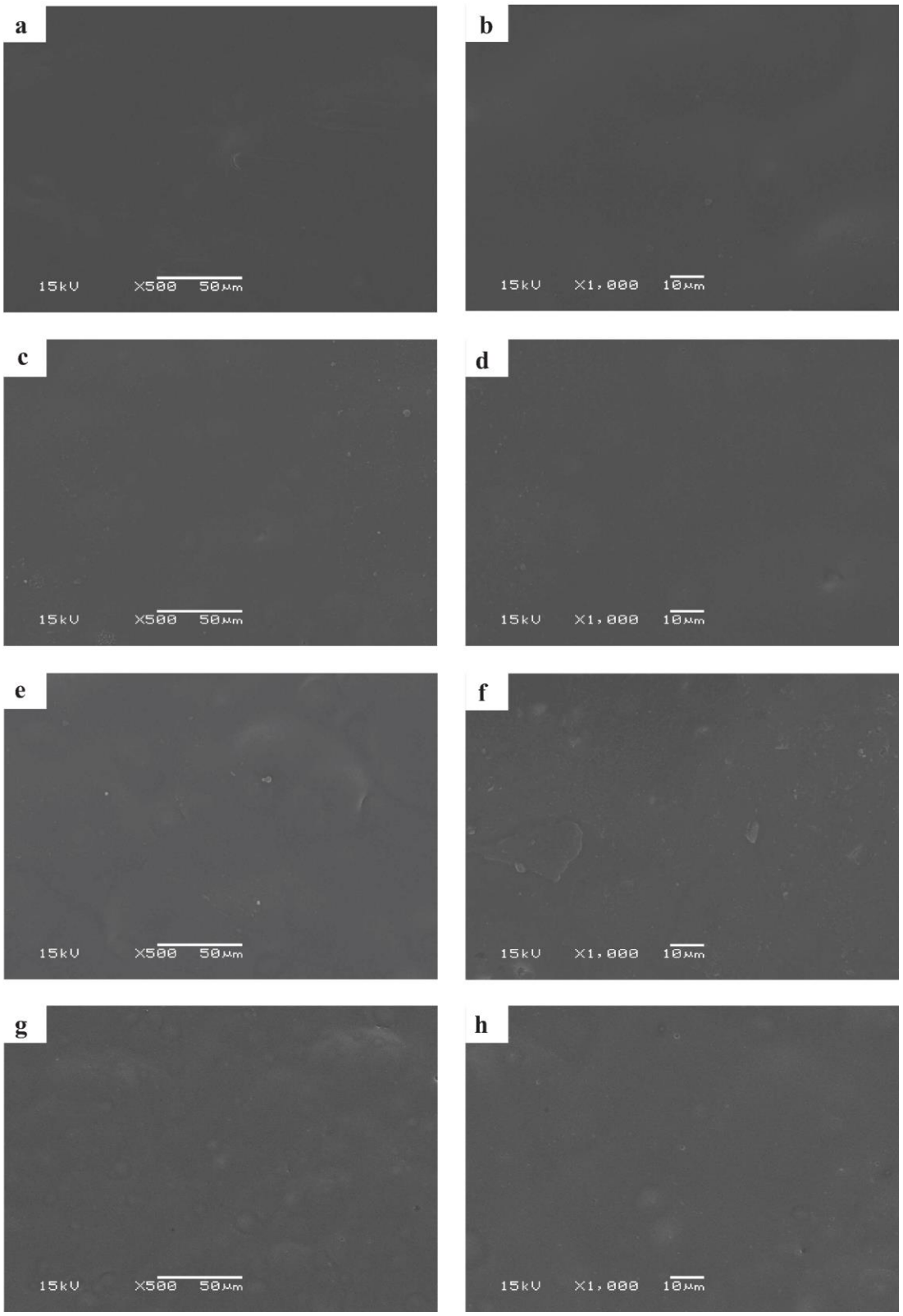

Figure 39 SEM images of surface for pure PLLA film (a,b) and PLLA/NC composite films in the ratios 1%wt (c,d), 3%wt (e,f) and 5%wt (g,h) at magnification 500X, bar 50 µm (a,c,e,g) and magnification 1000X, bar 10 µm (b,d,f,h)

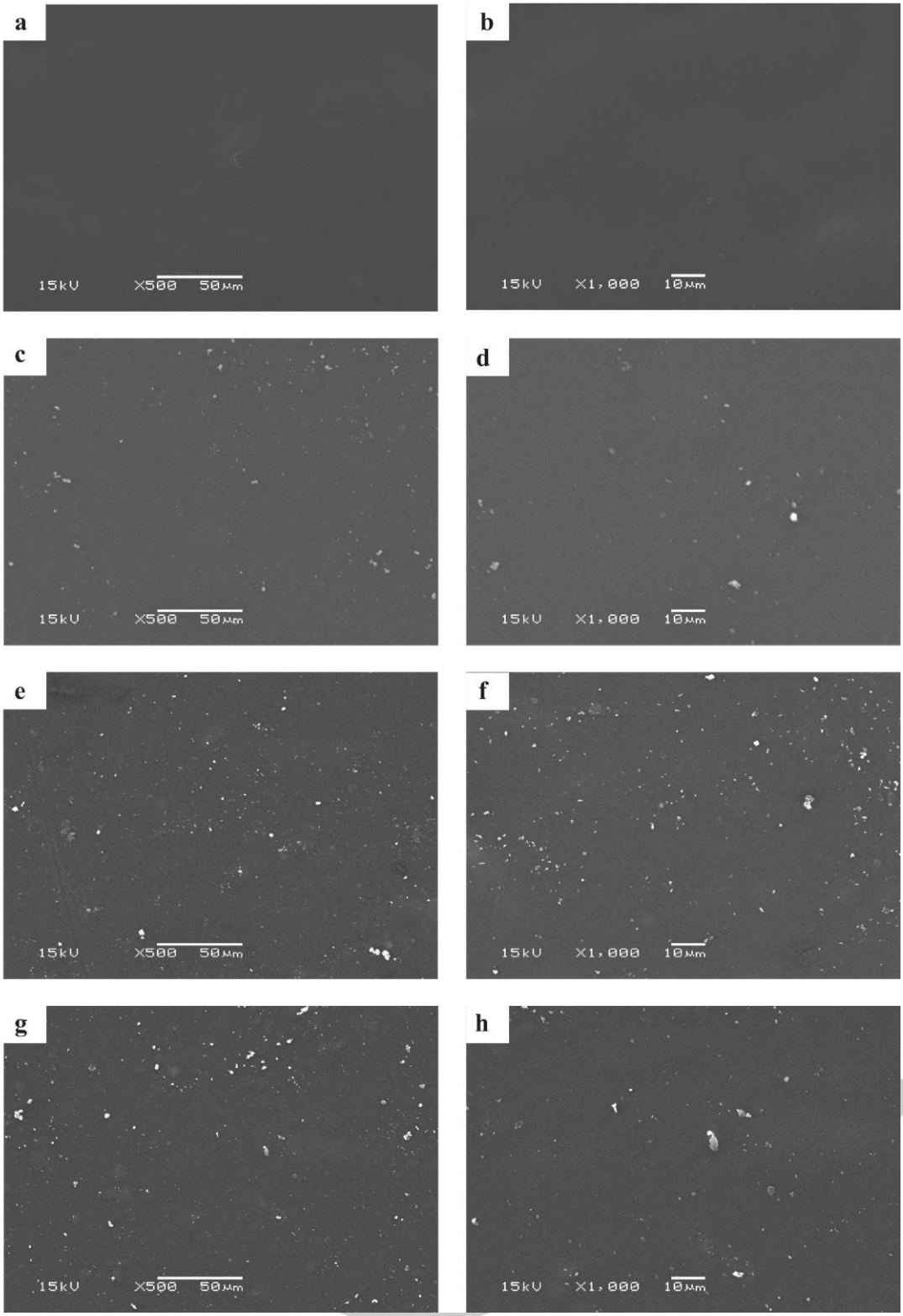

Figure 40 SEM images of surface for pure PLLA film (a,b) and PLLA/modified NC composite films in the ratios 1%wt (c,d), 3%wt (e,f) and 5%wt (g,h) at magnification 500X, bar 50 μm (a,c,e,g) and magnification 1000X, bar 10 μm (b,d,f,h)

4.2.5.2 Cross-section morphology of PLLA/NC and PLLA/modified NC composite films

The cross-section PLLA/NC composite films are shown in Figure 41. For pure PLLA film displayed smooth and uniform. The addition of NC (1-5 %wt) into the PLLA surface showed higher irregular and intermingle than pure PLLA film. While the PLLA/modified NC composite films are shown in Figure 42 when increasing modified NC exhibited slightly irregular and intermingle than pure films (PLLA100). When compare PLLA/NC and PLLA/modified NC, the PLLA/modified NC composite films displayed smooth and uniform than PLLA/NC. It can be seen the cracks in both phases indicate poor adhesion between PLLA/NC, while PLLA / modified NC showed good phase adhesion. Therefore, it can be concluded that modified NC good compatibility with PLLA. However, the modified NC high content will be effective on poor adhesion due to modified NC has aggregation [119].

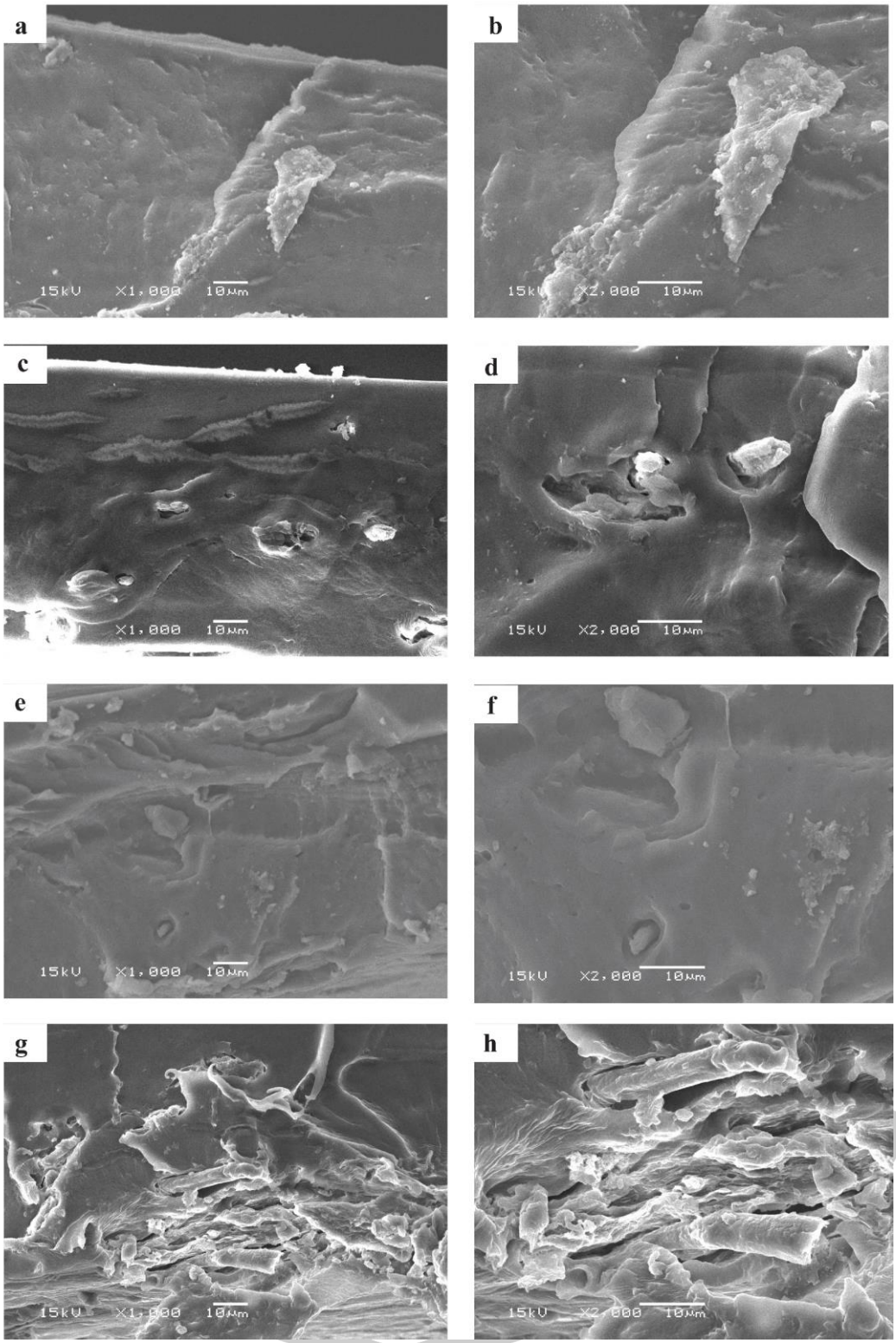

Figure 41 SEM images of cross-section for pure PLLA film (a,b) and PLLA/NC composite in the ratios 1%wt (c,d), 3%wt (e,f) and 5%wt (g,h) at magnification 1000X, bar 10 µm (a,c,e,g), magnification 2000X, bar 10 µm (b,d,f,h)

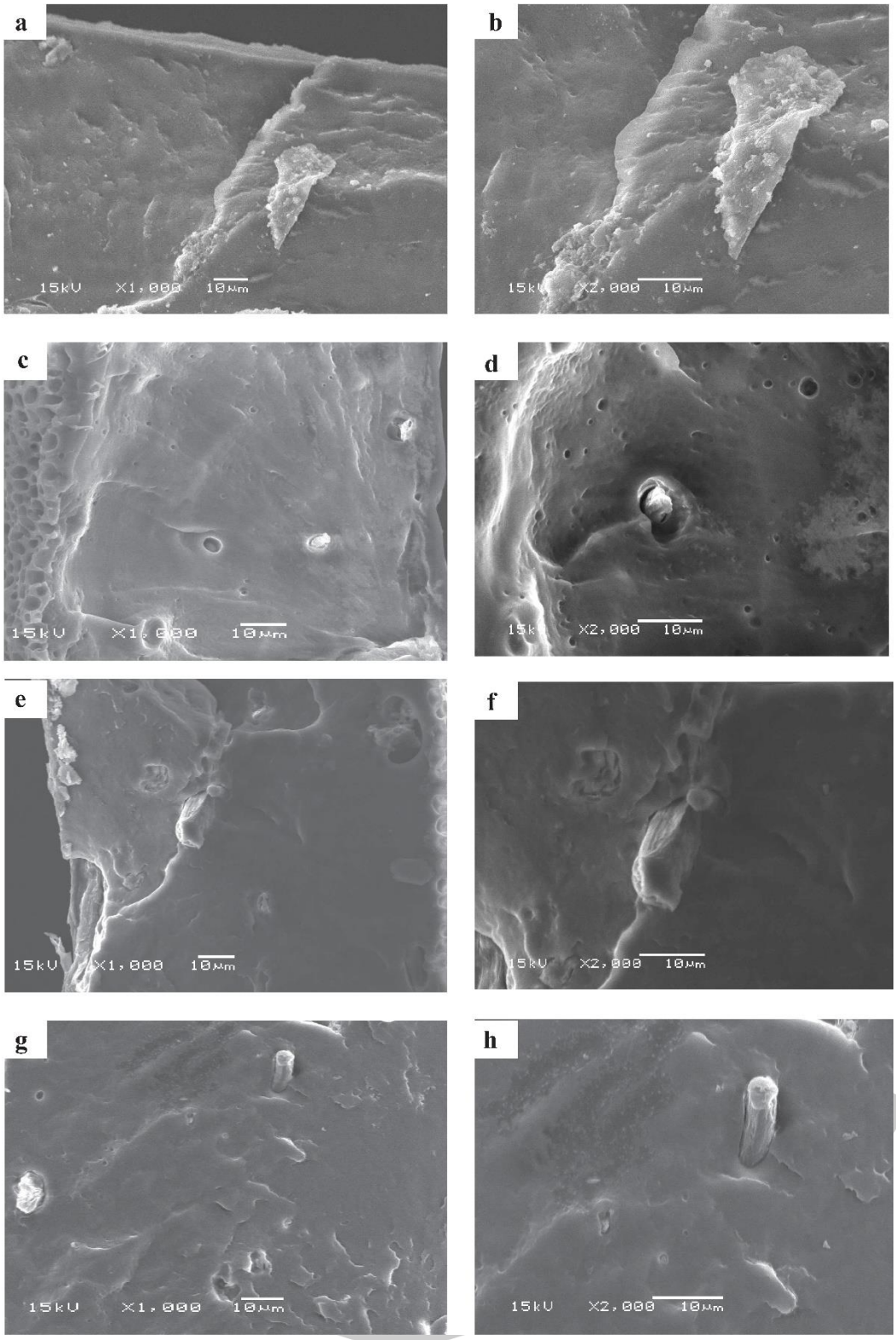

Figure 42 SEM images of cross-section for pure PLLA film (a,b) and PLLA/modified NC composite in the ratios 1%wt (c,d), 3%wt (e,f) and 5%wt (g,h) at magnification 1000X, bar 10 μm (a,c,e,g), magnification 2000X, bar 10 μm (b,d,f,h)

4.2.6 Thermogravimetric analysis

The study of thermal stability of composite films are shown in Figure 43. The TGA and DTG curves of composite films can be divided two steps. The first region in the range 100-150 °C temperature range was observed evaporation of water adsorption and second step in the range of 250-380 °C assigned to decomposition of backbone for composite films. In pure film (PLLA100) showed upper temperature 300°C [25]. When addition NC, the composite films (a, b) displayed slightly increased from 358 to 367 °C as shown in Figure 43 and Table 17 compared pure films (PLLA100). The residue at 600 ºC of pure PLLA film and composite films displayed the increasing thermal stability when addition of NC and modified NC. This may be due to the hydrogen bond between PLLA and NC. However, the addition of moreover nanocellulose content showed agglomerate. While the PLLA/modified NC composite films (c,d) presented higher thermal stability than pure films (PLLA100). Because PLLA and modified NC exhibited strong interaction [12, 81]. When compare composite PLLA/NC and PLLA/modified NC, PLLA/modified NC showed higher thermal stability than PLLA/NC due to good adhesion of modified NC consistent with the SEM results.

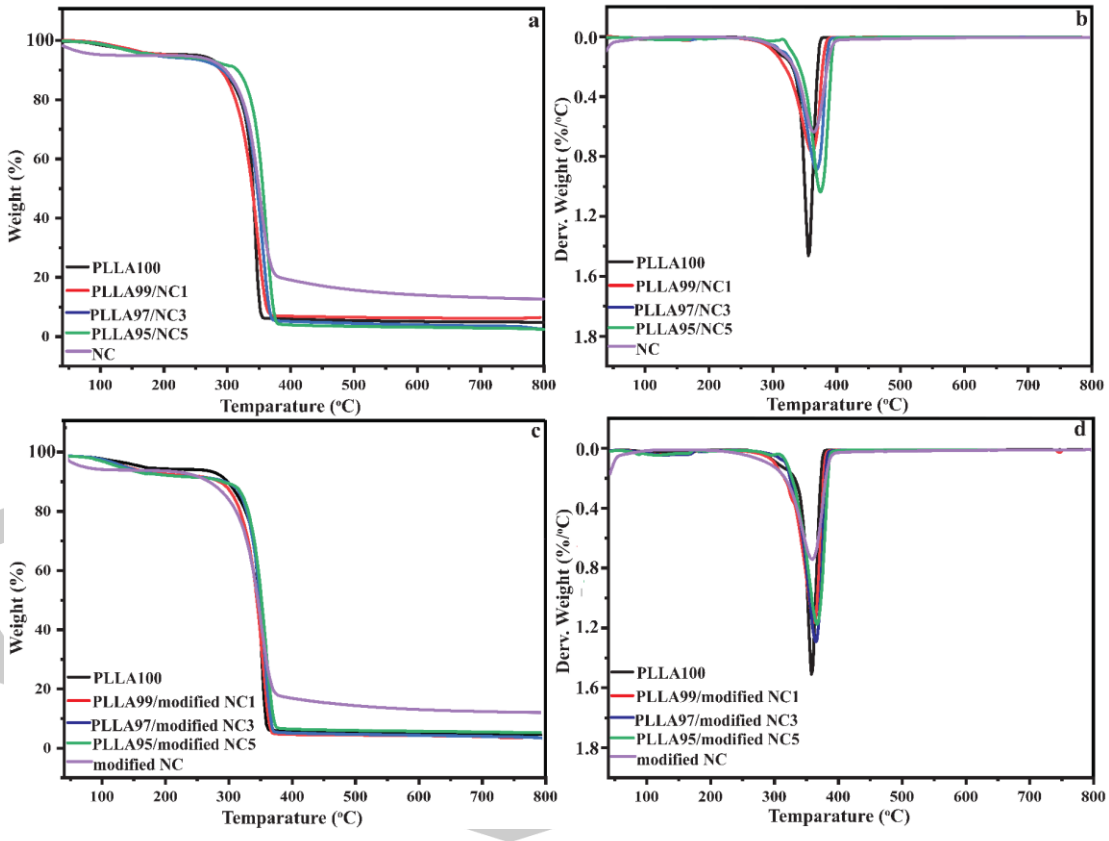

Figure 43 TGA and DTG curves of PLLA/NC (a,b) and PLLA/modified NC (c,d) composite films

Table 17 TGA analysis of NC, modified NC, PLLA/NC and PLLA/modified NC composite films

Sample	$T_{d, max}$ (^{o} C)	Residue at 600 ^{o}C (%)
NC	366	21.4
modified NC	360	22.4
PLLA100	358	0.94
PLLA99/NC1	362	1.01
PLLA97/NC3	365	1.29
PLLA95/NC5	367	1.73
PLLA99/modified NC1	364	1.19
PLLA97/modified NC3	370	1.31
PLLA95/modified NC5	377	2.59

4.2.7 Differential scanning calorimetry analysis

The DSC analyses (Figure 44, Figure 45 and Table 18) allowed the observation of multiphase separation, as evidenced by multiple thermal transitions of the composite films (PLLA/NC, PLLA/modified NC) component segments: glass transition (T_g), cold crystallization (T_{cc}) and melting temperatures (T_m). The T_g, T_m, and T_{cc} peaks of the pure PLLA films were in the ranges 50-65°C [62], 169-172°C [85] and 95-110°C [7] respectively. For influent NC on PLLA matrix, displayed decreased T_g (from 50 °C to 45°C), T_m (from 97°C to 92°C), and T_{cc} (from 172°C to 169°C), but increased X_c. For PLLA/modified NC (1-5%) composite films were observed slightly decreases T_g (from 50 °C to 47°C), T_m (from 97°C to 94°C), and T_{cc} (from 172°C to 170°C), but increase X_c. Because NC and modified as nucleating affected the fast crystallinity of composite films. [94, 120, 121]. Comparision PLLA/NC and PLLA/modified NC composite films, the results show that not different, however X_c of PLLA/modified NC composite films higher than PLLA/NC. Because the modified NC displayed lower hydrophilicity than NC interaction and good dispersion of modified NC on PLLA matrix [76, 82, 96]. The X_c was studied from DSC and XRD are shown in Figure 46. The X_c of pure PLLA film was observed by 7.91% [80] (for DSC), and 12.6 % (from XRD) [7]. The addition of NC (1-5%) into the PLLA matrix was observed the X_c increased from 7.91 to 28.3% from DSC and 12.6 to 20.4% from XRD. While addition modified NC into PLLA matrix was considered the X_c increased from 7.91 to 29.9% from DSC and 12.6 to 24.8% from XRD. The result showed that the addition of NC and modified NC on PLLA affect the

X_c of composite films. This can be explained the filler act as a nucleation agent [80, 81, 122, 123].

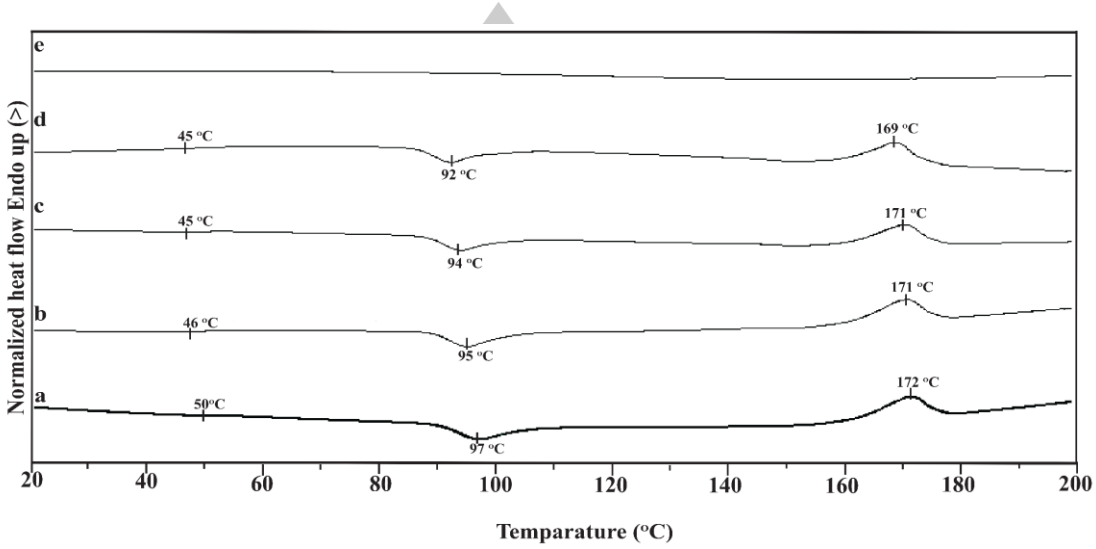

Figure 44 DSC curves of pure PLLA film (a) and PLLA/NC composite films in the ratios 1%wt (b), 3%wt (c), 5%wt (d) and pure NC (e)

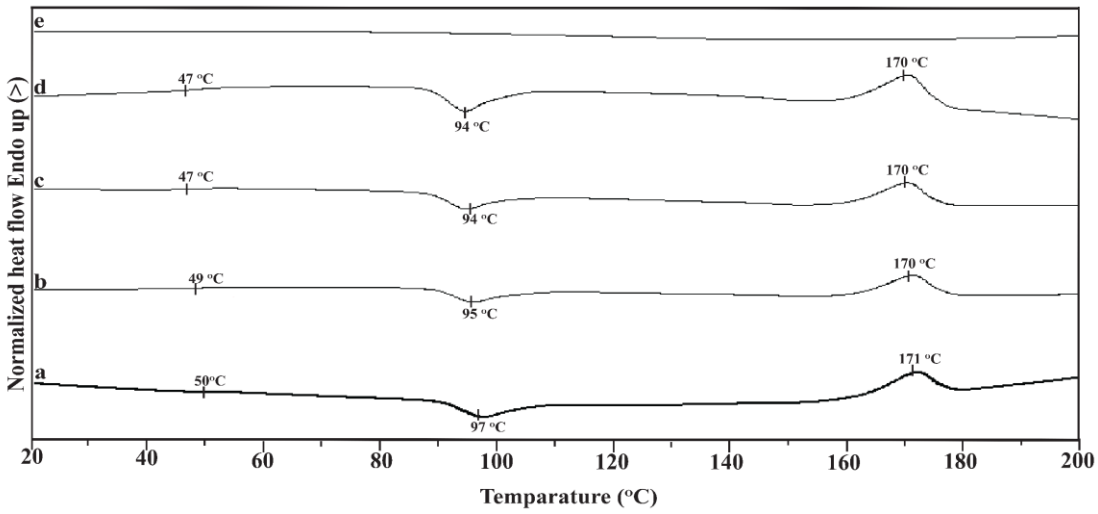

Figure 45 DSC curves of pure PLLA film (a) and PLLA/modified NC composite films in the ratios 1%wt (b), 3%wt (c), 5%wt (d) and pure modified NC (e)

Table 18 Thermal transition properties of PLLA/NC and PLLA/modified NC composite films

Sample	Filler content (wt%)	T_g (°C)	T_m (°C)	T_{cc} (°C)	ΔH_m (J/g)	ΔH_{cc} (J/g)	Xc (%)
PLLA100	0	50	171	97	40.385	32.972	7.91
PLLA99/NC1	1.0	46	171	95	39.868	27.474	13.4
PLLA97/NC3	3.0	45	171	94	42.651	23.417	21.2
PLLA95/NC5	5.0	45	169	92	45.639	20.437	28.3
PLLA99/modified NC1	1.0	49	170	95	41.203	24.318	18.2
PLLA97/modified NC3	3.0	47	170	94	47.787	25.368	24.7
PLLA95/modified NC5	5.0	47	170	94	52.324	25.629	29.9

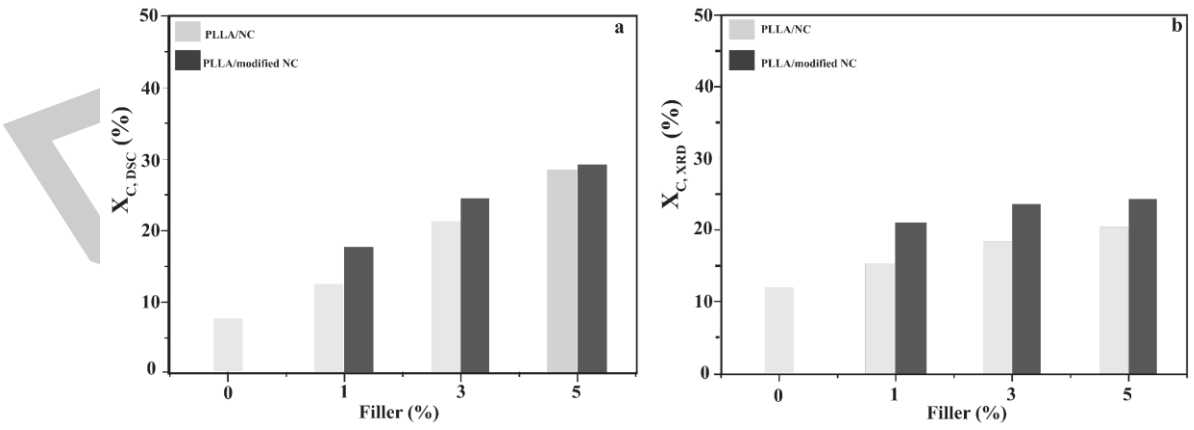

Figure 46 Degree of crystallinity (□) PLLA/NC and (■) PLLA/modified NC composite films from DSC (a) and XRD (b)

4.2.8 Tensile testing

The mechanical properties were measured for the solvent casted composite films using a Tensile testing machine (Figure 47). For pure PLLA film, the tensile strength showed 65 MPa, Elongation at break 6.28 % and Young's modulus 1198 MPa consistent with previous research [7, 62, 95]. After the addition of NC in PLLA matrix, the composite films displayed a slightly increased Young's modulus but decreased stress at break and elongation at break. This may be due to high NC content effect on aggregation [81, 114]. For PLLA/modified NC composite films was increased tensile stress and Young's modulus, followed by a reduction of elongation at break compare pure PLLA films. These values indicate the strength of the film. When addition modified NC more content (1-5%) found that increased stress at break and Young's modulus but decreased of elongation at break. While increasing modified NC content affected aggregation [119]. Compare mechanical properties of PLLA/NC and modified NC observed PLLA/modified NC higher mechanical properties than PLLA/NC. This may be due to the interaction between modified NC and PLLA and good dispersion of modified NC consistent with SEM results.

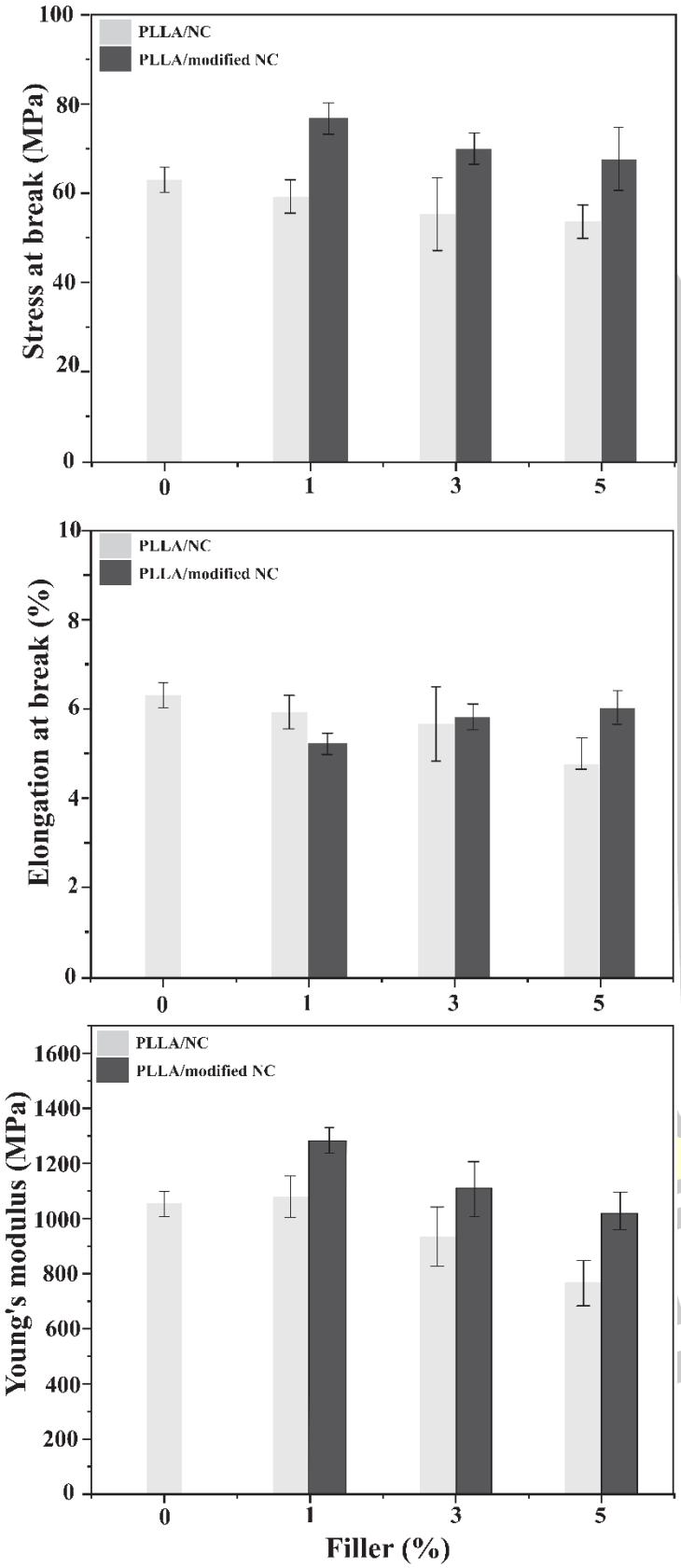

Figure 47 Tensile properties of (□) PLLA/NC and (■) PLLA/modified NC film

4.2.9 Water absorption

The water absorption chart displayed in Figure 48. The pure PLLA film showed the lowest water absorption due to hydrophobic properties of PLLA. For PLLA/NC composite films, the result showed that water absorption increased when increasing NC contents. For PLLA/modified NC composite films were observed water absorption increase according to modified NC content (1-5%). After 25 days the PLLA/NC and PLLA/modified NC composite films, the composite films showed higher degradation than pure PLLA film. The PLLA/NC slightly increased water absorption than PLLA/ modified NC due to hydrophilicity properties of NC. The result show that water absorption increased with increasing amount of NC and modified NC [98, 124].

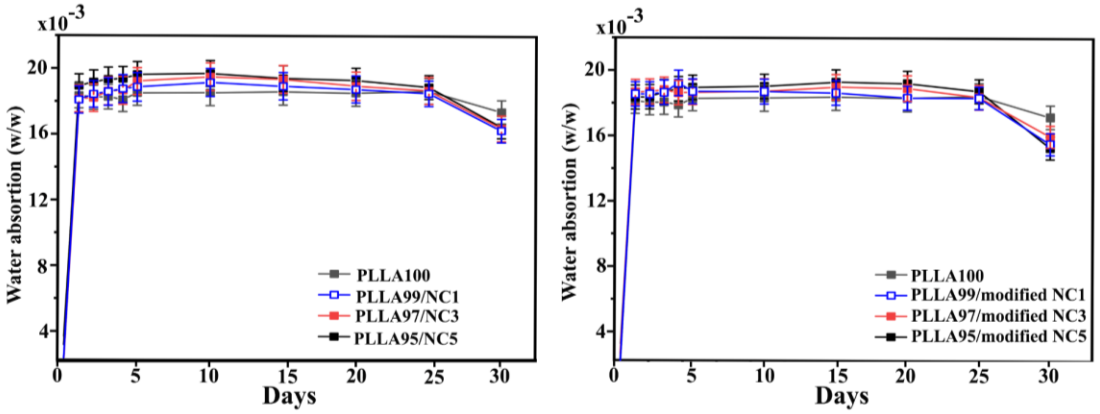

Figure 48 Water absorption of pure PLLA film, PLLA/NC (a) and PLLA/modified NC (b) composite films

4.3 Characterization of PLLA-PEG-PLLA/NC and PLLA-PEG-PLLA/modified NC composite films

4.3.1 Physical appearances

The unmodified and modified NC were used to produce composite films by solvent casting method. The physical appearances of PLLA-PEG-PLLA/NC and PLLA-PEG-PLLA/modified NC composite films displayed in Figure 49. The composite films were placed on a printed paper. For study influence NC (1-5wt%) on the PLLA-PEG-PLLA matrix, it was found that slightly lower transparent than pure PLLA-PEG-PLLA film. Meanwhile, PLLA-PEG-PLLA/modified NC composite films showed a more homogeneous dispersion of the modified NC for all amounts added; however, the films showed opacity, which increased upon the addition of higher amounts of modified NC, as observed earlier [119].

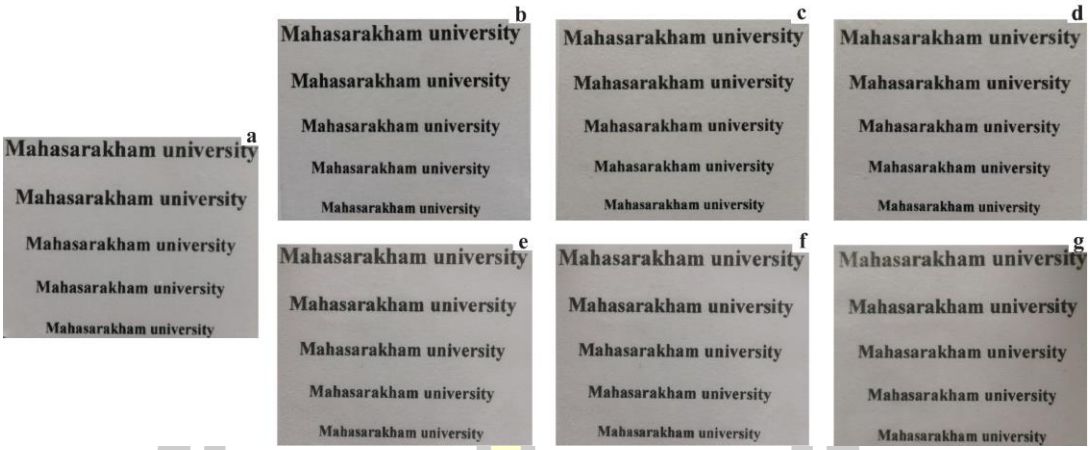

Figure 49 Physical appearances of pure PLLA-PEG-PLLA film (a), PLLA-PEG-PLLA /NC composite films in the ratios 1%wt (b), 3%wt (c) and 5%wt (d) as well as PLLA-PEG-PLLA /modified NC composite films in the ratios 1%wt (e), 3%wt (f) and 5%wt (g)

4.3.2 UV-Vis spectrophotometry analysis

The optical properties of pure PLLA-PEG-PLLA film, PLLA-PEG-PLLA/NC and PLLA-PEG-PLLA/modified NC are show in Figure 50. The pure PLLA-PEG-PLLA film showed high transparency. The PLLA-PEG-PLLA/NC and PLLA-PEG-PLLA/modified NC composite films displayed slightly decreased transparency [110].

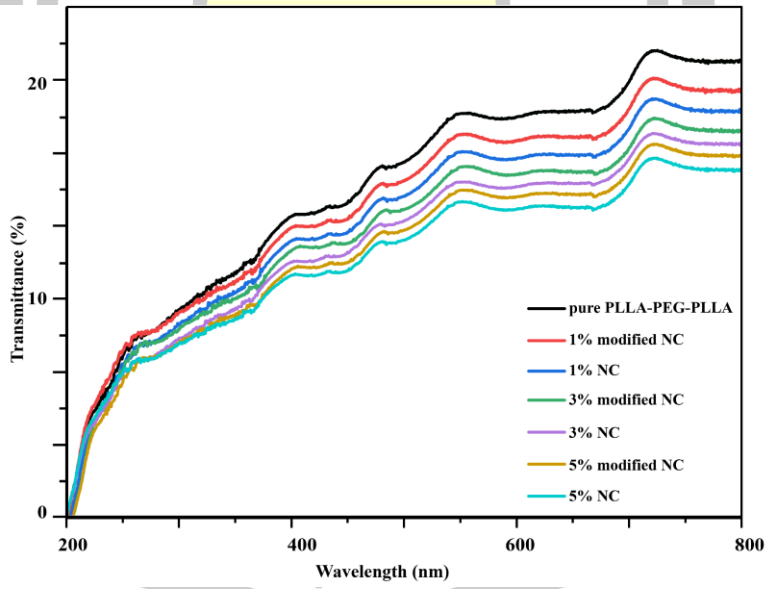

Figure 50 Transparency of pure PLLA-PEG-PLLA film, PLLA-PEG-PLLA/NC and PLLA-PEG-PLLA/modified NC with 210 μm thickness

4.3.3 Fourier transform infrared spectroscopy analysis

The main functional groups of pure PLLA-PEG-PLLA film, PLLA-PEG-PLLA/NC and PLLA-PEG-PLLA/modified NC were examined by ATR-FTIR (Figure 51). The dominant function of NC, the 3500-3000 cm^{-1} spectrum was broad spectrum and high intensity of OH stretching, 1450-1420 cm^{-1} was C-H stretching and at 950 cm^{-1} was C-O-C glycosidic ether. While, the dominant function of modified NC showed similar to NC. However, 700- 1150 cm^{-1} was assigned to Si-O or Si-O-Si [100] has a high intensity. For pure PLLA-PEG-PLLA film, the dominant function was observed at 1750 cm^{-1}, 1103 cm^{-1} the presence of carboxylic ester (C=O), ether (C–O) groups [41] and 1450-1420 cm^{-1} was presented C-H stretching. The influence of NC and modified NC on PLLA-PEG-PLLA, exhibited broad-spectrum and high intensity of 3500 - 3000 cm^{-1} (OH stretching) because of the hydroxyl (–OH) groups in NC. For this result, it can be confirmed that CNCs appears in the polymer matrix. The PLLA-PEG-PLLA/modified NC composite films were observed Si-O-Si (700-1150 cm^{-1}). The results were confirmed to be modified NC on the PLLA-PEG-PLLA matrix [41].

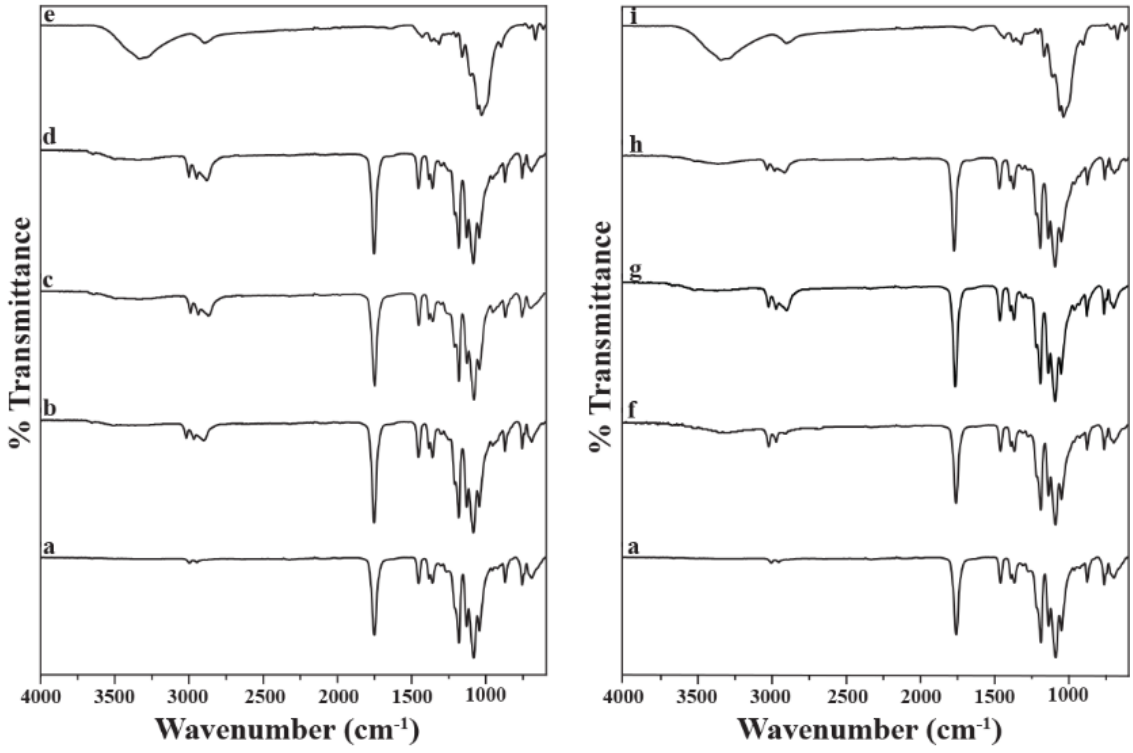

Figure 51 ATR-FTIR analysis of pure PLLA-PEG-PLLA film (a), PLLA-PEG-PLLA/NC composite films in the ratios 1%wt (b), 3%wt (c) 5%wt (d) and pure NC (e) as well as PLLA-PEG-PLLA/modified NC composite films in the ratios 1%wt (f), 3%wt (g), 5%wt (h) and pure modified NC (e)

4.3.4 X-ray diffractometer analysis

The XRD analysis of pure PLLA-PEG-PLLA film, PLLA-PEG-PLLA/NC and PLLA-PEG-PLLA/modified NC composite films was studied for crystallinity are shown in Figure 52. The NC and modified NC presented a small and broad peak at 2θ = 15.7°, 22.8°, and 34° [7].The characteristic high-intensity diffraction peak of 16◦ was attributed to the PLLA block, and the peaks of 18.9°and 23.2°[43] were attributed to the PEG block, which revealed the existence of a natural crystalline form of PLLA-PEG-PLLA. When added, NC and modified NC on PLLA-PEG-PLLA composite film content found that peaks at position 15.7°, 18°, and 22° showed higher intensity compared to pure PLLA-PEG-PLLA film. When comparing PLLA-PEG-PLLA/NC and PLLA-PEG-PLLA/modified NC composite films, the PLLA-PEG-PLLA/modified NC exhibited higher intensity than PLLA-PEG-PLLA/NC.

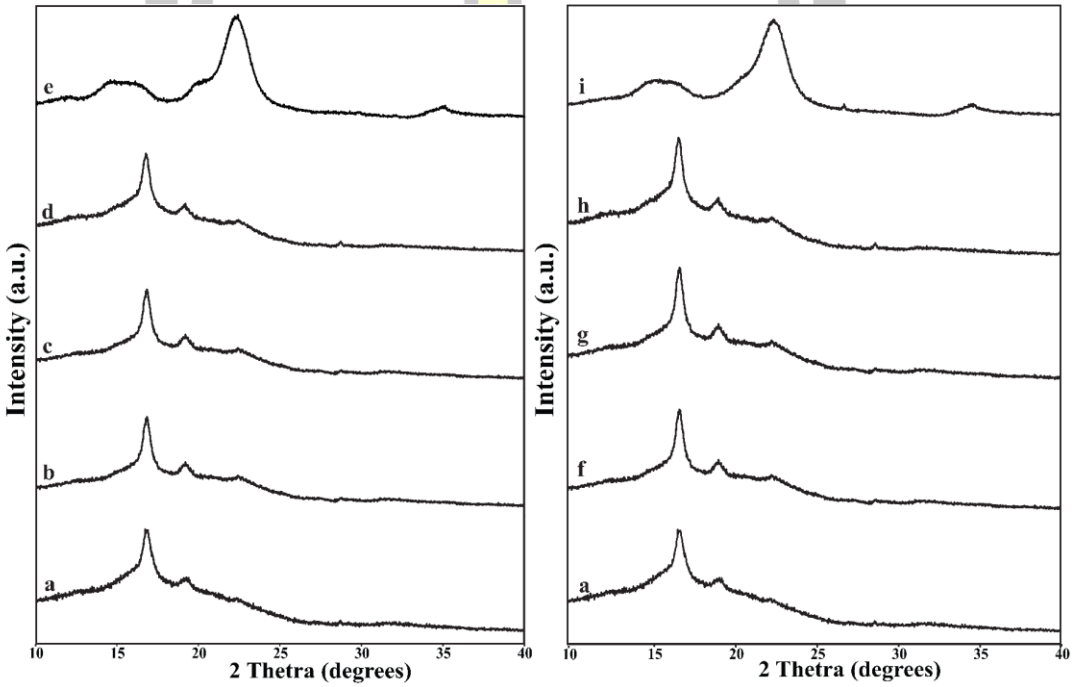

Figure 52 XRD patterns of pure PLLA-PEG-PLLA film (a), PLLA-PEG-PLLA/NC composite films in the ratios 1%wt (b), 3%wt (c), 5%wt (d) and pure NC (e) as well as PLLA-PEG-PLLA/modified NC composite films in the ratios 1%wt (f), 3%wt (g), 5%wt (h) and pure modified NC (i)

4.3.5 Scanning electron microscopy analysis

4.3.5.1 Surface morphology of PLLA-PEG-PLLA/NC and PLLA-PEG-PLLA/modified NC composite films

The smooth surface was observed in neat PLLA-PEG-PLLA (Figure 53) film while PLLA-PEG-PLLA film with NC showed separation phase of uniform bubble phase (NC phase) in PLLA-PEG-PLLA matrix. When to increasing modified NC into PLLA-PEG-PLLA are shown in Figure 54 displayed slightly irregular compare pure PLLA-PEG-PLLA film. When comparing PLLA-PEG-PLLA/NC and PLLA-PEG-

PLLA/modified NC, the PLLA-PEG-PLLA/ modified NC composite films exhibited smooth and uniform than PLLA-PEG-PLLA/NC.

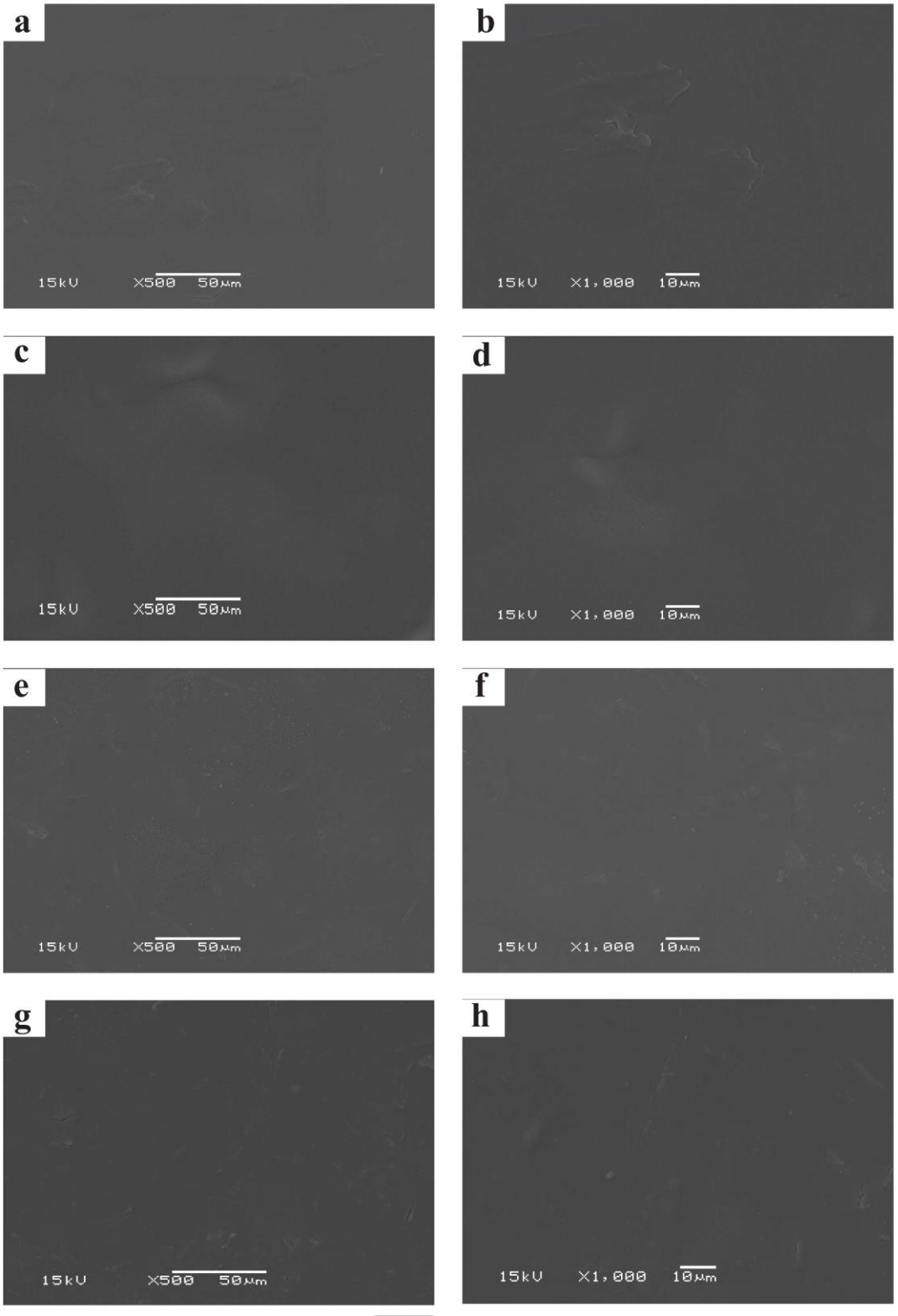

Figure 53 SEM images of surface for pure PLLA-PEG-PLLA film (a,b) and PLLA-PEG-PLLA/NC composite films in the ratios 1%wt (c,d), 3%wt (e,f) and 5%wt (g,h) at magnification 500X, bar 50 µm (a,c,e,g) and magnification 1000X, bar 10 µm (b,d,f,h)

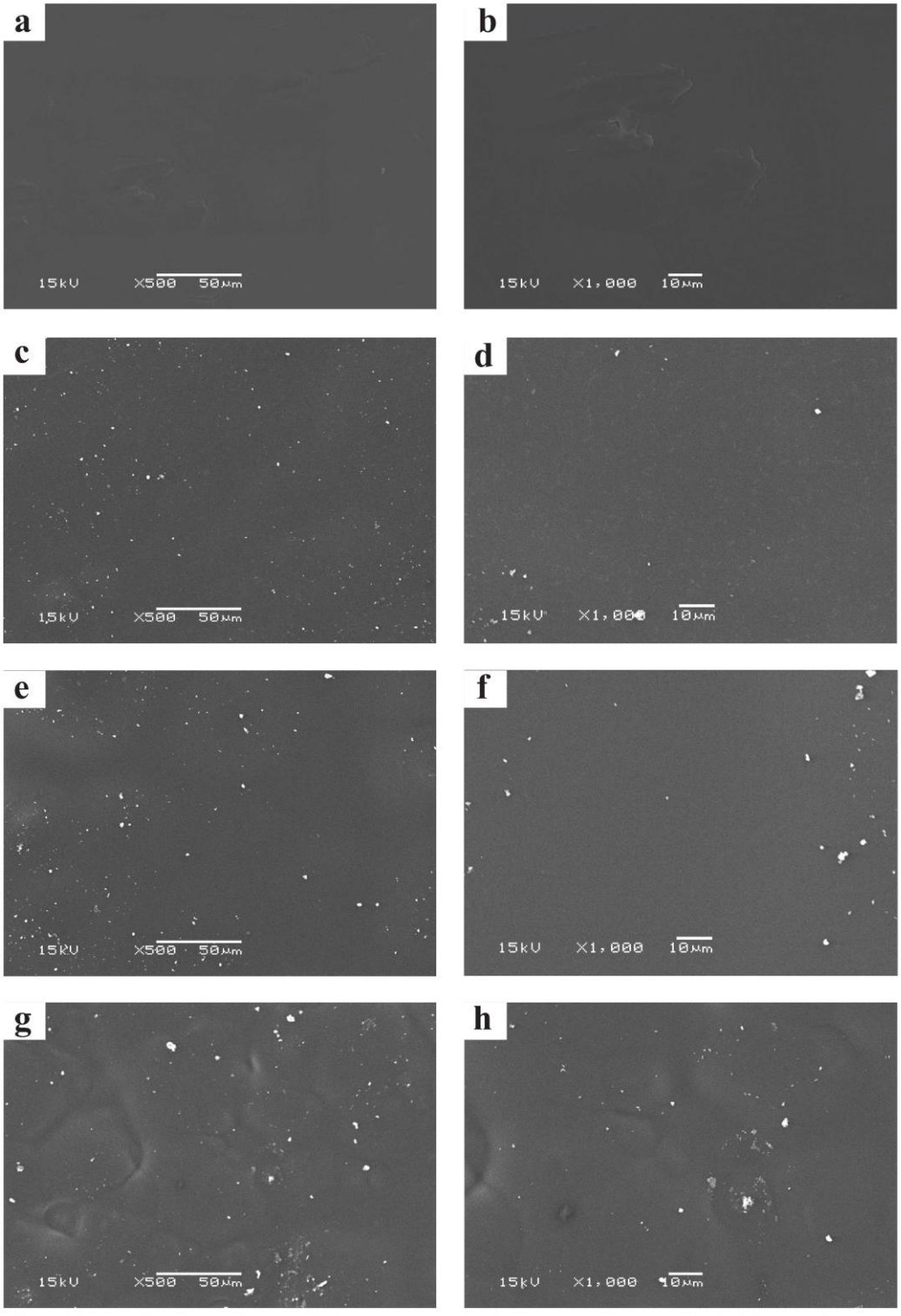

Figure 54 SEM images of surface for pure PLLA-PEG-PLLA film (a,b) and PLLA-PEG-PLLA/modified NC composite films in the ratios 1%wt (c,d), 3%wt (e,f) and 5%wt (g,h) at magnification 500X, bar 50 μm (a,c,e,g) and magnification 1000X, bar 10 μm (b,d,f,h)

4.3.5.2 Cross-section morphology of PLLA-PEG-PLLA/NC and PLLA-PEG-PLLA/modified NC composite film

The cross-section of pure PLLA-PEG-PLLA film and PLLA-PEG-PLLA/NC composite films are shown in Figure 55. The pure PLLA-PEG-PLLA film demonstrated smooth and uniform. Addition NC (1-5 %wt), the PLLA-PEG-PLLA/NC composite films presented higher irregular and intermingle than pure film. While the cross-section of PLLA-PEG-PLLA/modified NC composite films (Figure 56) showed slightly irregular and intermingle with increasing of modified NC content. When comparing PLLA-PEG-PLLA/NC and PLLA-PEG-PLLA/modified NC composite films, the PLLA-PEG-PLLA / modified NC composite films displayed smooth, uniform and good phase adhesion than PLLA-PEG-PLLA/NC due to interaction of PLLA-PEG-PLLA and modified NC. The composite films showed agglomerate of NC and modified NC with increasing high content [119].

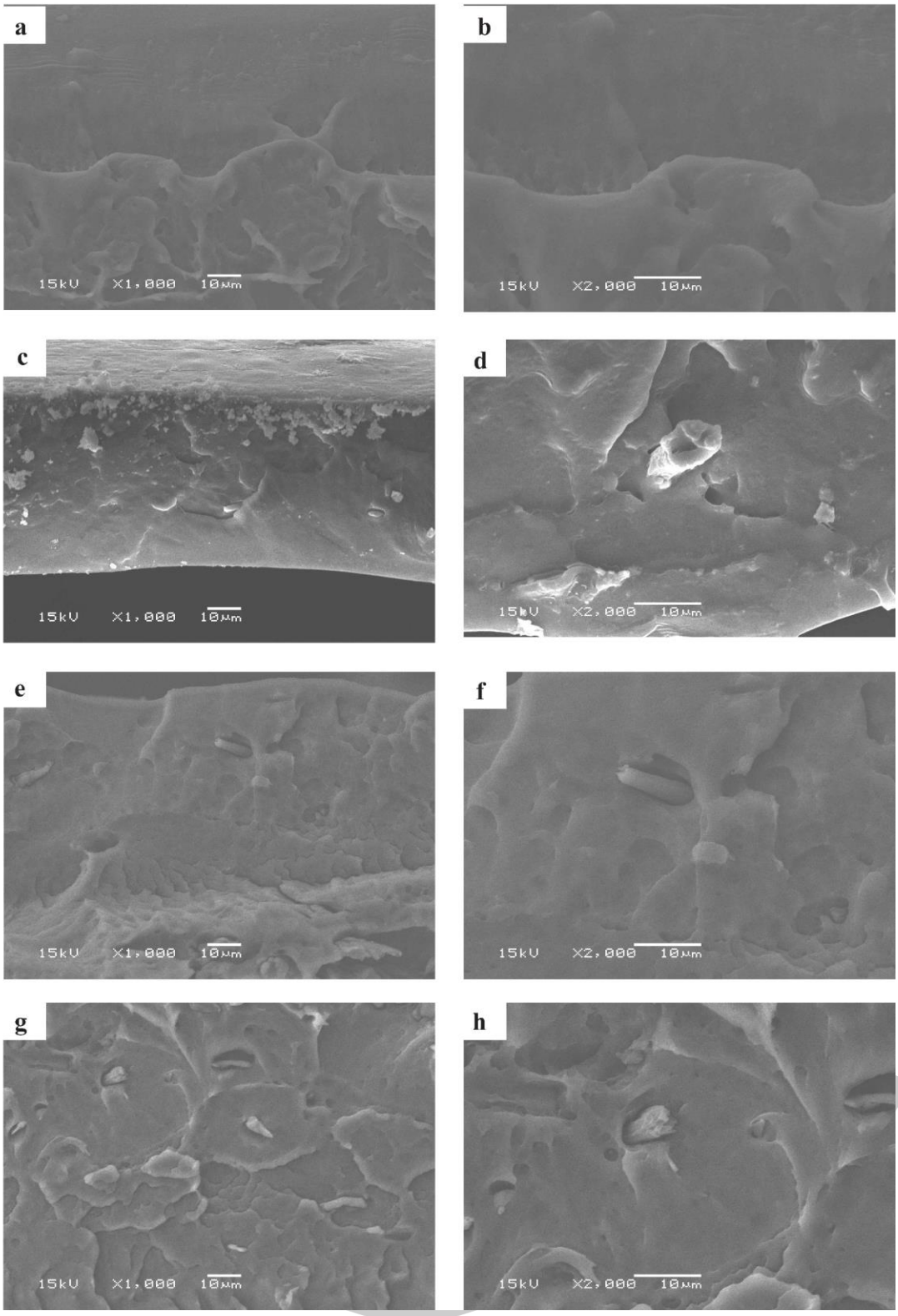

Figure 55 SEM images of cross-section for pure PLLA-PEG-PLLA film (a,b) and PLLA-PEG-PLLA/NC composite in the ratios 1%wt (c,d), 3%wt (e,f) and 5%wt (g,h) at magnification 1000X, bar 10 µm (a,c,e,g), magnification 2000X, bar 10 µm (b,d,f,h)

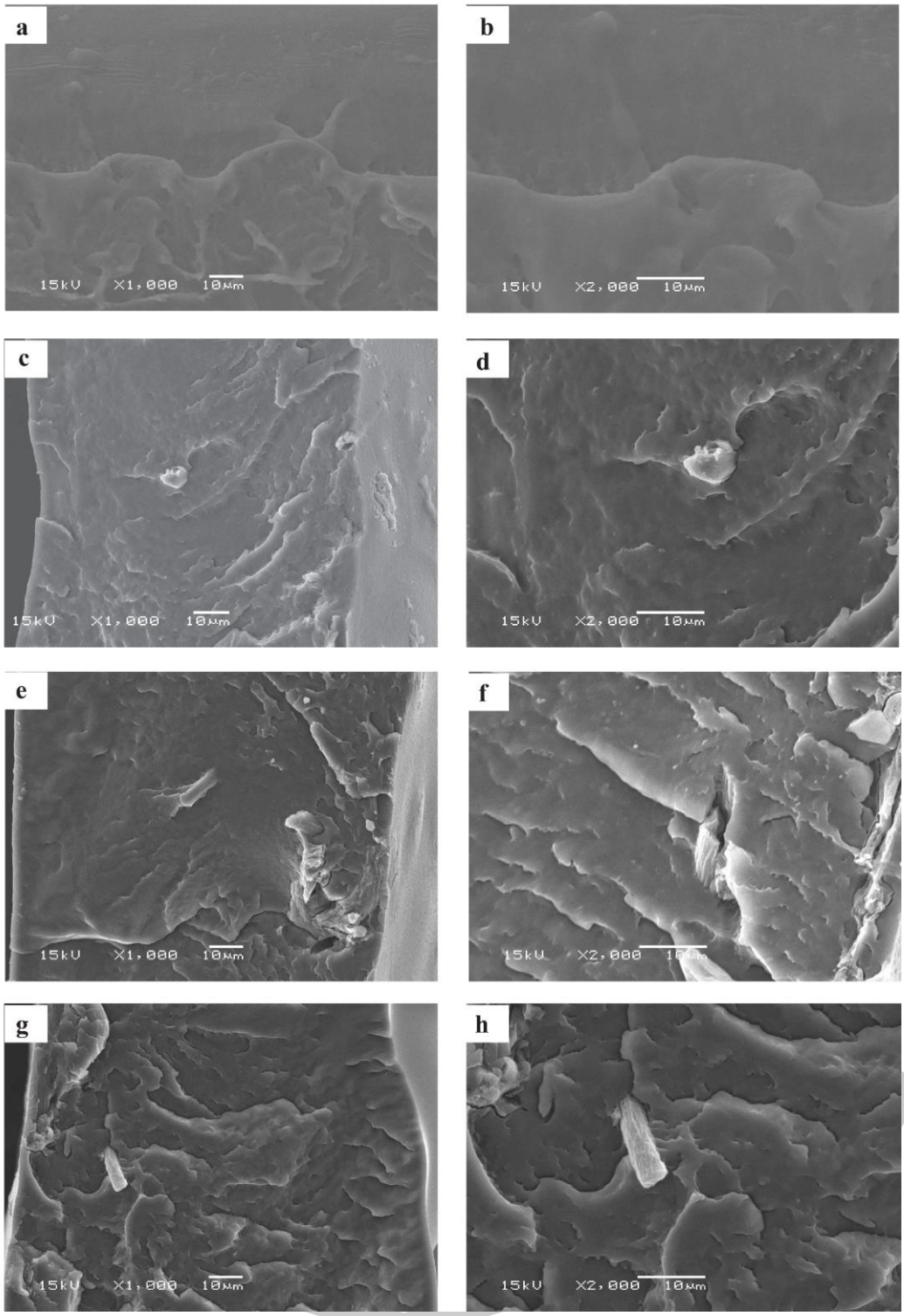

Figure 56 SEM images of cross-section for pure PLLA-PEG-PLLA film (a,b) and PLLA-PEG-PLLA/modified NC composite in the ratios 1%wt (c,d), 3%wt (e,f) and 5%wt (g,h) at magnification 1000X, bar 10 μm (a,c,e,g), magnification 2000X, bar 10 μm (b,d,f,h)

4.3.6 Thermogravimetric analysis

The study of thermal stability of PLLA-PEG-PLLA/NC and PLLA-PEG-PLLA/ modified NC composite films are shown in Figure 57. The TGA and DTG of PLLA-PEG-PLLA/NC slightly increased from 270 to 276, 367-376 ºC (Table 19) compared pure PLLA-PEG-PLLA films. This may be due to the hydrogen bond between PLLA-PEG-PLLA and NC. While the PLLA-PEG-PLLA/ modified NC composite films exhibited higher than pure PLLA-PEG-PLLA film because the strong interaction between PLLA-PEG-PLLA and modified NC. The residue of composite films slightly increased when addition of NC and modified NC are shown in Table 19 When compare PLLA-PEG-PLLA/NC and PLLA-PEG-PLLA/modified NC composite films, PLLA-PEG-PLLA/modified NC showed higher thermal stability properties than PLLA-PEG-PLLA/NC due to good dispersion on surface and interaction of them [7].

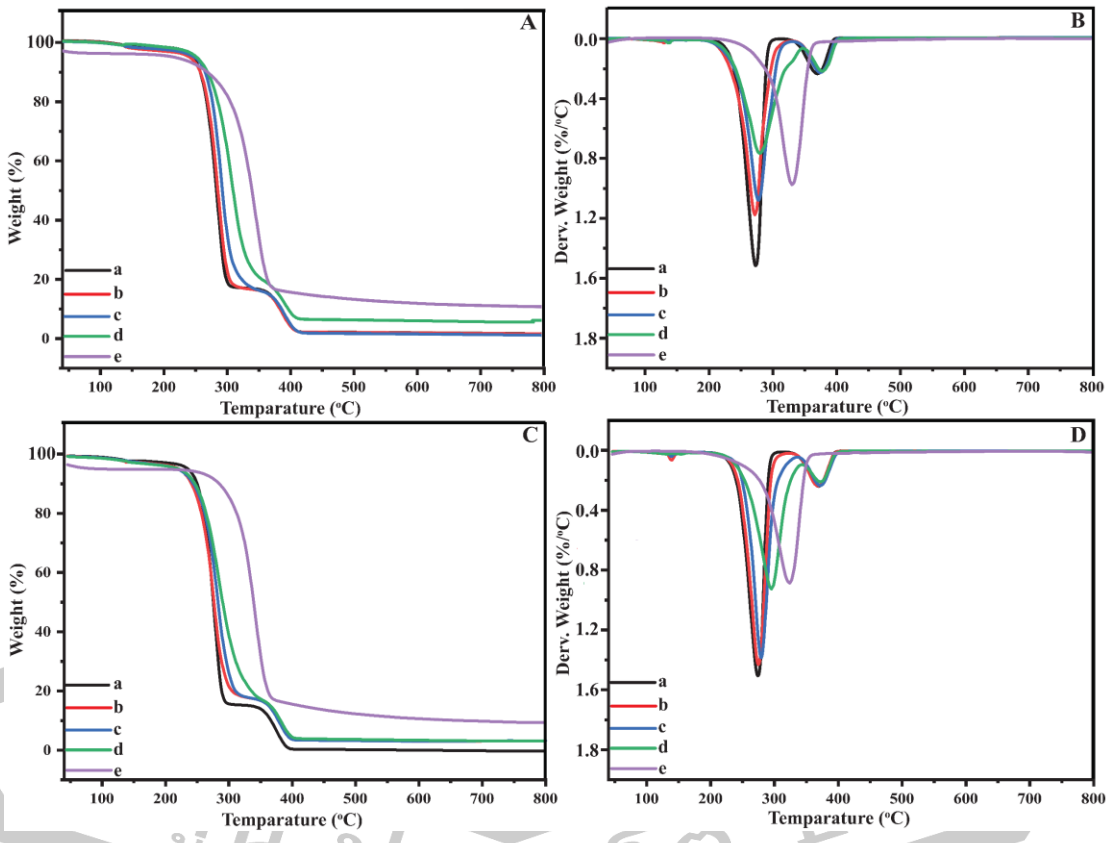

Figure 57 TGA and DTG curves of pure PLLA-PEG-PLLA film (a), PLLA-PEG-PLLA/NC (A,B) and PLLA-PEG-PLLA/modified NC (C,D) composite films ratios 1%(b), 3%(c), 5% (d) and 100% (e)

Table 19 TGA analysis of NC, modified NC, PLLA-PEG-PLLA/NC and PLLA-PEG-PLLA/ modified NC

Sample	$T_{d1, max}$ (° C)	$T_{d2, max}$ (° C)	Residue at 600 °C (%)
NC	366	-	21.4
modified NC	360	-	22.4
Pure PLLA-PEG-PLLA	270	367	1.43
PLLA-PEG-PLLA99/NC1	269	368	3.65
PLLA-PEG-PLLA97/NC3	274	372	3.67
PLLA-PEG-PLLA95/NC5	276	376	3.99
PLLA-PEG-PLLA99/modified NC1	274	368	2.26
PLLA-PEG-PLLA97/modified NC3	276	371	2.34
PLLA-PEG-PLLA95/ modified NC5	291	377	4.65

4.3.7 Differential scanning calorimeter analysis

The thermal properties of pure PLLA-PEG-PLLA film, PLLA-PEG-PLLA/NC and PLLA-PEG-PLLA/modified NC composite films are shown in Figure 58, Figure 59 and Table 20. The sample allowed the observation of multiphase separation, as evidenced by multiple thermal transitions of the composite film component segments: glass transition (T_g), cold crystallization (T_{cc}) and melting temperature (T_m). The T_g, T_m, and T_{cc} peaks of the pure PLLA-PEG-PLLA films were in the ranges 27-30°C [7], 165–170°C [39] and 63-65°C. For PLLA-PEG-PLLA/NC composite films, it was found that slightly decreased T_g (from 27°C to 25°C) and T_{cc} (from 65°C to 63°C) while T_m (from 168°C to 167°C) not different due to weak interaction and poor dispersion NC. For PLLA-PEG-PLLA/modified NC composite films (1-5%) were observed T_g (from 27°C to 26°C) and T_m (from 168°C to 167°C) not different. The T_{cc} (from 65°C to 63°C) slightly decreased, but X_c increased compare pure PLLA-PEG-PLLA film due to weak interaction and poor dispersion modified NC. Comparison PLLA-PEG-PLLA/NC and PLLA-PEG-PLLA/modified NC composite films, the results show that not different, however X_c of PLLA-PEG-PLLA/modified NC composite films higher than PLLA-PEG-PLLA/NC because of the interaction and good dispersion of modified NC on PLLA-PEG-PLLA matrix . The X_c was studied from DSC and XRD are shown in Figure 60. The X_c of pure PLLA film was observed by 37.4% (for DSC), and 4.28 % (from XRD) [7]. The

addition of NC (1-5%) into the PLLA-PEG-PLLA matrix were observed X_c increased from 37.4 to 49.6% from DSC and 4 to 19.2% from XRD. While addition modified NC into PLLA-PEG-PLLA matrix were considered the crystalline increased from 37.4 to 61.3% from DSC and 4.28 to 24.2% from XRD. The result showed that the addition modified NC into PLLA-PEG-PLLA matrix affected to X_c of composite films due to interaction of the modified NC and polymer matrix [125, 126].

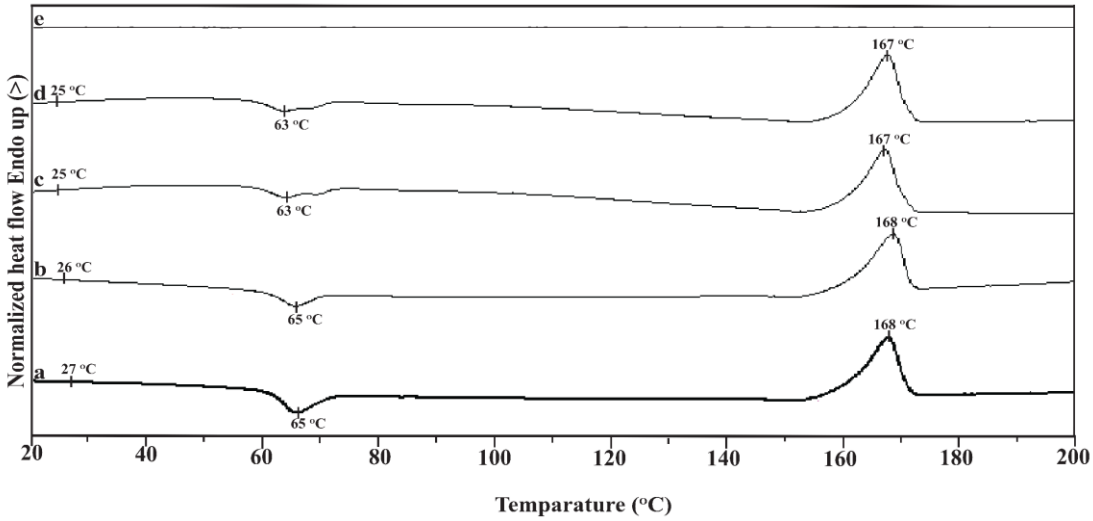

Figure 58 DSC curves of pure PLLA-PEG-PLLA film (a) and PLLA-PEG-PLLA/NC composite films in the ratios 1%wt (b), 3%wt (c), 5%wt (d) and pure NC (e)

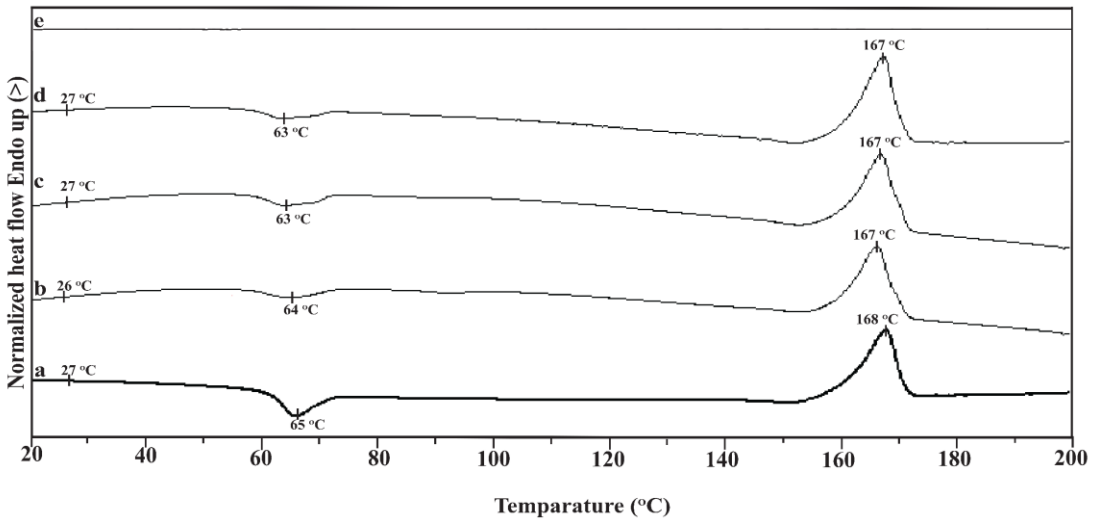

Figure 59 DSC curves of pure PLLA-PEG-PLLA film (a) and PLLA-PEG-PLLA/modified NC composite films in the ratios 1%wt (b), 3%wt (c), 5%wt (d) and pure modified NC (e)

Table 20 Thermal transition properties of PLLA-PEG-PLLA/NC and PLLA-PEG-PLLA/modified NC composite films

Sample	Filler conten (wt%)	T_g (°C)	T_m (°C)	T_{cc} (°C)	ΔH_m (J/g)	ΔH_{cc} (J/g)	Xc (%)
PLLA-PEG-PLLA100	0	27	168	65	42.410	13.260	37.5
PLLA-PEG-PLLA99/NC1	1.0	26	168	65	39.795	7.246	42.3
PLLA-PEG-PLLA97/NC3	3.0	25	167	63	41.986	6.851	46.6
PLLA-PEG-PLLA95/NC5	5.0	25	167	63	44.271	7.618	49.6
PLLA-PEG-PLLA99/ modified NC1	1.0	26	166	64	40.936	6.512	44.7
PLLA-PEG-PLLA97/ modified NC3	3.0	27	167	63	46.332	7.278	51.8
PLLA-PEG-PLLA95/ modified NC5	5.0	27	167	63	51.025	5.670	61.4

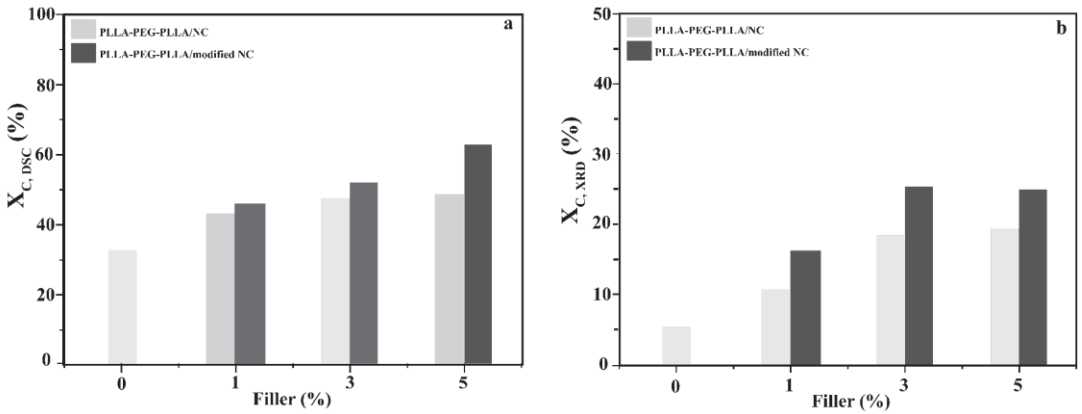

Figure 60 Degree of crystallinity of (□) PLLA-PEG-PLLA/NC and (■) PLLA-PEG-PLLA/modified NC composite films from DSC(a) and XRD (b)

4.3.8 Tensile testing

The mechanical properties were measured for the solvent casting composite films using a Tensile testing machine (Figure 61).The pure PLLA-PEG-PLLA film, the stress at break showed 28 MPa, Elongation at break (18.1 %) and Young's modulus (543 MPa) consistent with previous research [7]. After the addition NC, the composite films displayed slightly increased Young's modulus (500-540 MPa), stress at break (23-27 MPa) and elongation at break compare pure PLLA-PEG-PLLA film due to high NC content effect on aggregation. For PLLA-PEG-PLLA/modified NC composite films increased stress at break (29-32 MPa) and Young's modulus (535-612 MPa), followed by a reduction of elongation at break (12-15 %) compare pure PLLA-PEG-PLLA film. While addition modified NC more content (1-5%) found that slightly decreased stress at break Young's modulus and elongation at break because moreover modified NC presented aggregation of them [127]. Compare mechanical properties of composite films, the PLLA-PEG-PLLA/modified NC showed higher mechanical properties than PLLA-PEG-PLLA/NC due to the interaction and good dispersion of modified NC on PLLA-PEG-PLLA matrix consistent with SEM results.

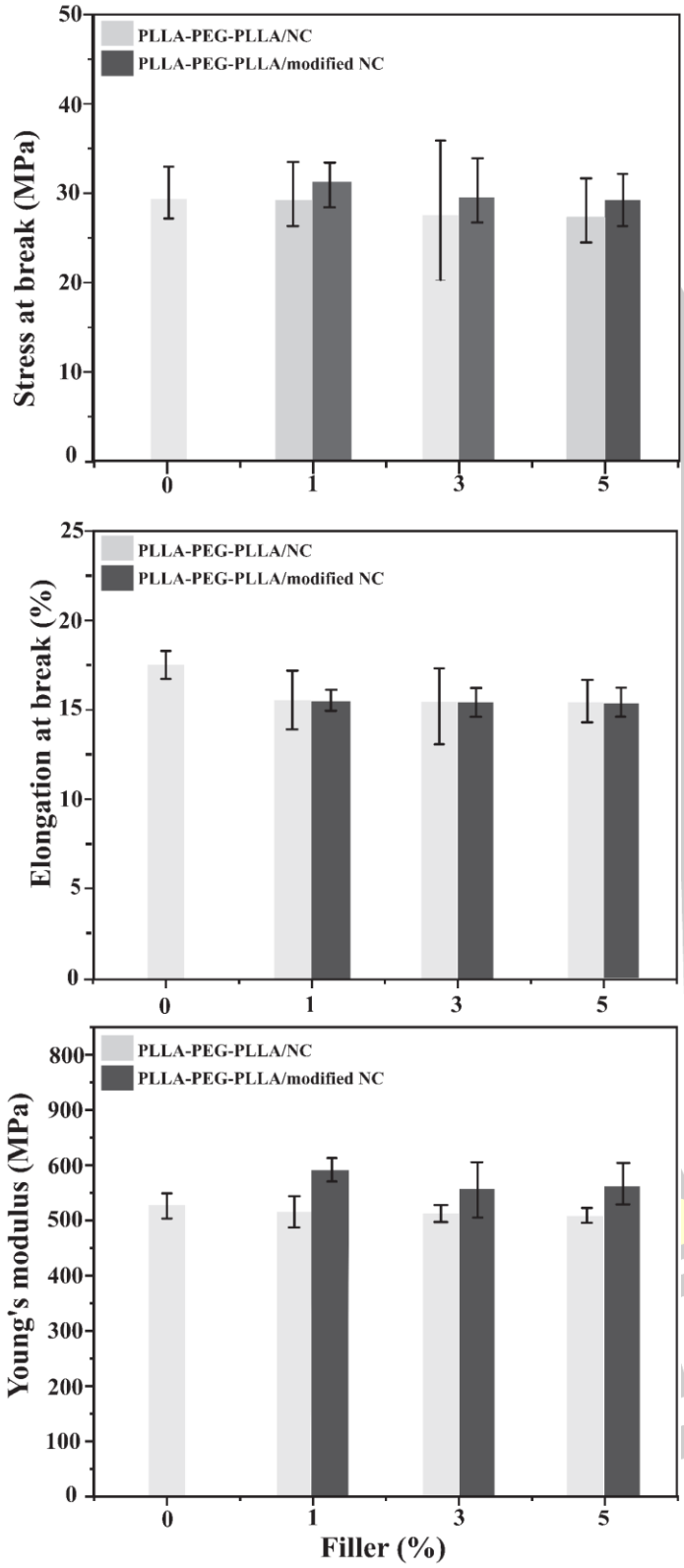

Figure 61 Tensile properties of (□) PLLA-PEG-PLLA/NC and (■) PLLA-PEG-PLLA/modified NC composite films

4.3.9 Water absorption

Water absorption is one of the most important functions of food packaging to decrease the moisture between the food and the surrounding atmosphere; the water absorption of the packaging material should be as low as possible[124]. The water absorption chart is shown Figure 62. The pure PLLA-PEG-PLLA film showed the lowest water absorption due to the hydrophobic properties of them. For PLLA-PEG-PLLA/NC composite films, the water absorption increased with increasing of NC content. For PLLA-PEG-PLLA/modified NC composite films were observed water absorption increased according to modified NC content (1-5%). After 20 days, the composite films presented higher degraded than pure PLLA-PEG-PLLA film because of NC and modified NC displayed a larger of OH group. The comparison between PLLA-PEG-PLLA/NC and PLLA-PEG-PLLA /modified NC composite films, the PLLA-PEG-PLLA /modified NC slightly increased water absorption than PLLA-PEG-PLLA /NC. This may be due to NC has a lot of hydroxyl groups compare modified NC [98].

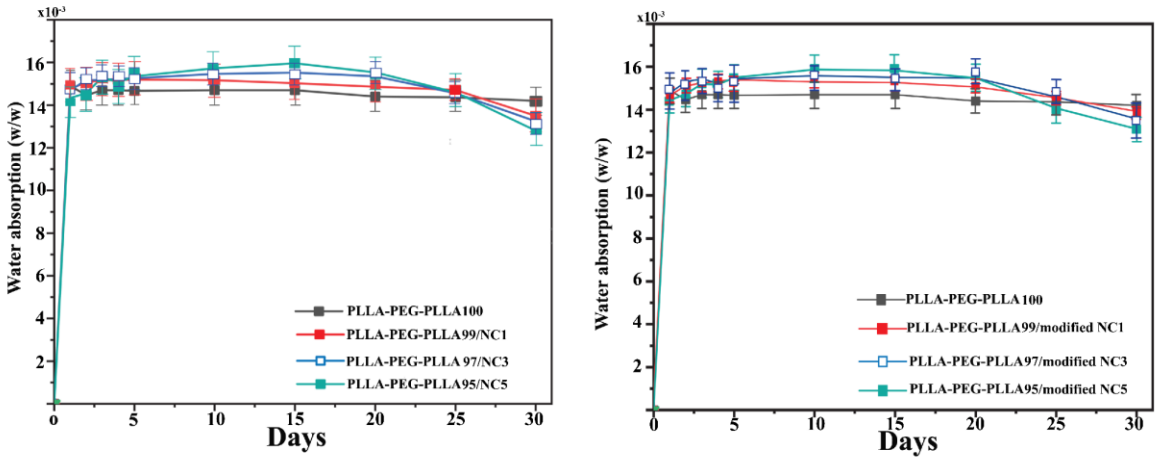

Figure 62 Water absorption of pure PLLA-PEG-PLLA film, PLLA-PEG-PLLA/NC (a) and PLLA-PEG-PLLA/modified NC (b) composite film

CHAPTER 5
CONCLUSION

This research was studied and extracted cellulose from rice straw by alkali treatment (NaOH), bleaching process with H_2O_2 and hydrolysis with H_2SO_4. The size of the cellulose was obtained (after the hydrolysis process) around 50-91 nm and 225-396 nm. The characterization was confirmed by particle size analyzers. While, diameter of size NC from Transmission electron microscope (TEM) displayed 30.22+1.7 nm. Therefore, the extracted was called nanocellulose and NC. However, NC extracted high hydrophilicity (with a lot of OH function) which has low compatibility with polymer matrix (hydrophobicity). Therefore, in this research, the was modified function groups of NC with [3-(2,3-Epoxypropoxy)-propyl]-trimethoxysilane. The modified NC will be called modified nanocellulose or modified NC. The size of the modified NC was 225-396 nm (particle size analyzer) and 35.53$\pm$1.6 nm (TEM). These characteristics were examined using fourier transform infrared spectroscopy (FTIR) and X-ray photoelectron spectrometry (XPS) for an analysis functional group, X-ray diffractometer (XRD) for studies crystallinity, scanning electron microscope (SEM)and transmission electron microscopy (TEM) for analysis morphology, differential scanning calorimeter (DSC) and thermogravimetric analysis (TGA) for examining the thermal property.

After studying and extracting nanocellulose (NC) from rice straw, The PLLA/NC, PLLA/modified NC, PLLA-PEG-PLLA/NC and PLLA-PEG-PLLA/modified NC composite films were prepared by the solvent casting process. The composite films were prepared in the weight ratios of 100/0, 99/1, 97/3, and 95/5. The PLLA/NC and PLLA/modified NC composite films decreased transparently. While the PLLA-PEG-PLLA result is similar to composite PLLA film. For ATR-FTIR analysis of the PLLA/NC, PLLA/modified NC, PLLA-PEG-PLLA/NC and PLLA-PEG-PLLA/modified NC composite films were confirmed the presence of NC and modified NC on the polymer matrix. The XRD result was showed the crystallinity index and position of crystals when increasing NC and modified NC content into the polymer matrix (PLLA or PLLA-PEG-PLLA). The result showed that the crystallinity index slightly increasing. In the case position of crystals for composite films, can confirm the existence of the polymer matrix (PLLA or PLLA-PEG-PLLA) and NC or modified NC. The study morphology of composite films was divided 2 types: surface and cross-section for composite films (PLLA/NC, PLLA/modified NC, PLLA-PEG-PLLA/NC and PLLA-PEG-PLLA/modified NC). For the surface, when increasing NC and modified NC content (1-5%) on the polymer matrix (PLLA or PLLA-PEG-PLLA) has a higher irregularity than pure films. For the cross-section, when increasing NC and modified NC content (1-5%) on the polymer matrix (PLLA or PLLA-PEG-PLLA) was observed composite films of modified NC filler good compatibility and good adhesion than NC fillers. The thermal stability of the composite films (PLLA/NC, PLLA/modified NC, PLLA-PEG-PLLA/NC and PLLA-PEG-PLLA/modified NC) showed that the film containing cellulose slightly increased thermal stability (358-367 ^{o}C for PLLA/NC, 358-377 ^{o}C for PLLA/modified NC, 367-376 ^{o}C for PLLA-PEG-PLLA/NC and 367-377 ^{o}C for PLLA-PEG-PLLA/modified NC).The thermal properties of the composite films (PLLA/NC, PLLA/modified NC,

PLLA-PEG-PLLA/NC and PLLA-PEG-PLLA/modified NC) was examined by DSC. When addition NC and modified NC content (1-5%), the result showed that decreases T_g, T_m, and T_{cc} but increase X_c for composite PLLA/NC and PLLA/modified NC films. In order hand on, the composite PLLA-PEG-PLLA/NC and PLLA-PEG-PLLA/modified NC slightly decreased T_g,and T_{cc} while T_m not different because of the interaction and good dispersion of modified NC on PLLA-PEG-PLLA matrix. The mechanical properties of composite films were analyzed by tensile testing. For PLLA/NC composite films, slightly increased Young's modulus was observed, followed by a reduction of tensile stress and elongation at break compare pure PLLA films. For PLLA/modified NC composite films increased tensile stress and Young's modulus, followed by a reduction of elongation at break compare pure PLLA films. In case pure PLLA-PEG-PLLA films, the PLLA-PEG-PLLA/NC found that slightly decreased tensile stress (23-27 MPa), Young's modulus (500-540 MPa). The elongation at break has not different compare pure PLLA-PEG-PLLA film. For PLLA-PEG-PLLA/modified NC composite films were increased tensile stress (29-32 MPa) and Young's modulus (535-612 MPa), followed by a reduction of elongation at break (12-15%) compare pure PLLA-PEG-PLLA film. Compare mechanical properties of PLLA-PEG-PLLA/NC and modified NC has been observed PLLA-PEG-PLLA/modified NC higher mechanical properties than PLLA-PEG-PLLA/NC. This may be due to the interaction and good dispersion of modified NC on PLLA-PEG-PLLA matrix.The water absorption of PLLA/NC, PLLA/modified NC, PLLA-PEG-PLLA/NC and PLLA-PEG-PLLA/modified NC composite films found that when addition filler (NC or modified NC) on polymer matrix increasing water absorption compare pure films. This may be due to NC has a lot of hydroxyl groups compare modified NC. After 25 days (composite PLLA films) and 20 days (composite PLLA-PEG-PLLA films) can be degraded.

It can be used as reinforcing agents to increase the thermal and mechanical properties of PLLA and PLLA-PEG-PLLA. The composite films containing 1% modified NC showed the best thermal and mechanical properties, suitable for packaging applications.

พหุน ปณฺ ฑิโต ชีเว

REFERENCES

REFERENCES

[1] F. Z. Benabid and F. Zouai, “Natural polymers: cellolose, chitin, chitosan, gelatin, starch, carrageenan, xylan and dextran,” vol. 4, no. 3, pp. 348–357, 2017.

[2] A. Cipurkovic and M. Saletovic, “Biodegradable Polymers: Production, properties and application in medicine,” vol. 11, no. 1, pp. 25–35, 2018.

[3] R. Auras, B. Harte, and S. Selke, “An overview of polylactides as packaging materials,” *Macromol. Biosci.*, vol. 4, no. 9, pp. 835–864, 2004.

[4] Y. Ikada and H. Tsuji, “Biodegradable polyesters for medical and ecological applications,” *Macromol. Rapid Commun.*, vol. 21, no. 3, pp. 117–132, 2002.

[5] A. R. Webb, J. Yang, and G. A. Ameer, “Biodegradable polyester elastomers in tissue engineering,” vol 4, no. 6 pp. 801–812, 2004.

[6] J. Ahmed, S. K. Varshney, J. Ahmed, and S. K. Varshney, “Polylactides-Chemistry, Properties and Green Packaging Technology: A Review. Polylactide (PLA),” vol 14, no.1, pp. 37–58, 2011.

[7] Y. Baimark, W. Rungseesantivanon, and N. Prakymoramas, “Improvement in melt flow property and flexibility of poly(L-lactide)-b-poly(ethylene glycol)-b-poly(L-lactide) by chain extension reaction for potential use as flexible bioplastics,” *Mater. Des.*, vol. 154, pp. 73–80, 2018.

[8] Y. Hu, Y. S. Hu, V. Topolkaraev, A. Hiltner, and E. Baer, “Crystallization and phase separation in blends of high stereoregular poly(lactide) with poly(ethylene glycol),” *Polymer*, vol. 44, no. 19. pp. 5681–5689, 2003.

[9] H. Danafar, K. Rostamizadeh, S. Davaran, and M. Hamidi, “Drug-conjugated PLA-PEG-PLA copolymers: a novel approach for controlled delivery of hydrophilic drugs by micelle formation.,” *Drug Dev. Ind. Pharm.*, vol. 40, no. 10, pp. 1411–1420, 2014.

[10] A. Wang, R. Qi, C. Xiong, and M. Huang, “Effects of coupling agent and interfacial modifiers on mechanical properties of poly(lactic acid) and wood flour biocomposites,” *Iran. Polym. J.*, vol. 20, no. 4, pp. 281–294, 2011.

[11] S. C. Pech-Cohuo, G. Canche-Escamilla, A. Valadez-González, V. V. A. Fernandez-Escamilla, and J. Uribe-Calderon, “Production and Modification of Cellulose Nanocrystals from Agave tequilana Weber Waste and Its Effect on the Melt Rheology of PLA,” *Int. J. Polym. Sci.*, vol. 2018, pp. 1-14, 2018.

[12] T. Niemela and M. Kellomaki, “Bioactive glass and biodegradable polymer composites.,” *Bioactive glasses.*, pp. 227-245, 2011.

[13] R. A. Gross, “Biodegradable Polymers for the Environment,” *Science.*, vol. 803, no. 2002, pp. 803–808, 2012.

[14] J. H. Clark, “Chemistry goes green,” *Nat. Chem.*, vol. 1, no. 1, pp. 12–13, 2009.

[15] V. Isabelle and T. Lan, “Biodegradable Polymers,” *Materials.*, vol. 2, no.1, pp. 307-344, 2009.

[16] S. A. Ashter, “Types of Biodegradable Polymers,” in *Introduction to Bioplastics Engineering*, vol. 8, no. 4, pp. 81-15, 2016.

[17] F. Gironi and V. Piemonte, “Bioplastics and petroleum-based plastics: Strengths and weaknesses,” *Energy Sources, Part A Recover. Util. Environ. Eff.*, vol. 33, no. 21, pp. 1949–1959, 2011.

[18] A. Sofia, L. Machado, I. G. De, A. V. De Sá, A. Vera, and A. Machado, *10 - Biodegradable polymer nanocomposites for packaging applications. Food Packaging.*, pp. 329-363, 2017.

[19] J. Pretula, S. Slomkowski, and S. Penczek, “Polylactides-Methods of synthesis and characterization,” *Adv. Drug Deliv. Rev.*, vol. 107, pp. 3–16, 2016.

[20] G. Kale, R. Auras, S. P. Singh, and R. Narayan, “Biodegradability of polylactide bottles in real and simulated composting conditions,” *Polym. Test.*, vol. 26, no. 8, pp. 1049–1061, 2007.

[21] D. Garlotta, “A Literature Review of Poly(Lactic Acid),” *Springer*, vol. 9, no. 2, pp. 63-84, 2002.

[22] S. Jia, D. Yu, Y. Zhu, Z. Wang, L. Chen, and L. Fu, “Morphology, crystallization and thermal behaviors of PLA-based composites: Wonderful effects of hybrid GO/PEG via dynamic impregnating,” *Polymers (Basel).*, vol. 9, no. 10, pp. 1–18, 2017.

[23] N. Jabeen, I. Majid, and G. A. Nayik, “Bioplastics and food packaging: A review,” *Cogent Food Agric.*, vol. 1, no. 1, pp. 1–6, 2015.

[24] M. B. Khajeheian and A. Rosling, “Preparation and characterization of linear and star-shaped poly L -lactide blends,” *J. Appl. Polym. Sci.*, vol. 133, no. 2, pp. 1–8, 2016.

[25] J. C. Bogaert and P. Coszach, “Poly(lactic acids): A potential solution to plastic waste dilemma,” *Macromol. Symp.*, vol. 153, pp. 287–303, 2000.

[26] J. Herzberger, K. Niederer, H. Pohlit, J. Seiwert, M. Worm, F. R. Wurm, and H. Frey., "Polymerization of ethylene oxide, propylene oxide, and other alkylene oxides: Synthesis, novel polymer architectures, and bioconjugation," *Chem. Rev.*, vol. 116, no. 4, pp. 2170–2243, 2016.

[27] L. T. Lim, R. Auras, and M. Rubino, "Processing technologies for poly(lactic acid)," *Prog. Polym. Sci.*, vol. 33, no. 8, pp. 820–852, 2008.

[28] M. H. Chisholm, "Concerning the ring-opening polymerization of lactide and cyclic esters by coordination metal catalysts," *Pure Appl. Chem.*, vol. 82, no. 8, pp. 1647–1662, 2010.

[29] Z. Wang, L. Yu, M. Ding, H. Tan, J. Li, and Q. Fu, "Preparation and rapid degradation of nontoxic biodegradable polyurethanes based on poly(lactic acid)-poly(ethylene glycol)-poly(lactic acid) and l-lysine diisocyanate," *Polym. Chem.*, vol. 2, no. 3, pp. 601–607, 2011.

[30] H. Danafar, K. Rostamizadeh, S. Davaran, and M. Hamidi, "PLA-PEG-PLA copolymer-based polymersomes as nanocarriers for delivery of hydrophilic and hydrophobic drugs: Preparation and evaluation with atorvastatin and lisinopril," *Drug Dev. Ind. Pharm.*, vol. 40, no. 10, pp. 1411–1420, 2014.

[31] W. Liu, A. Yang, Z. Li, H. Xu, and X. Yang, "PEGylated PLGA nanoparticles as tumor ecrosis factor-α receptor blocking peptide carriers: Preparation, characterization and release in vitro," *J. Wuhan Univ. Technol. Mater. Sci. Ed.*, vol. 22, no. 1, pp. 112–116, 2007.

[32] J. Ren, H. Hong, T. Ren, and X. Teng, "Preparation and characterization of magnetic PLA-PEG composite nanoparticles for drug targeting," *React. Funct. Polym.*, vol. 66, no. 9, pp. 944–951, 2006.

[33] L. F. Zhang, R. Sun, L. Xu, J. Du, Z. C. Xiong, H. C. Chen, C. D. Xiong., "Hydrophilic poly (ethylene glycol) coating on PDLLA/BCP bone scaffold for drug delivery and cell culture," *Mater. Sci. Eng. C*, vol. 28, no. 1, pp. 141–149, 2008.

[34] H. Asadi, K. Rostamizadeh, D. Salari, and M. Hamidi, "Preparation and characterization of tri-block poly(lactide)-poly(ethylene glycol)-poly(lactide) nanogels for controlled release of naltrexone," *Int. J. Pharm.*, vol. 416, no. 1, pp. 356–364, 2011.

[35] L. Li, Z. Q. Cao, R. Y. Bao, B. H. Xie, M. B. Yang, and W. Yang, "Poly(L-lactic acid)-polyethylene glycol-poly(L-lactic acid) triblock copolymer: A novel macromolecular plasticizer to enhance the crystallization of poly(L-lactic acid)," *Eur. Polym. J.*, vol. 97, pp. 272–281, 2017.

[36] K. L. Kadam, L. H. Forrest, and W. A. Jacobson, “Rice straw as a lignocellulosic resource: collection, processing, transportation, and environmental aspects,” *Biomass and Bioenergy*., vol. 18, no. 5, pp. 369-389, 2000.

[37] P. Cheewaphongphan, A. Junpen, S. Garivait, and O. Kamnoet, “Study on the Potential of Rice Straws as a Supplementary Fuel in Very Small Power Plants,” *Energies*., vol. 11, no. 2, pp. 1–21, 2018.

[38] P. Phanthong, P. Reubroycharoen, X. Hao, G. Xu, A. Abudula, and G. Guan, “Nanocellulose: Extraction and application,” *Carbon Resour. Convers.*, vol. 1, no. 1, pp. 32–43, 2018.

[39] A. Isogai, “Wood nanocelluloses : fundamentals and applications as new bio-based nanomaterials,” *J Wood Sci*., vol. 59, no. 6, pp. 449–459, 2013.

[40] L. Brinchi, F. Cotana, E. Fortunati, and J. M. Kenny, “Production of nanocrystalline cellulose from lignocellulosic biomass: Technology and applications,” *Carbohydr. Polym.*, vol. 94, no. 1, pp. 154–169, 2013.

[41] C. Bilbao-sainz, J. Bras, T. Williams, T. Sénechal, and W. Orts, “HPMC reinforced with different cellulose nano-particles,” *Carbohydr. Polym.*, vol. 86, no. 4, pp. 1549–1557, 2011.

[42] D. Bandera, J. Sapkota, S. Josset, C. Weder, P. Tingaut, X. Gao, E. J. Foster, and T. Zimmermann.,“Influence of mechanical treatments on the properties of cellulose nanofibers isolated from microcrystalline cellulose,” *React. Funct. Polym.*, vol. 85, pp. 134–141, 2014.

[43] H. P. S. Abdul Khalil, C. K.Saurabh, A.S. Adnan, M.R.N. Fazita, M.I.Syakira, M.Rafatullah, C.K.Abdullah, M.K.M. Haafiz and R.Dunganid., “A review on chitosan-cellulose blends and nanocellulose reinforced chitosan biocomposites: Properties and their applications,” *Carbohydr. Polym.*, vol. 150, no.5, pp. 216–226, 2016.

[44] I. Siro and D. Plackett, “Microfibrillated cellulose and new nanocomposite materials: A review,” *Cellulose*, vol. 17, no. 3, pp. 459–494, 2010.

[45] S. Edge, D. F. Steele, A. Chen, M. J. Tobyn, and J. N. Staniforth, “The mechanical properties of compacts of microcrystalline cellulose and silicified microcrystalline cellulose,” *Int. J. Pharm.*, vol. 200, no. 1, pp. 67–72, 2000.

[46] C. C. S. Coelho, M. Michelin, M. A. Cerqueira, C. Goncalves, R. V. Tonon, L. M. Pastrana, O. Freitas-Silva, A. A. Vicente, L. M. C. Cabral and J. A. Teixeira “Cellulose nanocrystals from grape pomace: Production, properties and

cytotoxicity assessment," *Carbohydrate Polymers*, vol. 192. pp. 327–336, 2018.

[47] P. Lu and Y. Lo Hsieh, "Preparation and characterization of cellulose nanocrystals from rice straw," *Carbohydr. Polym.*, vol. 87, no. 1, pp. 564–573, 2012.

[48] J. Liu, R. Korpinen, K. S. Mikkonen, S. Willför, and C. Xu, "Nanofibrillated cellulose originated from birch sawdust after sequential extractions: A promising polymeric material from waste to films," *Cellulose*, vol. 21, no. 4, pp. 2587–2598, 2014.

[49] H. Dong, J. F. Snyder, D. T. Tran, and J. L. Leadore, "Hydrogel, aerogel and film of cellulose nanofibrils functionalized with silver nanoparticles," *Carbohydr. Polym.*, vol. 95, no. 2, pp. 760–767, 2013.

[50] C. Miao and W. Y. Hamad, "In-situ polymerized cellulose nanocrystals (CNC)-poly(L-lactide) (PLLA) nanomaterials and applications in nanocomposite processing," *Carbohydr. Polym.*, vol. 153, pp. 549–558, 2016.

[51] R. M. D. Santos, W. P. Flauzino Neto, H. A. Silvério, D. F. Martins, N. O. Dantas, and D. Pasquini, "Cellulose nanocrystals from pineapple leaf, a new approach for the reuse of this agro-waste," *Ind. Crops Prod.*, vol. 50, pp. 707–714, 2013.

[52] P. Phanthong, Y. Ma, G. Guan, and A. Abudula, "Extraction of Nanocellulose from Raw Apple Stem," *J. Japan Inst. Energy*, vol. 94, no. 8, pp. 787–793, 2015.

[53] M. Cheng, Z. Qin, Y. Liu, Y. Qin, T. Li, L. Chen and M. Zhua, "Efficient extraction of carboxylated spherical cellulose nanocrystals with narrow distribution through hydrolysis of lyocell fibers by using ammonium persulfate as an oxidant," *J. Mater. Chem. A*, vol. 2, no. 1, pp. 251–258, 2014.

[54] I. Shahabi-Ghahfarrokhi, F. Khodaiyan, M. Mousavi, and H. Yousefi, "Preparation and characterization of nanocellulose from beer industrial residues using acid hydrolysis/ultrasound," *Fibers Polym.*, vol. 16, no. 3, pp. 529–536, 2015.

[55] K. Xu, C. Liu, K. Kang, Z. Zheng, S. Wang, Z. Tang, W. Yang, "Isolation of nanocrystalline cellulose from rice straw and preparation of its biocomposites with chitosan: Physicochemical characterization and evaluation of interfacial compatibility," *Compos. Sci. Technol.*, vol. 154, no. 2018, pp. 8–17, 2018.

[56] Y. Nishiyama, "Structure and properties of the cellulose microfibril," *J. Wood*

Sci., vol. 55, no. 4, pp. 241–249, 2009.

[57] Q. Cheng and S. Wang, "A method for testing the elastic modulus of single cellulose fibrils via atomic force microscopy," *Compos. Part A Appl. Sci. Manuf.*, vol. 39, no. 12, pp. 1838–1843, 2008.

[58] H. Fukuzumi, T. Saito, and A. Isogai, "Influence of TEMPO-oxidized cellulose nanofibril length on film properties," *Carbohydr. Polym.*, vol. 93, no. 1, pp. 172–177, 2013.

[59] Y. C. Hsieh, H. Yano, M. Nogi, and S. J. Eichhorn, "An estimation of the Young's modulus of bacterial cellulose filaments," *Cellulose*, vol. 15, no. 4, pp. 507–513, 2008.

[60] X. Wu, R. J. Moon, and A. Martini, "Crystalline cellulose elastic modulus predicted by atomistic models of uniform deformation and nanoscale indentation," *Cellulose*, vol. 20, no. 1, pp. 43–55, 2013.

[61] F. Tanaka and T. Iwata, "Estimation of the elastic modulus of cellulose crystal by molecular mechanics simulation," *Cellulose*, vol. 13, no. 5, pp. 509–517, 2006.

[62] P. J. Jandas, S. Mohanty, and S. K. Nayak, "Surface treated banana fiber reinforced poly (lactic acid) nanocomposites for disposable applications," *J. Clean. Prod.*, vol. 52. pp. 392–401, 2013.

[63] N. Wang, E. Ding, and R. Cheng, "Thermal degradation behaviors of spherical cellulose nanocrystals with sulfate groups," *Polymer.*, vol. 48, no. 12, pp. 3486–3493, 2007.

[64] G. Dorez, L. Ferry, R. Sonnier, A. Taguet, and J. M. Lopez-Cuesta, "Effect of cellulose, hemicellulose and lignin contents on pyrolysis and combustion of natural fibers," *J. Anal. Appl. Pyrolysis*, vol. 107, pp. 323–331, 2014.

[65] P. Nascimento, R. Marim, G. Carvalho, and S. Mali, "Nanocellulose Produced from Rice Hulls and its Effect on the Properties of Biodegradable Starch Films," *Mater. Res.*, vol. 19, no. 1, pp. 167–174, 2016.

[66] W. P. F. Neto, H. A. Silverio, N. O. Dantas, and D. Pasquini, "Extraction and characterization of cellulose nanocrystals from agro-industrial residue - Soy hulls," *Ind. Crops Prod.*, vol. 42, no. 1, pp. 480–488, 2013.

[67] A. Alemdar and M. Sain, "Isolation and characterization of nanofibers from agricultural residues - Wheat straw and soy hulls," *Bioresour. Technol.*, vol. 99, no. 6, pp. 1664–1671, 2008.

[68] G. Siqueira, S. Tapin-Lingua, J. Bras, D. da Silva Perez, and A. Dufresne,

"Mechanical properties of natural rubber nanocomposites reinforced with cellulosic nanoparticles obtained from combined mechanical shearing, and enzymatic and acid hydrolysis of sisal fibers," *Cellulose*, vol. 18, no. 1, pp. 57–65, 2011.

[69] T. Ramanathan, A. A. Abdala, S. Stankovich, D. A. Dikin, M. Herrera-Alonso, R. D. Piner, D. H. Adamson, H. C. Schniepp, X. Chen, R. S. Ruoff, S. T. Nguyen, I. A. Aksay, R. K. Prud'Homme and L. C. Brinson., "Functionalized graphene sheets for polymer nanocomposites," *Nat. Nanotechnol.*, vol. 3, no. 6, pp. 327–331, 2008.

[70] F. V. Ferreira, B.R.C. Menezes, W. Franceschi, and Gilmar Thim, "Influence of carbon nanotube concentration and sonication temperature on mechanical properties of HDPE/CNT nanocomposites," *Fullerenes Nanotub. Carbon Nanostructures*, vol. 25, no. 9, pp. 531–539, 2017.

[71] J. Chen, D. Wu, K. C. Tam, K. Pan, and Z. Zheng, "Effect of surface modification of cellulose nanocrystal on nonisothermal crystallization of poly(β-hydroxybutyrate) composites," *Carbohydr. Polym.*, vol. 157, pp. 1821–1829, 2017.

[72] A. Pei, Q. Zhou, and L. A. Berglund, "Functionalized cellulose nanocrystals as biobased nucleation agents in poly(l-lactide) (PLLA) - Crystallization and mechanical property effects," *Compos. Sci. Technol.*, vol. 70, no. 5, pp. 815–821, 2010.

[73] E. Espino-Perez, J. Bras, V. Ducruet, A. Guinault, A. Dufresne, and S. Domenek, "Influence of chemical surface modification of cellulose nanowhiskers on thermal, mechanical, and barrier properties of poly(lactide) based bionanocomposites," *Eur. Polym. J.*, vol. 49, no. 10, pp. 3144–3154, 2013.

[74] E. Luiz, D. Paula, V. Mano, E. Aparecida, R. Duek, and F. Vargas, "Hydrolytic degradation behavior of plla nanocomposites reinforced with modified cellulose nanocrystals" vol. 38, no. 8, pp. 1014–1020, 2015.

[75] E. Robles, J. Labidi, and L. Serrano, "Surface-modified nano-cellulose as reinforcement in poly (lactic acid) to conform new composites," vol. 71, pp. 44–53, 2015.

[76] K. M. Choi, S. W. Lim, M. C. Choi, Y. M. Kim, D. H. Han, and C. S. Ha, "Thermal and mechanical properties of poly(lactic acid) modified by poly(ethylene glycol) acrylate through reactive blending," *Polym. Bull.*, vol. 71, no. 12, pp. 3305–3321, 2014.

[77] J. G. Gwon, S. Y. Lee, S. J. Chun, G. H. Doh, and J. H. Kim, “Effects of chemical treatments of hybrid fillers on the physical and thermal properties of wood plastic composites,” *Compos. Part A Appl. Sci. Manuf.*, vol. 41, no. 10, pp. 1491–1497, 2010.

[78] E. Luiz, D. Paula, F. Roig, A. Mas, J.P. Habas, V. Mano, F. V. Pereira and J. J. Robin, “Effect of surface-grafted cellulose nanocrystals on the thermal and mechanical properties of PLLAA based nanocomposites,” *Eur. Polym. J.*, vol. 84, pp. 173–187, 2016.

[79] M. K. M. Haafiz, A. Hassan, Z. Zakaria, I. M. Inuwa, M. S. Islam, and M. Jawaid, “Properties of polylactic acid composites reinforced with oil palm biomass microcrystalline cellulose,” *Carbohydr. Polym.*, vol. 98, no. 1, pp. 139–145, 2013.

[80] C. Xu, J. Chen, D. Wu, Y. Chen, Q. Lv, and M. Wang, “Polylactide/acetylated nanocrystalline cellulose composites prepared by a continuous route: A phase interface-property relation study,” *Carbohydr. Polym.*, vol. 146, pp. 58–66, 2016.

[81] B. Schartel, B. Dittrich, K. Wartig, D. Hofmann, and M. Rolf, “The influence of layered, spherical, and tubular carbon nanomaterials’ concentration on the flame retardancy of polypropylene,” *Polym. Compos.*, no. 36, pp. 1230–1241, 2015.

[82] C. Miao and W. Y. Hamad, “Alkenylation of cellulose nanocrystals (CNC) and their applications,” *Polymer.*, vol. 101, pp. 338–346, 2016.

[83] H. Wu, S. Nagarajan, L. Zhou, Y. Duan, and J. Zhang, “Synthesis and characterization of cellulose nanocrystal-graft-poly(D-lactide) and its nanocomposite with poly(L-lactide),” *Polymer*, vol. 103. pp. 365–375, 2016.

[84] N. Johar, I. Ahmad, and A. Dufresne, “Extraction, preparation and characterization of cellulose fibres and nanocrystals from rice husk,” *Ind. Crops Prod.*, vol. 37, no. 1, pp. 93–99, 2012.

[85] M. Aminu, “Acid Hydrolysis-Mediated preparation of Nanocrystalline Cellulose from Rice Straw,” *Int. J. Nanomater. Nanotechnol. Nanomedicine*, vol. 3, pp. 051–056, 2017.

[86] M. Thakur, A. Sharma, V. Ahlawat, M. Bhattacharya, and S. Goswami, “Process optimization for the production of cellulose nanocrystals from rice straw derived a -cellulose,” *Mater. Sci. Energy Technol.*, vol. 3, pp. 328–334, 2020.

[87] S. Hyun, Y. Chang, and J. Han, “Development of polylactic acid nanocomposite films reinforced with cellulose nanocrystals derived from coffee silverskin Development of polylactic acid nanocomposite films reinforced with cellulose nanocrystals derived from coffee silverskin,” *Carbohydr. Polym.*, vol. 169, no. January, pp. 495–503, 2018.

[88] L. Du, J. Wang, Y. Zhang, C. Qi, M. P. Wolcott, and Z. Yu, “Preparation and characterization of cellulose nanocrystals from the bio-ethanol residuals,” *Nanomaterials*, vol. 7, no. 3, pp. 1–12, 2017.

[89] J. Luis Orellana, D. Wichhart, and C. L. Kitchens, “Mechanical and optical properties of polylactic acid films containing surfactant-modified cellulose nanocrystals,” *J. Nanomater.*, vol. 2018, 2018.

[90] V. A. Online, J. Gwon, H. Cho, S. Chun, S. Lee, and Q. Wu, “Physiochemical, optical and mechanical properties of poly(lactic acid) nanocomposites filled with toluene diisocyanate grafted cellulose nanocrystals,” *RSC Adv.*, vol. 69438–9445, pp. 9438–9445, 2016.

[91] R. Gunti, A.V. R. Prasad, and A. Gupta, “Mechanical and degradation properties of successive alkali treated completely biodegradable sisal fiber reinforced poly lactic acid composites,” *J. Reinf. Plant Comp.*, vol. 34, no. 12, pp. 951-961, 2015.

[92] S. Islam, N. Kao, S. N. Bhattacharya, R. Gupta, and P. K. Bhatt, “Effect of low pressure alkaline delignification process on the production of nanocrystalline cellulose from rice husk,” *J. Taiwan Inst. Chem. E.*, vol. 80, pp. 820-834, 2017.

[93] A. B. D. Nandiyanto, T. Rahman, M. A. Fadhlulloh, A. G. Abdullah, I. Hamidah and B. Mulyanti, “Synthesis of silica particles from rice straw waste using a simple extraction method,” *IOP. Conf. Ser. Mater. Sci. Eng.*, vol. 128, pp.1-8, 2016.

[94] L. Yue, A. Maiorana, F. Khelifa, A. Patel, J.M. Raquez, L. Bonnaud, R. Gross, P. Dubois and I.M. Zloczower, “Surface-modified cellulose nanocrystals for biobased epoxy nanocomposites,” *Polymer*, vol. 134, pp. 155–162, 2018.

[95] F. V Ferreira, M. Mariano, S. C. Rabelo, R. F. Gouveia, and L. M. F. Lona, “Isolation and surface modification of cellulose nanocrystals from sugarcane bagasse waste : From a micro- to a nano-scale view,” *Appl. Surf. Sci.*, vol. 436, pp. 1113–1122, 2018.

[96] Y. Yin, J. Ma, X. Tian, X. Jiang, and H. Wang, “Cellulose nanocrystals functionalized with amino-silane and epoxy-poly (ethylene glycol) for reinforcement and flexibilization of poly (lactic acid): material preparation

and compatibility mechanism," *Cellulose*, vol. 25, no. 11, pp. 6447–6463, 2018.

[97] M. Mariano, N. E. Kissi, and A. Dufresne, "Cellulose Nanocrystals and Related Nanocomposites: Review of some Properties and Challenges," *Polym Sci B Polym Phys*, vol. 52, no. 12, pp. 791–806, 2014.

[98] S. Hindi, "Suitability of Date Palm Leaflets for Sulphated Cellulose Nanocrystals Synthesis," *J Nanosci Nanotechno*, vol. 4, no. 1, pp. 6–16, 2017.

[99] L. C. Malucelli, L. G. Lacerda, M. Dziedzic, and M. A. da Silva Carvalho Filho, "Preparation, properties and future perspectives of nanocrystals from agro-industrial residues: a review of recent research," *Rev. Environ. Sci. Biotechnol.*, vol. 16, no. 1, pp. 131–145, 2017.

[100] Z. Liu, M. He, G. Ma, G. Yang, and J. Chen, "Preparation and characterization of cellulose nanocrystals from wheat straw and corn stalk," *Palpu Chongi Gisul/Journal Korea Tech. Assoc. Pulp Pap. Ind.*, vol. 51, no. 2, pp. 40–48, 2019.

[101] S. Girdthep, J. Sirirak, D. Daranarong, R. Daengngern, and S. Chayabutra, "Physico-chemical characterization of natural lake pigments obtained from Caesalpinia Sappan Linn. and their composite films for poly(lactic acid)-based packaging materials," *Dye. Pigment.*, vol. 157, pp. 27–39, 2018.

[102] J. Luo, M. Zhang, B. Yang, G. Liu, J. Tan, J. Nie and S. Song, "A promising transparent and UV-shielding composite film prepared by aramid nanofibers and nanofibrillated cellulose," *Carbohydr. Polym.*, vol. 203, no. September 2018, pp. 110–118, 2019.

[103] K. Saitou and M. Yamaguchi, "Transparent poly (lactic acid) film crystallized by annealing beyond glass transition temperature," *J Polym Res.*, vol. 104, pp. 22–29, 2020.

[104] J. Gwon, H. Cho, S. Chun, and S. Lee, "Physiochemical, optical and mechanical properties of poly(lactic acid) nanocomposites filled with toluene diisocyanate grafted cellulose nanocrystals," *RSC. Adv.*, vol. 12, pp. 9438–9445, 2016.

[105] C. C. Satam. C. W. Irvin, A. W. Lang, J. C. R. Jallorina, M. L. Shofner, J. R. Reynolds and J. C. Meredith, "Spray-Coated Multilayer Cellulose Nanocrystal -Chitin Nanofiber Films for Barrier Applications," *ACS Sustainable Chem. Eng.*, vol. 6, no. 8, pp.10637–10644, 2018.

[106] M. Vestena, I. P. Gross, C. M. O. Müller, and A. T. N. Pires, "Nanocomposite

of poly(lactic acid)/cellulose nanocrystals: Effect of CNC content on the polymer crystallization kinetics," *J. Braz. Chem. Soc.*, vol. 27, no. 5, pp. 905–911, 2016.

[107] P. Dubois, J. Dorgan and G. L. Re, "Polylactide / cellulose nanocrystal nanocomposites : Efficient routes for nanofiber modification and effects of nanofiberchemistry on PLA reinforcement," *Polymer.*, vol. 65, pp. 9–17, 2015.

[108] X. Zhang, P. Ma, and Y. Zhang, "Structure and properties of surface-acetylated cellulose nanocrystal/poly(butylene adipate-co-terephthalate) composites," *Polym. Bull.*, vol. 73, no. 7, pp. 2073–2085, 2016.

[109] D. Bagheriasl, P. J. Carreau, B. Riedl, and C. Dubois, "Enhanced properties of polylactide by incorporating cellulose nanocrystals," *Polym. Compos.*, vol. 39, no. 8, pp. 2685–2694, 2018.

[110] S. Gardebjer, A. Bergstrand, A. Idstrom, C. Borstell, S. Naana, L. Nordstierna and A. Larsson., "Solid-state NMR to quantify surface coverage and chain length of lactic acid modified cellulose nanocrystals, used as fillers in biodegradable composites," *Compos. Sci. Technol.*, vol. 107, pp. 1–9, 2015.

[111] R. Z. Khoo, H. Ismail, and W. S. Chow, "Thermal and Morphological Properties of Poly (lactic acid)/Nanocellulose Nanocomposites Nomenclature CNC Cellulose Nanocrystals DSC Differential Scanning Calorimetry EFTEM Energy Filtered Transmission Electron Microscope MCC Microcrystalline Cellulose NC ," *Procedia Chemistry*, vol. 19. pp. 788–794, 2016.

[112] Z. C. B. and M. P. of P. A. in the P. of a C. N. A. Yang, H. Peng, W. Wang, and T. Liu, "The Crystallization Behavior and Mechanical Properties of Polylactic Acid in the Presence of a Crystal Nucleating Agent," *J. Appl. Polym. Sci.*, vol. 125, pp. 1108–1115, 2012.

[113] D. Battegazzore, S. Bocchini, J. Alongi, A. Frache, and F. Marino, "Cellulose extracted from rice husk as filler for poly(lactic acid): Preparation and characterization," *Cellulose*, vol. 21, no. 3, pp. 1813–1821, 2014.

[114] S. Qian and K. Sheng, "PLA toughened by bamboo cellulose nanowhiskers: Role of silane compatibilization on the PLA bionanocomposite properties," *Compos. Sci. Technol.*, vol. 148, pp. 59–69, 2017.

[115] M. L. Sanyang, S. M. Sapuan, M. Jawaid, M. R. Ishak, and J. Sahari, "Development and characterization of sugar palm starch and poly (lactic acid) bilayer films," *Carbohydr. Polym.*, vol 146, pp.36-45, 2016.

[116] R. Abouzeid, M. A. Diab, S. A. A. Mohamed, and H. Aljohani, "Surfactant-

Assisted Poly (lactic acid)/ Cellulose Nanocrystal as a Bionanocomposite for Potential Application in Paper Coating," *J. Renew. Mater*. vol.6, no.4, pp.394-401, 2018.

[117] M. Ho, K. Lau, H. Wang, and D. Hui, "Improvement on the properties of polylactic acid (PLA) using bamboo charcoal particles," *Compos. Part B*, vol. 81, pp. 14–25, 2015

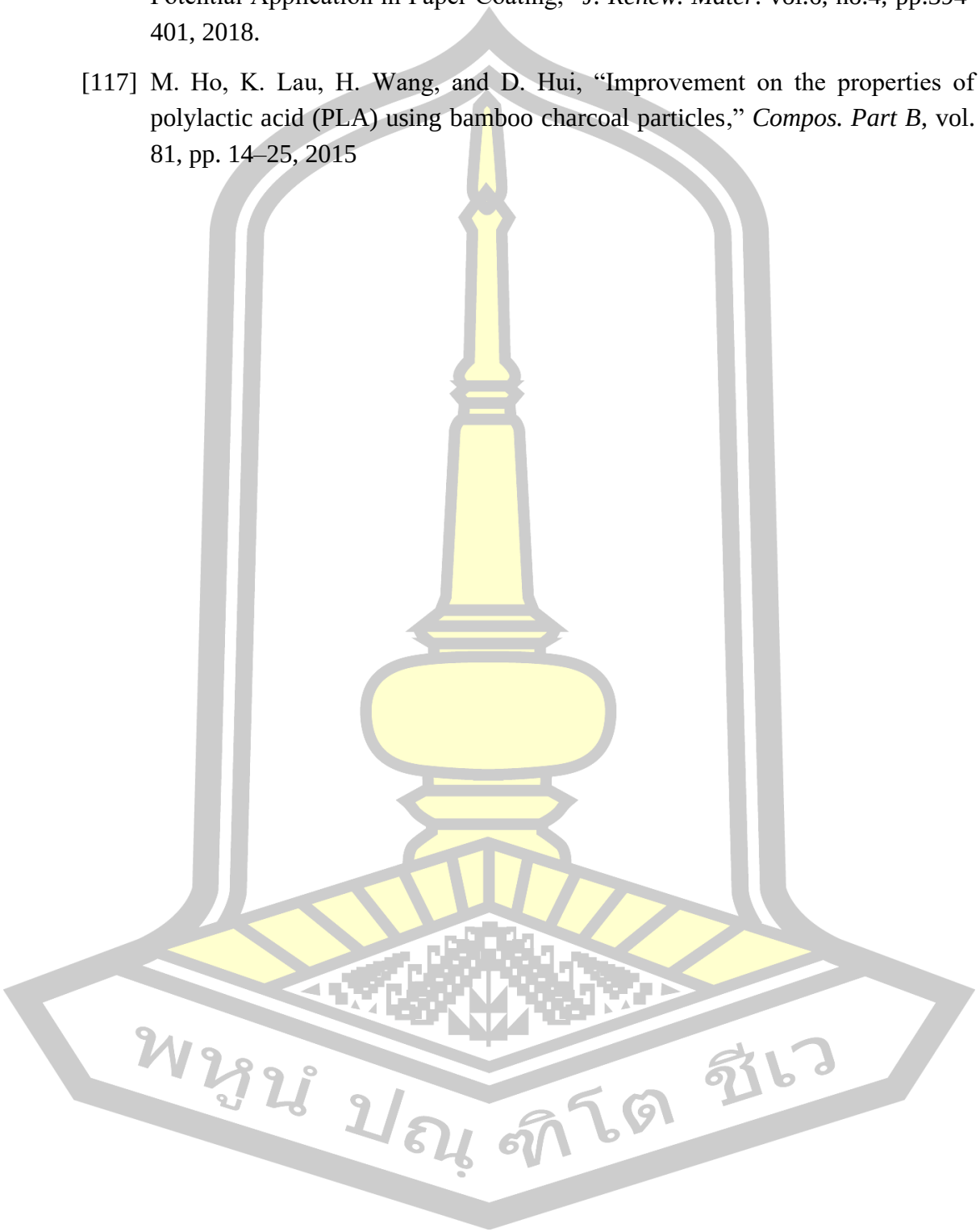

APPENDIX

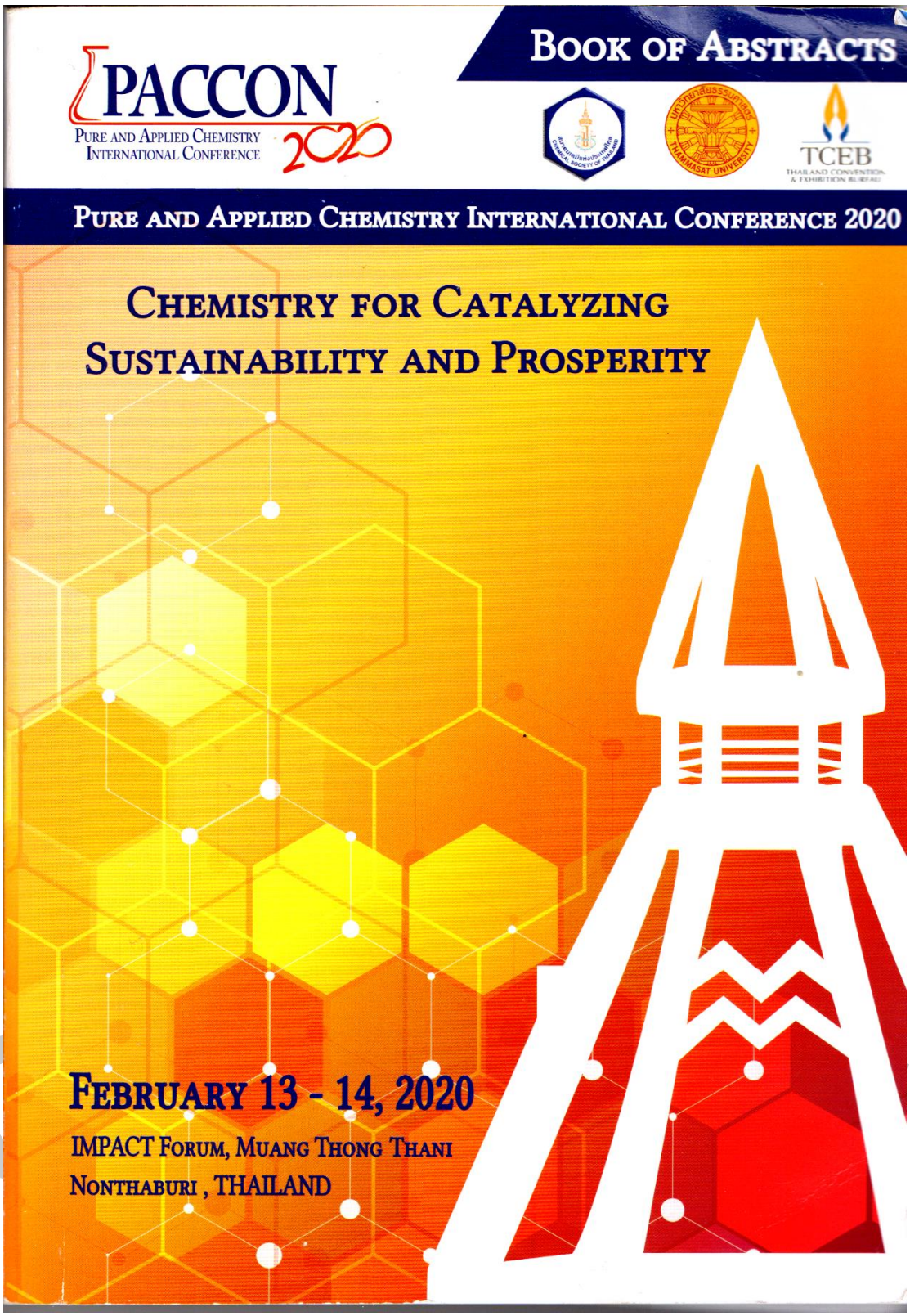
PACCON 2020
PURE AND APPLIED CHEMISTRY INTERNATIONAL CONFERENCE
BOOK OF ABSTRACTS
TCEB
THAILAND CONVENTION & EXHIBITION BUREAU
PURE AND APPLIED CHEMISTRY INTERNATIONAL CONFERENCE 2020
CHEMISTRY FOR CATALYZING SUSTAINABILITY AND PROSPERITY
FEBRUARY 13 - 14, 2020
IMPACT FORUM, MUANG THONG THANI
NONTHABURI , THAILAND

Pure And Applied Chemistry International Conference 2020
Chemistry for Catalyzing Sustainability and Prosperity
February 13-14, 2020
IMPACT Forum, Muangthong Thani, Bangkok, Thailand

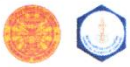

The Pure and Applied Chemistry International Conference 2020 - PACCON 2020

Chemistry for Catalyzing Sustainability and Prosperity

February 13-14, 2020

IMPACT Forum, Mauangthong Thani, Bangkok, Thailand

Dear Participant ,

Thank you for your payment. Please use the attached registration confirmation letter as your proof of registration to get the receipt, name tag and all other congress materials at the registration counter in the congress.

You can download your confirmation letter by go to https://www.paccon2020.com/app/print_confirmation_letter.php?id=2221&rk=0006601250

If you have any enquiries, please do not hesitate to contact us.

Sincerely yours,
PACCON 2020 Secretariat Officer.

Pure And Applied Chemistry International Conference 2020
Secretariat Office:
Department of Chemistry, Faculty of Science and Technology, Thammasat University
E-mail: paccon2020@sci.tu.ac.th Web site: https://www.paccon2020.com

PC-P-017	**Homogeneous Acetylation of Cellulose with Acetyl Chloride to Cellulose Acetate from Water Hyacinth** Malinee Leekrajang*, Borwon Narupai, Nattaporn Chutichairattanaphum, Siriporn Larpkiattaworn
PC-P-018	**Thermal Properties of Polycaprolactone Blended with Benzoxazine Resins of Different Functionalities** Chanidapa Rachniyom, Suphachok Angsuworapurk, Sarawut Rimdusit, Sunan Tiptipakorn*
PC-P-019	**Synthesis and Characterization of Chitosan Hydrogels and Chitosan Hydrogel-ZnO-nanocomposites** Wilawan Nuansri, Srichalai Khunthon, Krisana Siralertmukul*
PC-P-020	**Modified Nanocrystals Cellulose as Green Fillers to Improve Crystallization Property of Poly(L-lactide) Bionanocomposite Films** Chutima Banthao, Yodthong Baimark, Kansiri Pakkethati*
PC-P-021	**Enhancing Dye Adsorption by UiO-67/Cellulose Acetate Composite Film** Jarinphorn Pukkao, Penwisa Pisitsak, Thitirat Inprasit*
PC-P-022	**The Modified Ion Exchange Cigarette Filters Applied for Heavy Metals Removal** Wichayasith Inthakusol, Saisuree Prateeptongkum, Ngampuk Tayana, Nongnaphat Duangdee*
PC-P-023	**Utilization of KOH Activated Molasses Carbon Powder as an Alternative Filler in Natural Rubber** Perawat Kittipitak, Waroporn Sopradit, Thanunya Saowapark*
PC-P-024	**Construction of Aptamer Complex by Hybridization** Paphada Watcharapo, Boonchoy Soontornworajit*
PC-P-025	**Integration of Collagen into Chitosan Blend Film Composite: Physico-Chemical Properties Aspect for Pharmaceutical Material** Kitiyaporn Thongchai, Piyachat Chuysinuan, Thanyaluck Thanyacharoen, Sarute Ummartyotin*

PC

PC-P-020	**Modified Nanocrystals Cellulose as Green Fillers to Improve Crystallization Property of Poly (L- Lactide) Bionanocomposite Films**

Chutima Banthao, Yodthong Baimark, Kansiri Pakkethati*

Department of chemistry, Faculty of science, Mahasarakham University, Mahasarakham 44150, Thailand

**E-mail: kansiri.p@msu.ac.th*

Modified cellulose nanocrystals which were extracted from rice straw by hydrolysis method improved crystallization property of poly (L-lactide) bionanocomposite films. The nanocrystals cellulose were obtained a diameter between 50 and 100 nm by particle size analyzer. The bionanocomposite films were prepared by solution casting method using poly (L-lactide) and modified cellulose nanocrystals with different weight ratios (100/0, 99/1, 97/3, 95/5). The films were characterized by thermal gravimetric analysis (TGA), differential scanning calorimetry (DSC), X-ray powder diffraction (XRD) and scanning electron microscopy (SEM). The thermal properties and crystallinity of bionanocomposite films were increased by increasing the amount of modified cellulose nanocrystals. The results of this study showed that modified cellulose nanocrystals from rice straw can enhance the thermal properties and crystallinity of bionanocomposite films.

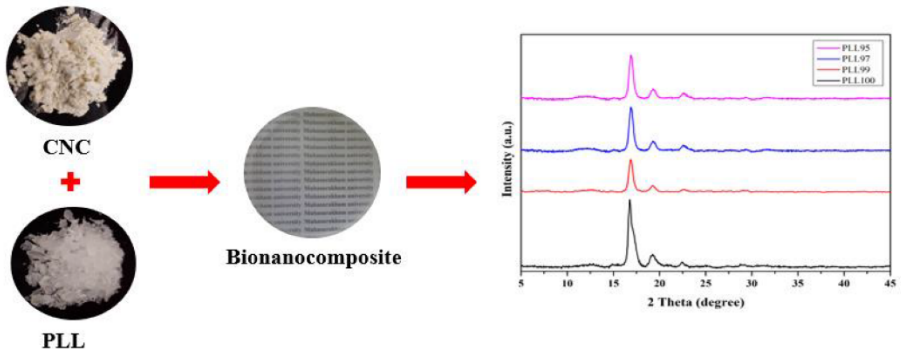

Keywords: Bionanocomposite film; Poly (L-lactide); Nanocrystals cellulose

PACCON 2020
Pure and Applied Chemistry International Conference
Chemistry for Catalyzing Sustainability and Prosperity

Modified nanocrystal cellulose as green fillers to improve crystallization property of poly (L- lactide) bionanocomposite films

Chutima Banthao[1], Yodthong Baimark[1], Sujitra Wongkasemjit[2], Kansiri Pakkethati[1]*

[1]*Department of chemistry, Faculty of science, Mahasarakham University, Mahasarakham 44150, Thailand*
[2]*Petroleum and petrochemical college, Chulalongkorn University, Bangkok 10330, Thailand*
**E-mail: kansiri.p@msu.ac.th*

Abstract:

Modified nanocrystal cellulose which were extracted from rice straw by hydrolysis method improved crystallization property of poly (L-lactide) bionanocomposite films. The nanocrystal cellulose were obtained a diameter between 50 and 600 nm by particle size analyzer. The bionanocomposite films were prepared by solution casting method using poly (L-lactide) and modified nanocrystal cellulose with different weight ratios (100/0, 99/1, 97/3, 95/5). The films were characterized by thermal gravimetric analysis (TGA), differential scanning calorimetry (DSC), X-ray diffraction (XRD) and scanning electron microscopy (SEM). The thermal properties and crystallinity of bionanocomposite films were increased by increasing the amount of modified nanocrystals cellulose. The results of this study showed that modified nanocrystal cellulose from rice straw can enhance the thermal properties and crystallinity of bionanocomposite films.

1. Introduction

In current, "green chemistry" is popular all over the world. The tendency to use biodegradable polymers is increasing in various industries to reduce the accumulation of fossil plastic waste and to protect the green environment. Biodegradable polymers can be divided according to their source into 3 types: naturally produced renewable polymers, synthetic polymers derived from renewable resources, and synthetic polymers derived from petroleum-based resources.[1] Polylactide (PLL) is a popular biodegradable polymer due to its outstanding properties as high mechanical, biodegradability, transparent, low density and biocompatibility. However, it presents some disadvantages, such as low thermal stability, brittleness and low crystallization rate, which hinders its use in many applications.[2] Thus improving the properties of the PLL is using nucleating agents. The crystallization behavior of polylactic acid (PLA) was studied in the presence of a crystal nucleating agent.

The nanocrystal cellulose (CNCs) is classified as a nucleating agent, which has interesting properties such as high strength, low density renewability, very large surface area abundance in nature, biocompatibility and biodegradability.

The CNCs are very promising for using as reinforcement in high-performance nanocomposite with sustainable appeal. The large surface area and the presence of abundant surface hydroxyl groups allow the functionalization of CNCs. In previous work, Aihua[3] has improved the crystal properties of PLL. To compare properties of composite, PLL were added CNCs and modified CNCs (*n*-dodecyldimethylchlorosilane) using solution casting. The results show that the modified CNCs have higher crystallinity than CNCs. Consistent with the research of Orellana[2] that they compared the properties of PLL by filling their material with CNCs and modified CNCs(cetyltrimethylammonium bromide and decylamine). Cohuo[4] has modified nanocrystal cellulose(CNCs) using 2-ethyl hexyl acrylate (2-EHA). The results showed that the crystallinity index decreased. The aim of this work is to enhance the crystallization of PLL by the addition of mCNCs [3- (2,3-Epoxypropoxy) -propyl]-trimethoxysilane).

2.Materials and Methods

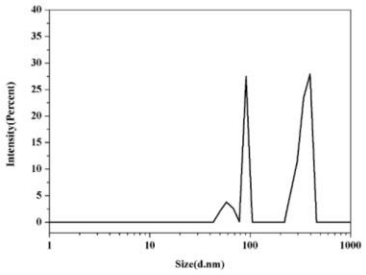

Fig.1. Particle size distributions of CNCs

3.2. The morphology analysis

The cross-sectional surface of a bionanocomposite was measured using a SEM shown in Fig.2. It shows that the surface area of the PLL films without mCNCs were smooth and uniform. while bionanocomposite films were irregularly and found mCNCs in the polymer matrix. Similar to the research of Xu *et al.*[7]

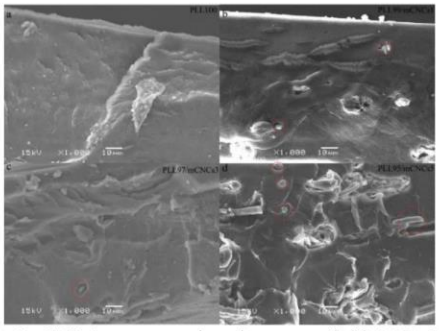

Fig.2. SEM cross-section images of (a) PLL100 and bionanocomposite films (b) PLL99/mCNCs1, (c) PLL97/mCNCs3 and (d) PLL95/mCNCs5

3.3 XRD analysis

The XRD analysis of pure film and bionanocomposite films were shown in Fig.3. CNCs and mCNCs presents a small and broad peak at 2θ = 14°, 22°, and 34°[8]. PLL shows a small and broad peak at 2θ=16°, 19°, and 22.7°[9] When mCNCs was composited with PLL, the crystallization was increased. This may be due to the mCNCs being nucleating agent.

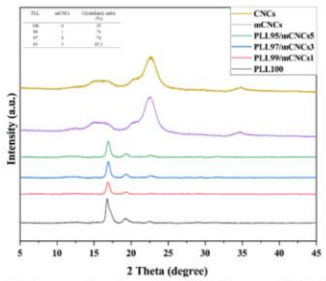

Fig.3. XRD analysis of CNCs, mCNCs, PLL films and bionanocomposite films

3.4 DSC and TGA analysis

The study of thermal properties of bionanocomposite films was shown in Fig.4. and Fig.5. The addition of mCNCs showed that the Tg decreased, but Tm and Tcc increased with addition of mCNCs. When increasing the concentration of mCNCs affected thermal stability of bionanocomposite increase. Because the interaction between mCNCs and PLL.[10]

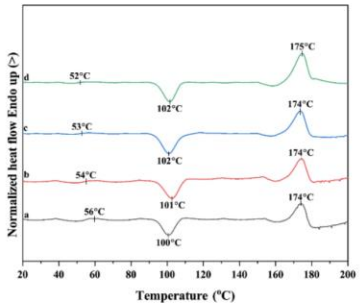

Fig.4. Heating DSC curves of (a) PLL100 and bionanocomposite films (b) PLL99/mCNCs1, (c) PLL97/mCNCs3 and (d) PLL95/mCNCs5

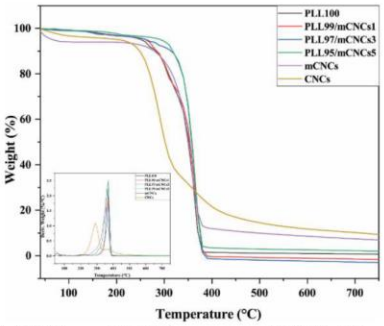

Fig.5. TGA and DTG curves of PLL films and bionanocomposite films

2.1 Materials

The PLL was supported by Assoc. Prof. Dr. Yodthong Baimark (Mn =100,000 g/mol). The nanocrystal cellulose was synthesized from rice straw (jasmine rice, Mahasarakham province). The chemicals were used extraction of nanocrystal cellulose, modified, and composite films H_2O_2 (30-32%, ANaPURE), NaOH (AR grade, Ajax Finechem, Australia), H_2SO_4 (98%, ANaPURE), CH_2Cl_2 (99.8%, AR grade, Fisher Chemical) and [3- (2,3-Epoxypropoxy)-propyl]-trimethoxysilane (Merck, China).

2.2 Experiment

2.2.1 Extraction of nanocrystal cellulose from rice straw

Rice straw was cut into small sizes, approximately 1-2 cm. It was washed with tap water and was dried in an oven at 80 °C. Next, these straws were eliminated hemicellulose using 5% NaOH and were removed lignin by 18.5% H_2O_2. The cellulose fibers were hydrolyzed using 64% H_2SO_4 at 45 °C for 1 h. according to a previously reported method[5] under constant stirring. After the hydrolysis, the solution was diluted with cold water to stop the hydrolysis reaction. The nanocrystal cellulose powder was dried by a freeze-dry machine and then stored in a desiccator.

2.2.2 Modified nanocrystals cellulose

Step I, in the process of preparation silanols, it was prepared by adding water to [3-(2,3-Epoxypropoxy)-propyl]-trimethoxysilane, then adding 95% ethanol, stirring for 30 min. Step II, coupling agents were prepared from silanol and nanocrystals cellulose, at 120 °C for 2 h., then reduced the temperature to 105 °C for 12 h. The modified nanocrystal cellulose powder was stored in a desiccator.

2.2.3 Fabrication PLL/ modified nanocrystal cellulose bionanocomposite films

PLL was added 10 ml of CH_2Cl_2 under stirring for 1 h. Then it was mixed with modified nanocrystal cellulose for 0.5 h. The PLL/ modified nanocrystal cellulose was poured into the petri dish and left at room temperature. After that, PLL/modified nanocrystal cellulose was perfumed by an oven vacuum for 24 h. The ratio of PLL/modified nanocrystal cellulose in this research were 100/0, 99/1, 97/3 and 95/5 (w/w).

2.3 Characterization

The particle size and distribution of the modified nanocrystal cellulose were evaluated by a particle size analyzer (Malvern instruments, Zetasizer Nano S90). The study of the crystallinity of the samples was measured using a Bruker D8 Advance X-ray diffractometer at room temperature using CuKα radiation at 40 kV and 40 mA. The scanning angle range of $2\theta = 5°–40°$ at a scan speed of rate 0.2 sec/degrees was used to determine the crystalline structures. The crystallinity index, CrI was determined using Segal's formula as given below[6]

$$CrI\,(\%) = I_{002} - I_{am} / I_{002}$$

Where I_{002} is the overall intensity of the peak at 2-theta about 16°, I_{am} is the intensity of the baseline at 2-theta about 19°.

The thermal properties of samples were measured out using differential scanning calorimeter (Perkin-Elmer, Pyris Diamond). Samples were first heated to 200 °C at 10 °C /min of heating rate and held for 2 min, and then cooled down to -40 °C at the same rate. Second heating was performed from 20 to 200 °C. All operations were studied under a nitrogen atmosphere. Also, the thermal stability properties of the samples were carried out using thermogravimetric Analyzers (TA-Instrument, TG SDT Q600). The sample was heated from 50 to 800 °C at a heating rate of 20 °C/min under a nitrogen purge.

The morphology of the samples was analyzed using scanning electron microscope; SEM (JEOL, JSM-64606V). The sample was fractured in liquid nitrogen, and the fracture surface was coated with gold to enhance conductivity before scanning.

3. Results & Discussion

3.1 The particle size distributions

The particle size distributions of CNCs were shown in Fig.1. The peak observed in the mass distribution was located at approximately 50- 600 nm.

4. Conclusion

Modified nanocrystal cellulose, which was extracted from rice straw by hydrolysis method improved crystallization property of PLL bionanocomposite films. The crystallinity index was increased from 37 to 87.5% when increasing mCNCs (1-5% w/w). The thermal properties of bionanocomposite films were slightly increased T_m (174-175 °C) and T_{cc} but decreased T_g.

Acknowledgements

This research was financially supported by Thailand Research Fund (TRF). The Center of Excellence for Innovation in Chemistry (PERCH-CIC), Ministry of Higher Education, Science, Research and Innovation is gratefully acknowledged. The department of chemistry, Faculty of Science, Mahasarakham University

References

1. Ashter, SA.; Types of Biodegradable Polymers. In: *Introduction to Bioplastics Engineering*. **2016**, 81-151.

2. Luis, OJ.; Wichhart, D.; Kitchens, CL.; Mechanical and optical properties of polylactic acid films containing surfactant-modified cellulose nanocrystals. *J Nanomater*. **2018**, 4, 1-12.

3. Pei, A.; Zhou, Q.; Berglund, LA.; Functionalized cellulose nanocrystals as biobased nucleation agents in poly(l-lactide) (PLLA) - Crystallization and mechanical property effects. *Compos Sci Technol*. **2010**, 70(5), 815-821.

4. Pech-Cohuo, SC.; Canche-Escamilla, G.; Valadez-González, A.; Fernández-Escamilla, VVA.; Uribe-Calderon, J.; Production and Modification of Cellulose Nanocrystals from Agave tequilana Weber Waste and Its Effect on the Melt Rheology of PLA. *Int J Polym Sci*. **2018**, 2, 1-14.

5. Du, L.; Wang, J.; Zhang, Y.; Qi, C.; Wolcott, MP.; Yu, Z.; Preparation and characterization of cellulose nanocrystals from the bio-ethanol residuals. *Nanomaterials*. **2017**, 7(3), 1-12.

6. Liu, Z.; He, M.; Ma, G.; Yang, G.; Chen, J.; Preparation and characterization of cellulose nanocrystals from wheat straw and corn stalk. *Palpu Chongi Gisul/Journal Korea Tech Assoc Pulp Pap Ind*. **2019**, 51(2), 40-48.

7. Xu, C.; Chen, J.; Wu, D.; Chen, Y.; Lv, Q.; Wang, M.; Polylactide/acetylated nanocrystalline cellulose composites prepared by a continuous route: A phase interface-property relation study. *Carbohydr Polym*. **2016**, 146, 58-66.

8. Bagheriasl, D.; Carreau, PJ.; Riedl, B.; Dubois, C.; Enhanced properties of polylactide by incorporating cellulose nanocrystals. *Polym Compos*. **2018**, 39(8), 2685-2694.

9. Bagheriasl, D.; Safdari, F.; Carreau, PJ.; Dubois, C.; Riedl, B.; Dubois, C.; Development of cellulose nanocrystal-reinforced polylactide: A comparative study on different preparation methods. *Polym Compos*. **2019**, 39(8), 2685-2694.

10. Miao, C.; Hamad, WY.; In-situ polymerized cellulose nanocrystals (CNC)—poly(L-lactide) (PLLA) nanomaterials and applications in nanocomposite processing. Carbohydr Polym. **2016**, 153, 549-558.

BIOGRAPHY

NAME	Miss Chutima Banthao
DATE OF BIRTH	07/01/1995
PLACE OF BIRTH	Udonthani
ADDRESS	73 Moo.10 Up-mung, Nongwuaso, Udonthani
POSITION	Student
PLACE OF WORK	Mahasarakham University
EDUCATION	2014 - High School, Nongwuasopittayakhom School, Udonthani, Thailand 2018 - Bachelor Degree of Science (B.Sc.) Major in Chemistry, Mahasarakham University, Mahasarakham Thailand
Research grants & awards	Center of Excellence for Innovation in Chemistry (PRECH-CIC)
Research output	-